High Frequency Transients in Large Wind Farm

Advanced Measurement and Characterization

Elforsk rapport 12:04

M. Reza, K. Srivastava, T. Abdulahovic, A. Marinopoulos, H.Breder

April 2012

Vindforsk Energimyndigheten ELFORSK

High Frequency Transients in Large Wind Farm

Advanced Measurement and Characterization

Elforsk rapport 12:04

M. Reza, K. Srivastava, T. Abdulahovic, A. Marinopoulos, H.Breder

April 2012

Foreword

Research on switching transient in a cable collection grid system was started already in Vindforsk II. The work has continued also during Vindforsk III. This report is the final report for the Vindforsk III project V-326 High frequency transients in large wind farm: advanced measurement and characterization

The work has been carried out by ABB Corporate Research with Dr. Muhamad Reza as project leader.

Vindforsk-III is funded by ABB, Arise windpower, AQ System, E.ON Elnät, E.ON Vind Sverige, EnergiNorge, Falkenberg Energi, Fortum, Fred. Olsen Renewables, Gothia Vind, Göteborg Energi, HS Kraft, Jämtkraft, Karlstads Energi, Luleå Energi, Mälarenergi, o2 Vindkompaniet, Rabbalshede Kraft, Skellefteå Kraft, Statkraft, Sena Renewable, Svenska kraftnät, Tekniska Verken i Linköping, Triventus, Wallenstam, Varberg Energi, Vattenfall Vindkraft, Vestas Northern Europe, Öresundskraft and the Swedish Energy Agency.

Comments on the work and the final report have been given by a reference group with the following members:

Anders Holm	Vattenfall
Sture Lindahl	Gothia Power
Stanislaw Gubanski	Chalmers
Philip Kjær	Vestas
Lars Gertmar	ABB
Arne Hejde Nielsen,	DTU
Thomas Johannesson	E.On elnät

Stockholm April 2012

Anders Björck

Programme manager Vindforsk-III

Electricity and heat production, Elforsk AB

Summary

Large cable-based systems such as collection grids for wind parks emerge worldwide. Transient overvoltages, appear, e.g., at grid energizing, de-energizing and fault handling. IEC test standards do not consider cable characteristics or repetitive re-strikes. This calls for a clarification of transients in wind park cable collection grids with respect to causes, prevention, and mitigation.

This work - High Frequency Transients in Large Wind Farm: Advanced Measurement and Characterization supported by Elfrosk program Vindforsk III, project V-326 - is a continuation of the cable system transient study done in 2007-2008 under support of Elforsk program Vindforsk II, project V-110 [1]. Within project V-110, a laboratory environment was created at ABB Corporate Research to enable measurements on typical apparatus within well-defined circuits and controlled parameters, where worst-case conditions can be tested with limited risks in terms of possible hazard and cost. In the present project V-326, the laboratory has been updated further so that, testing with higher voltage level (20 kV) can be performed as well as some electrical apparatus and transient overvoltages mitigation methods are additionally tested.

Results from the new experiment campaign V-326 confirm the characterizing transient overvoltages in a cable system obtained and presented in Vindforsk II project V-110.

- The experiments verify the consistent occurrence of repetitive prestrikes and re-ignitions in a cable system. The occurrence is determined by the electrical circuit and the point-on-wave of switching operations.
- Surge arresters always limit the maximum voltage magnitude but voltage steps with a magnitude twice the protective level can occur while the voltage can swing within a band in magnitude below the surge arrester protection level from negative to positive polarity.
- Surge capacitors and the RC-protection show mitigation effects although not removing the repetitive overvoltage transients completely. The number of repetitive reignitions can be considerably reduced.

Furthermore, results from the laboratory experiments (2007-2008 as well as 2010-2011) have been used to validate computer simulation models to be used for transient investigation in large wind farm. In this report, therefore, investigations on multiple reflection and refraction as well as impact of transient mitigation methods in large wind parks are performed using the validated models with higher degree of confidence.

Both experiment results and the extended simulation studies confirm voltage transients resulted from interactions of different apparatus and circuits and parameters (electrical, mechanical characteristics) and understanding transient characteristics will be useful for dimensioning related components, insulation coordination of the components within large cable-based systems as well as implementation of the effective mitigation methods.

Sammanfattning

Stora kabelbaserade uppsamlingssystem för vindkraft parker utvecklas globalt. Transienta överspänningar i dessa system uppkommer vid exempelvis spänningssättning och hantering av fel. IEC standard prov av kopplingsapparater tar inte hänsyn till varken kabelkaraktäristik eller fenomenet repetitiva återtändningar. Detta kräver klargörande av transienternas uppkomst och förebyggande samt hur skadliga verkningar kan förhindras.

Detta arbete med benämning ”Högfrekventa transienter i stora vindparker: Avancerade mätningar och karaktärisering” med stöd av Elforsk programmet Vindforsk III, projekt V-326, är en fortsättning på en kabelsystem-transientstudie som utfördes under åren 2007-2008 med stöd av Elforsk programmet Vindforsk II, projekt V-110 [1]. Inom projekt V-110 upprättades ett laboratorium som möjliggör detaljerade studier av typiska apparater i väl definierade kretsar med möjlighet att kontrollera viktiga parametrar. Svåra fall kan testas i laboratoriet vilka annars riskerar skada en anläggning inklusive risk för personskador och extra kostnader.Under pågående projekt V-326 har laboratoriet uppdaterats vidare så att prov kan utföras med elektriska apparater och komponenter för skydd mot överspänningar vid 20 kV driftspänning.

Resultaten från de nya experimenten under V 326 bekräftar den karaktärisering av transienta överspänningar i kabelsystem vilken presenterades under projekt V-110 vid lägre systemspänning.

- Experimenten visar ett konsistent uppträdande av repetitiva för- och återtändningar i kabel system. Förutsättningarna för förekomsten bestäms av den elektriska kretsen och fasvinkeln dvs. ögonblicket för den utförda kopplingen relativt strömmens grundfrekvens, så kallad ”point-on wave switching”.
- Ventilavledare begränsar alltid den maximala överspänningsamplituden i absolut mått, men spänningssteg av storlek motsvarande dubbla skyddsnivån, dvs. från negativ till positiv spännings skyddsnivå.
- Skyddskondensatorer visar skyddande effekt, delvis preventivt genom att starkt reducera antalet återtändningar i sekvens. Skyddet kan också reducera inkommande vågens branthet vid ett objekt, dock beroende på placering och aktuella parametrar.

Vidare har resultat från tidigare laboratorieexperiment 2007-2008 såväl som under 201-2011 använts för att validera datormodeller med syfte att studera spänningstransienter i stora vindparker. Således har multipla reflektioner och refraktion och effekten av skyddsmetoder kunnat studeras och redovisas i denna rapport. Användning av validerade modeller jämfört med mätningar ökar konfidensen för båda.

Resultat från experiment och simuleringar utöver experimenten bekräftar uppkomst av transienter genom samverkan av olika apparater och kretsar i anläggningen. Förståelse av transienternas uppkomst och karaktäristik kan vidare användas för dimensionering av relaterade skyddskomponenter inklusive isolationskoordinering.

Innehåll

1 Introduction

A new laboratory measurement campaign was planned at ABB wind cable laboratory where an advanced investigation and characterization of electrical transient phenomena is done on different cases with realistic interactions between electrical apparatus and power systems.

Quantification methods will be refined for characterizing the transients by taking into account new transient signals as well as transient indicators.

The results will be used as input to the activity within the IEEE and Cigre working groups that may lead to the definition of standards related to transients due to interaction between electrical apparatus and power systems.

1.1 Program motivation

It has been observed that within these recent years, attentions and concerns towards transient issues in wind farms are significantly increasing. This may be due to the fact that offshore wind farm applications (large scale cable systems) are relatively new, yet some failures occurred on components in some wind farms and it has been suspected that this can be due to transient phenomena, especially ones with high rise-of-time and repetitive nature. These attentions and concerns can be noticed by growing activities within IEEE and Cigré with a target of refining standards related to electrical transients in power systems, as well as by many questions addressed by ABB customers on this issue.

On the other hand, the occurrence of high rise-of-time and repetitive transients is determined to a large extent by the electrical circuit. Therefore it is important to identify the different major electrical circuits – i.e. different electrical apparatus and interaction between the apparatus and power systems - and characterize the transients in those circuits. The illustration shown in Figure 1, for instance, should be considered for the different major circuits.

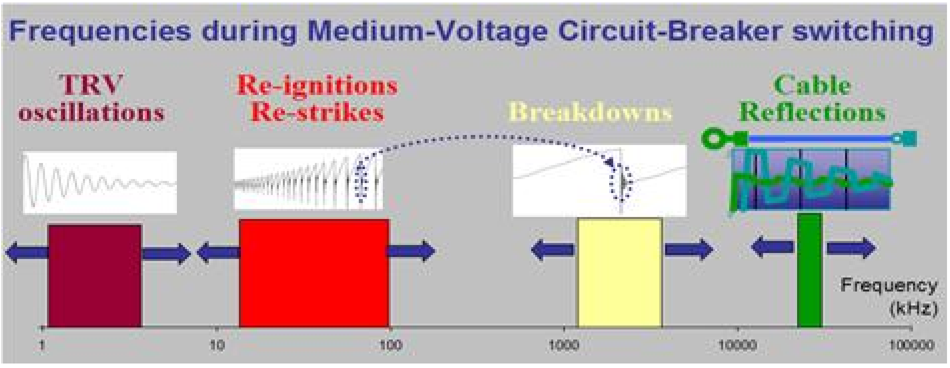

Figure 1 An overview of transient overvoltages caused by switching operations1

1.2 Background

Under the Vindforsk II research framework, a wind cable laboratory has been built at ABB Corporate Research Sweden, in which a measurement campaign has been done to investigate electrical transient phenomena in cable (wind) system [1]. So far, this wind cable laboratory is a unique facility, one of a kind in the world, where a testing facility has included a complete set of electrical apparatus within e.g. a wind cable system, partly with realistic cable length and voltage levels. The illustration of the wind park section reproduced within the ABB wind cable laboratory can be found in Figure 2.

The experiment conducted within the Vindforsk II program has mainly verified the consistent occurrence of repetitive pre-strikes and re-ignitions in a cable system that is determined by the electrical circuit and the point-on-wave of switching operation [1].

As continuation of the project conducted within Vindforsk II, the goal of this project Vindforsk III V-326 is to investigate further based on development done within the project in Vindforsk II program, where a measurement campaign is planned to investigate more realistic operating conditions in a wind park.

[1] Modified from Glinkowski, Electrical Environment of Transformers, Open Workshop, CIGRE JWG 12/13/23.21, http://cigre1.avenda.fr/WG12132321/workshopparis02/FinalPackageR5.ppt slide #61 (no longer available at internet), Paris, August 2002, Reported in prepared by CIGRE JWG A2-A3-B3.21. A similar picture can be found as Fig. 7 www.e cigre.org/Search/download.asp?ID=ELT_218_2.pdf in www.esat.kuleuven.ac.be/electa/publications/fulltexts/pub_954.pdf

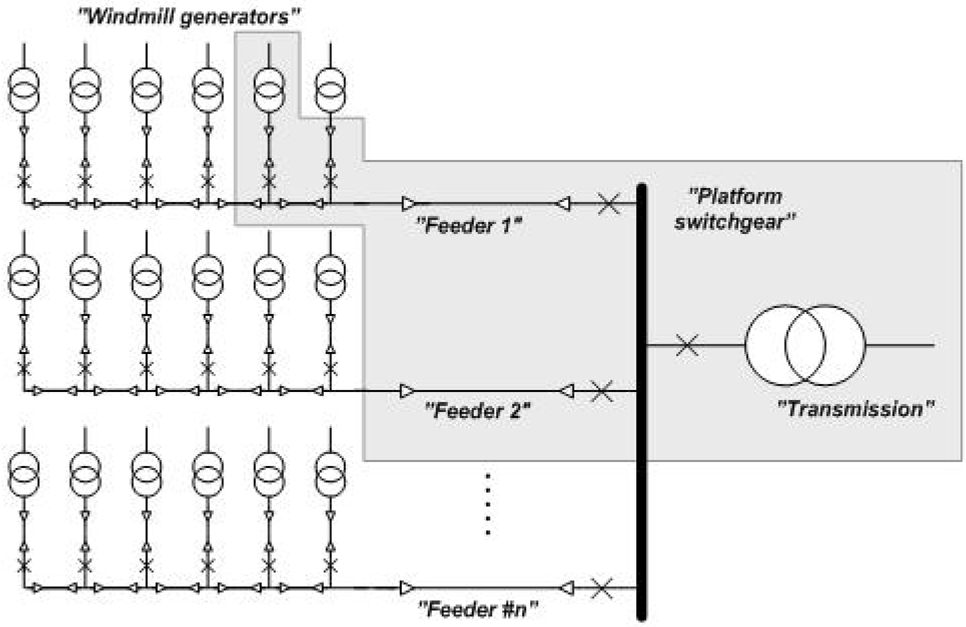

Figure 2 The part of wind park reproduced in the laboratory setup (grayed area)

1.3 Scope of work

This work - High Frequency Transients in Large Wind Farm: Advanced Measurement and Characterization supported by Elfrosk program Vindforsk III, project V-326 - is a continuation of cable system transient study done in 2007-2008 that was also under support of Elforsk program Vindforsk II, project V-110.

The scope of the work includes the following:

- Laboratory experiments with main advancement on the utilization of higher medium voltage level in the cable systems, tests with dry-type transformer, 24 kV vacuum switching device in a ring main unit and different mitigation methods using different protection levels of surge arresters and RC-protection.
- Validation of computer simulation models with results from the laboratory experiments obtained from both 2007-2008 as well as 2010-2011 experiment campaigns. The models are further used for investigation of transient phenomena in large wind farms, such as multiple reflection and refraction and impact of transient mitigation methods in large wind parks.
- In general, analysis and characterization of transients in cable systems.

1.4 Report structure

This report is structured as follows.

Chapter 2 is problem description. Basic laboratory circuit used throughout the experiment is presented in this Chapter. Main updates within the laboratory status compared to the one used throughout the Vindforsk II, V-110 project [1] are highlighted. The updates mainly focus on the new devices tested in this test campaign, namely ring main unit with vacuum switching device module, dry type transformer, and surge arresters and RC-protection with new setup.

Chapter 3 presents results of transient overvoltages obtained from the new laboratory test campaign and analysis around the results. The transient overvoltages data and corresponding currents are presented in time domain graphs as well as in scattered plots as function of magnitude and rise time for easier observation and comparison to current available standards.

In Chapter 4, validation of models to run in computer simulation PSCAD for transient studies is presented. Using the validated models, investigations on transient phenomena in large wind farm is performed and the results are presented along with the analysis.

In Chapter 5, phenomena of transients in large wind farms are investigated, namely multiple reflection and refraction in wind cable systems and transient characteristics due to switching operation of breaker in large wind farms. Investigation is performed by means of computer simulation models which are validated using laboratory experimental data. Simulations are further focused on the use of different choke concepts to mitigate transient in large wind farms. A transient characterization method is also proposed as tool to assess effectiveness of the mitigation methods.

Chapter 6 concludes the report and suggests some future works.

2 Problem description

2.1 Introduction

Lightning was for many years considered to be the only phenomenon that could create pulses with very steep fronts in the order of micro seconds (μs). If the traveling time of the wave pulses across the transmission line is longer than the rise time of the pulse itself, the wave pulses can be rejected off junctions at cable ends, consequently producing high overvoltages. Usually surge arresters are used for insulation coordination i.e. to control the voltage level of the overvoltages safely below the level that is considered to be harmful for insulation of equipment.

With the surge arrester protection the equipment failures were kept on an acceptable level. However, insulation failures of the equipment that was not exposed to such high overvoltages increasingly occurred with the introduction of some new technologies into the power systems. Insulation failures in dry-type transformers and inductors as well as motor windings appeared to increase, occasionally also cable terminations. The failure rate of the motor drives increased significantly with the introduction of the inverters in inverter fed drives systems. These inverters were built using switching devices that produce voltage pulses of a very short rise time. The pulse-width modulated (PWM) inverters built using fast switching insulated gate bipolar transistors (IGBT's) produce voltage pulses with a rise time as low as 0.1(μs), and even shorter [2]. This is more than ten times quicker than the rise time of a lightning pulse. The fast switching IGBT's were mainly used due to two major advantages over other switching devices, the switching losses and the total harmonic distortion (THD) are reduced significantly. Furthermore, breakers and interrupters create as well switching transients during their operation. The vacuum interruption technique used in modern breakers improved interruption and dielectric recovery characteristics of breakers [3]. The main advantage of vacuum circuit breakers are good durability and low maintenance costs. Vacuum circuit breakers provide the best breaker solution for medium voltage below 24 kV [4]. However, it was reported in many publications that many transformer failures may have occurred due to switching operations of VCBs, although the transformers have previously passed all the standard tests and complied to all quality requirements [5]-[9].

Furthermore, another study showed that it is not only the vacuum breaker that can create surges potentially dangerous to the transformers. Another new interruption technique that uses SF6 gas can create dangerous transient voltages as well [10]. Furthermore, the breakdown in SF6 medium can have a typical rise time between 2-20ns. Hartford Steam Boiler performed a 10 years long study in an investigation of failures of thousands of transformers. The study showed that the major cause of transformer failures is high frequency transients [11]. According to this study, the transformer failures caused by the high frequency transients reach a level of 33.9%. This makes the high frequency transients the most likely cause of a transformer insulation failure [11]Although, some studies claim that the direct proof of the negative impact of the high frequency transients on the transformer insulation is not yet found [10] some other studies give description of the phenomenon that produces very high overvoltages internally in the transformer winding[5],[12] that could possibly lead to an insulation failure during high frequency transients. Moreover, some studies for induction motors showed that the appearance of repetitive strikes is dangerous for the induction motors[12], [13]. It is very likely that the same phenomenon can be dangerous also for the insulation of dry-type transformers and reactors. A major problem with the dry-type transformer insulation failures occurred in the early wind parks (WP). In some of these WPs almost all the transformers had to be replaced with new ones due to the insulation failure [14], [15]. It is suspected that the breakers during regular switching operations caused these insulation failures.

Oil-filled transformers are also not failure-free in this aspect. Dry-type transformers due to its lower equivalent capacity to ground can suffer higher voltage surges, but on the other hand they have the following advantages:

- For the voltage stress between the HV-LV gap, most of it is withstood by the air, which is continuously renewed. On the contrary, in an oil-filled transformer, if the oil suffers ageing it remains inside the tank. In a dry-type transformer the solid insulation between HV-LV withstands a really low part of the total voltage, while in an oil-filled one it can withstand a significant part of the stress.
- For the voltage stress between different sections inside the HV winding, although the combination of epoxy with nets withstand less voltage than the combination of oil with solid material. Dry-type transformers have very low stress (1 kV/cm and less) to compensate this.

The problem of high frequency transients can be related to all types of breakers in principle. Some studies of insulation failures of motors caused by switching phenomenon showed that the surges generated while operating air magnetic circuit breakers can be similar to those of a vacuum devices[16]-[18]. One study shows that surges generated by air magnetic circuit breakers appear as 4,4 pu in magnitude and with rise times in the order of 0,2 µs. In the same case the vacuum breaker generated surges appear with 4,6 pu magnitude and a longer rise time of 0,6µs[16]. An important finding of this study is that although the vacuum breaker generates more surges in one burst, , surges generated by these two types of breakers have a similar typical magnitude and rise time[16].

Another important factor that contributed to the failures during the switching operations of IGBT's and VCB's is that in both low and medium voltage systems cables are used. A very small characteristic impedance of cables, which can be ten times lower than the characteristic impedance of transmission lines, results in a ten times shorter rise time of the transient overvoltage (TOV). For that reason, the wave reflection phenomenon is notable even at a 50 m long cable. Consequently the high frequent magnitudes with considerable magnitudes may not have been taken into account in design and validation of some components

2.2 Laboratory Setup

Figure 3 shows the single line diagram of ABB wind cable laboratory.

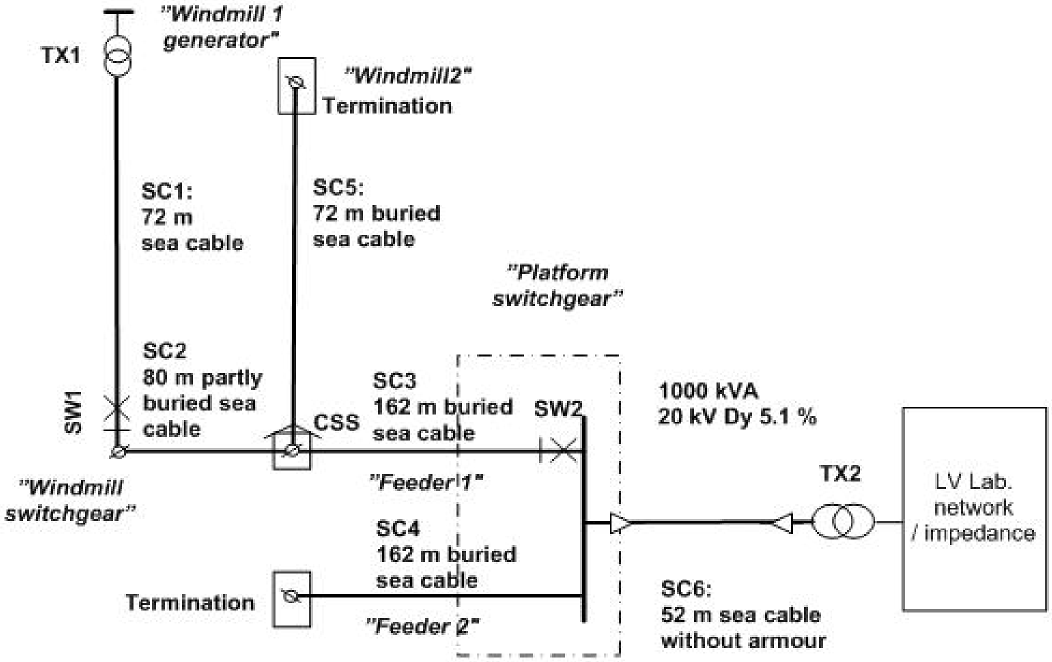

Figure 3 ABB wind cable laboratory system line diagram

2.3 Update laboratory status from Vindforsk II

Laboratory circuit used in Vindforsk III wasfurther developed from the circuit used in Vindforsk II so that details of the following components, namely: Cables 240 mm^2, Oil-type transformer installed at TX2, Platform switchgear, compact substation (CSS), inductive load, surge arrester blocks, control, measuring and recording devices can be found in[1]. The improvements of laboratory circuit done in Vindforsk are listed here as follows.

2.3.1 Ring main unit with vacuum switching device module

The switching device used throughout the tests is a vacuum module of ring main unit / compact switchgear rated at 24 kV with the installation in the laboratory setup shown in Figure 4 and technical data listed in Figure 5[1].

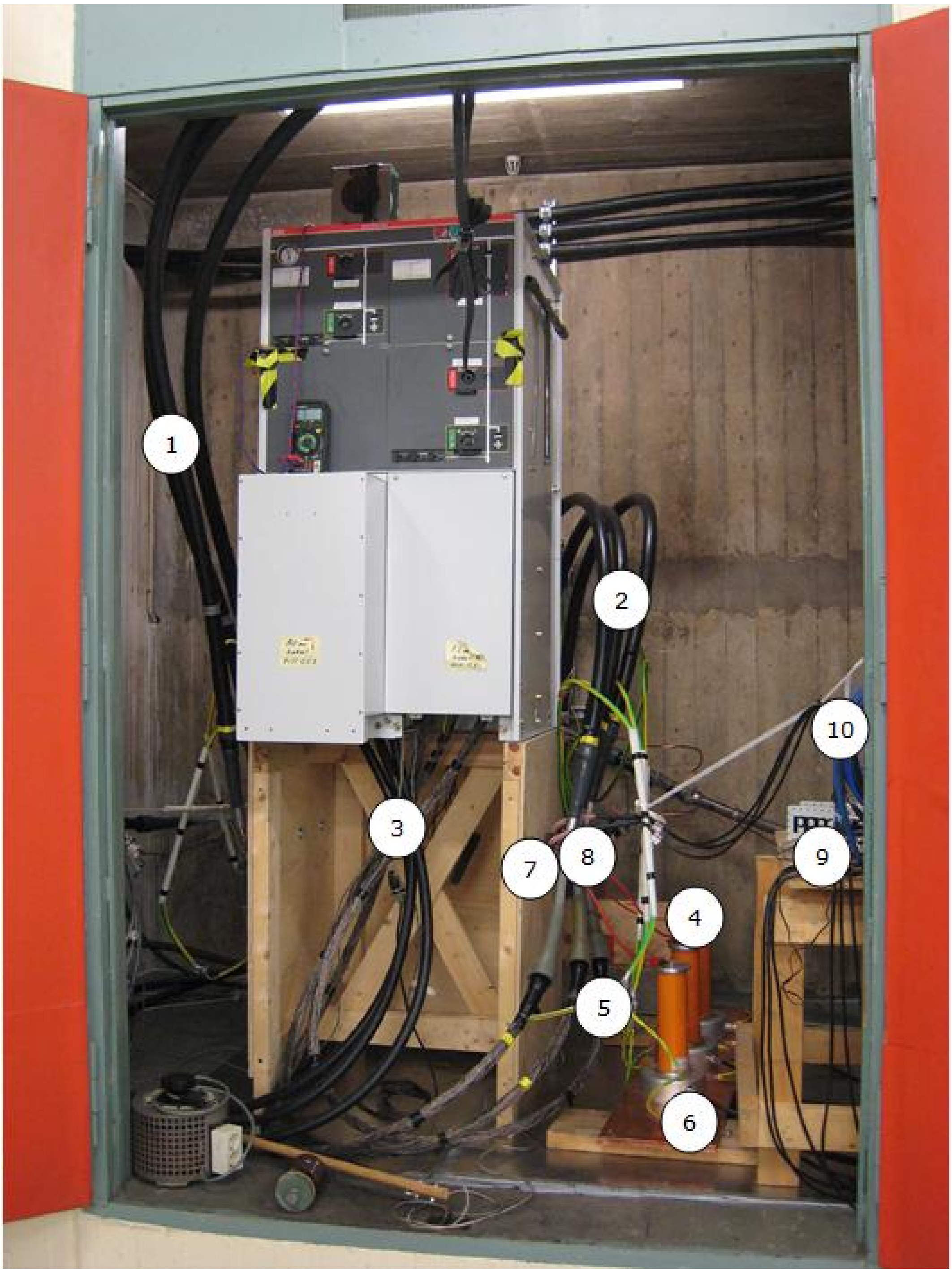

Figure 4 Ring main unit with switching device module used throughout tests: (1) "Feeder" cables, (2) Cables to "nacelle", (3) Joint cables to elbow connectors, (4) Voltage dividers, (5) Cable shield common point connected to copper earth plane, (6) Copper earth plane, (7) Bushings, (8) Current measurement device, (9) transmitter, (10) Fiber optics

SafeRing		V-module		F-module	
		Vacuum circuit breaker	Earthing switch	Switch fuse	Downstream earthing switch
Rated voltage	kV	12/17,5/24	12/17,5/24	12/17,5/24	12//17,5/24
Power frequency withstand voltage	kV	28/38/50	28/38/50	28/38/50	28/38/50
Impuls withstand voltage	kV	95/95/125	95/95/125	95/95/125	95/95/125
Rated current	A	200/200/200		see[1]	
Breaking capacities:					
active load	A				
closed loop	A				
off load cable charging	A				
of load transformer	A			20/20/20	
earth fault	A				
earth fault cable charging	A				
short circuit breaking current	kA	21/16/16		see[2]	
Making capacity	kA	52,5/40/40	52,5/40/40	see[2]	12,5/12,5/12,5
Short time current 1 sec.	kA	21/16/16			5/5/5
Short time current 3 sec.	kA		21/16/16		

Figure 5 Technical data of switching device

2.3.2 Dry type transformer

A dry type transformer rated at 20 kV was used throughout the laboratory tests, representing transformer TX1 in Figure 3. Figure 6 and Figure 7 show the installation of the transformer in the laboratory setup and Figure 8 shows the technical specification. A remark should be made that installation shown in Figure 7 is the installation where inductive load is connected and RC-protection mitigation devices are installed.

Figure 6 Dry trype transformer used in laboratory test (during preparation):
(1) Transformer

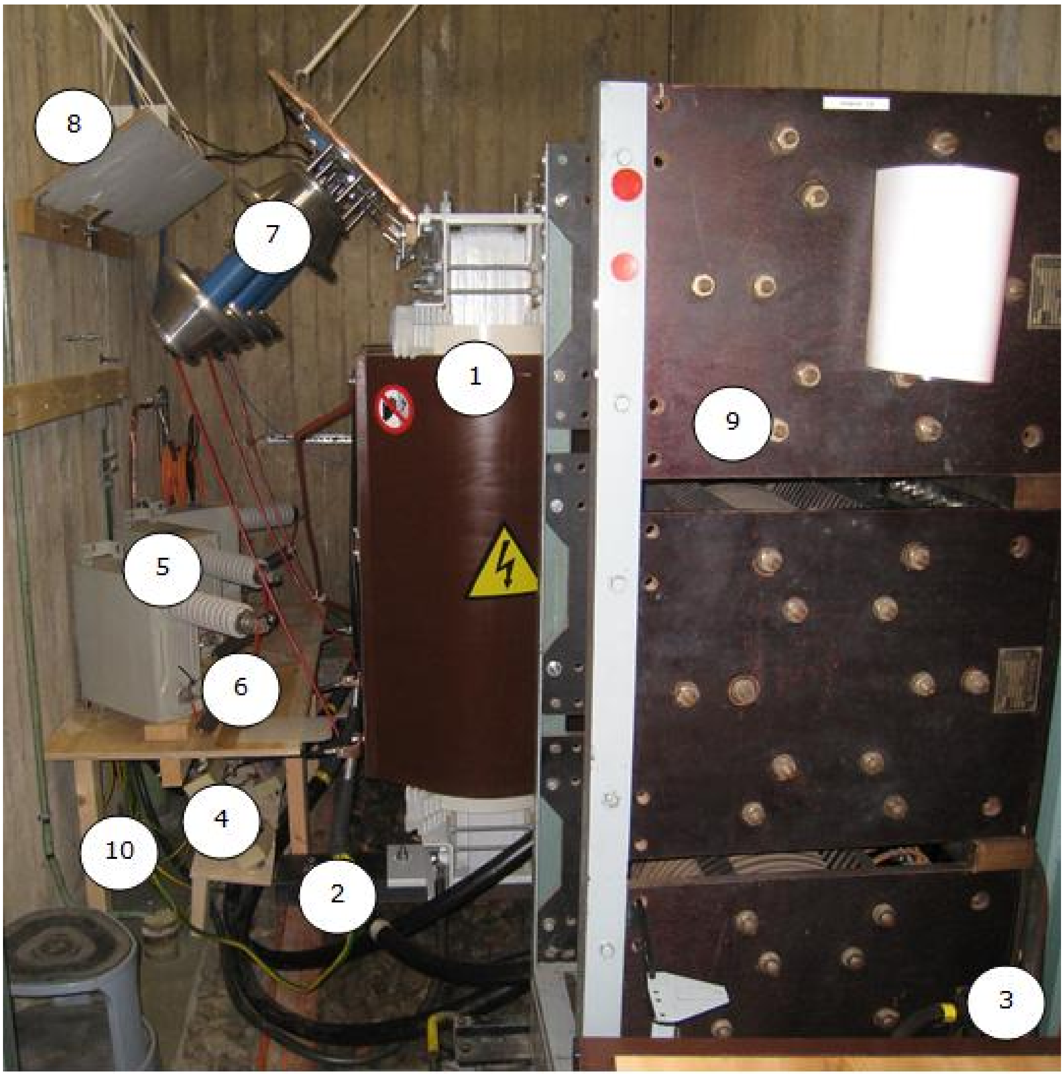

Figure 7 Dry type transformer installation during laboratory test preparation: (1) Transformer, (2) Cables toward collection grid (3) Cables towards load/generator, (4) Surge arresters, (5) Surge capacitors, (6) Resistors, (7) Voltage dividers, (8) Transmitter, (9) Inductive load, (10) Cable shield common point. Note: the reference ground for the voltage measurements is the transformer core/frame

2. GENERAL CHARACTERISTICS		
Description:	dry type transformer	
Type designation:	DTE-900/24	
Rated power:	900	kVA
Frequency:	50	Hz
Number of phases:	3	
Vector group:	Dyn11	
Cooling method:	AN	
Location:	indoor	
Standars:	IEC 60726	
3. HIGH VOLTAGE		
Voltage:	20000	V
Tap-changer (off-circuit):	±2.5±5	%
Manufacturing type:	encapsulated	
Material:	aluminum	
Insulation level:	24	kV
Rated power frequency withstand voltage:	50	kV
Rated lightning impulse withstand voltage (1.2/50 μs):	95	kV
4. LOW VOLTAGE		
Voltage:	690	V
Manufacturing type:	impregnated	
Material:	aluminum	
Insulation level:	1.1	kV
Rated power frequency withstand voltage:	3	kV
Rated lightning impulse withstand voltage (1.2/50 μs):	n.a.	kV

Figure 8 Technical specification of dry type transformer

2.3.3 Transient mitigation devices

Several transient mitigation devices were tested in this test campaign, namely: surge arresters and RC-protection. Two protection levels of surge arresters were used - in different cases - which are: 42 kV (3 x 14 kV blocks) as shown in Figure 9 and 56 kV (4 x 14 kV blocks) as shown in Figure 10 and Figure 13 (installation within the electrical diagram of laboratory setup). A case with RC protection was also tested with the following details:

- RC-protections of 3 x 20 Ohms and 3 x 83 nF are installed at terminals of dry transformer TX1 (Figure 11 and Figure 14), while at the same time
- RC-protections of 3 x 30 Ohms and 3 x 130 nF are installed at terminals of transformer TX2 (Figure 12 and Figure 14).

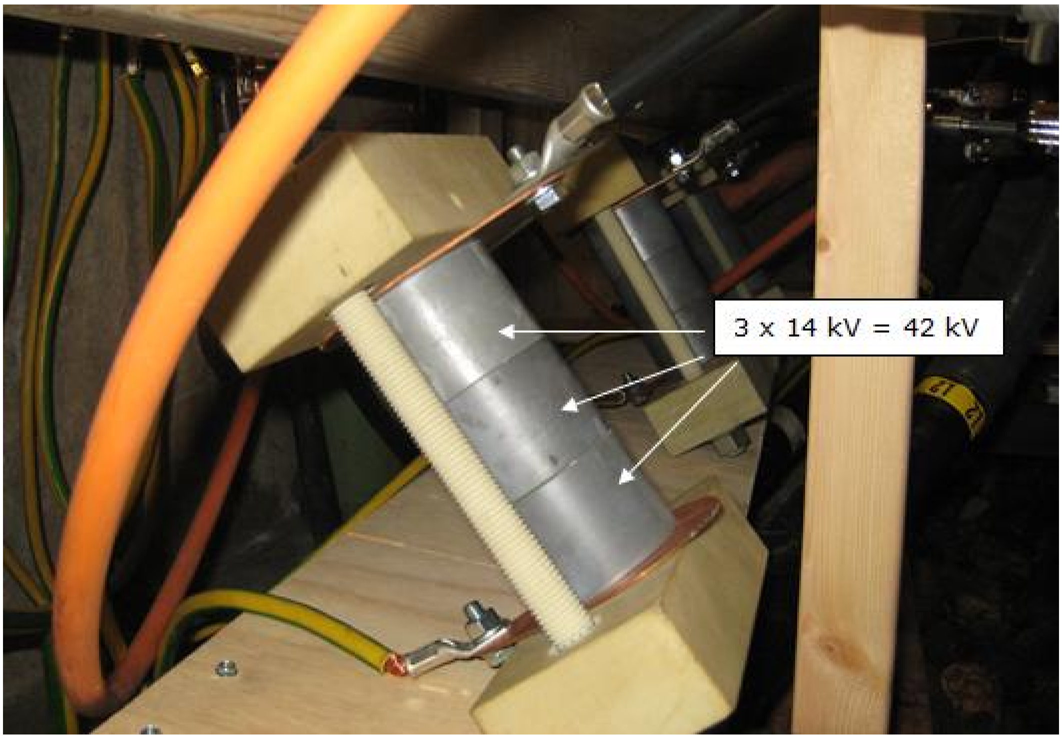

Figure 9 Surge arresters installed at terminals of transformer T1 with 42 kV protection level (3 x 14 kV)

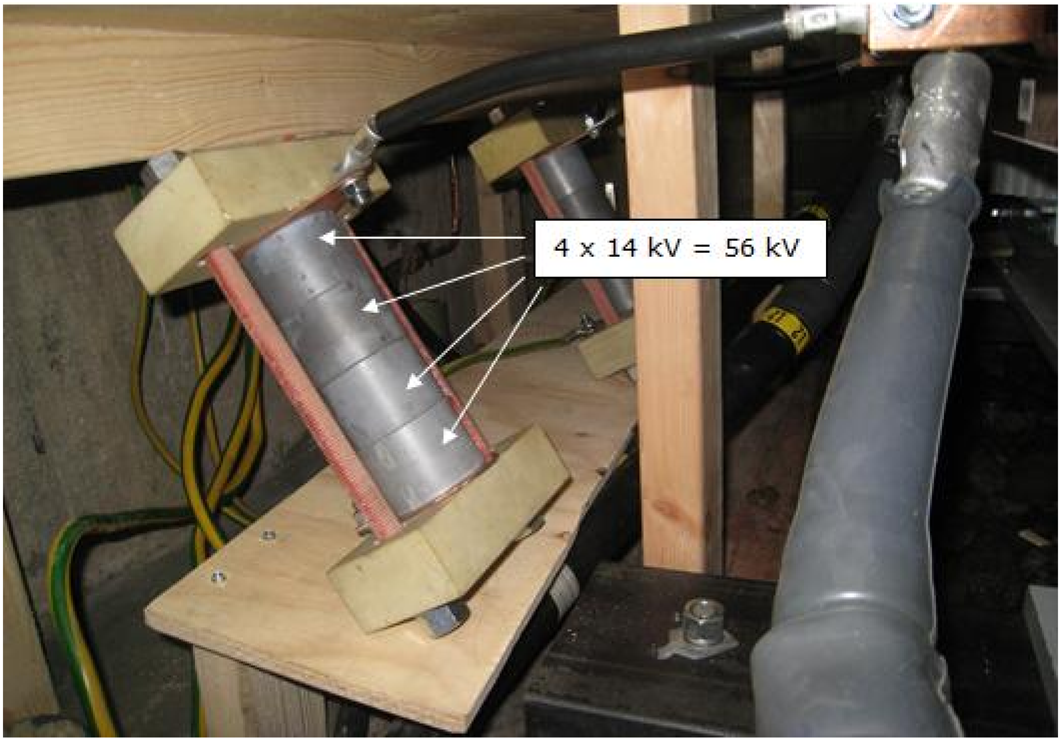

Figure 10 Surge arresters installed at terminals of transformer T1 with 56 kV protection level (4 x 14 kV)

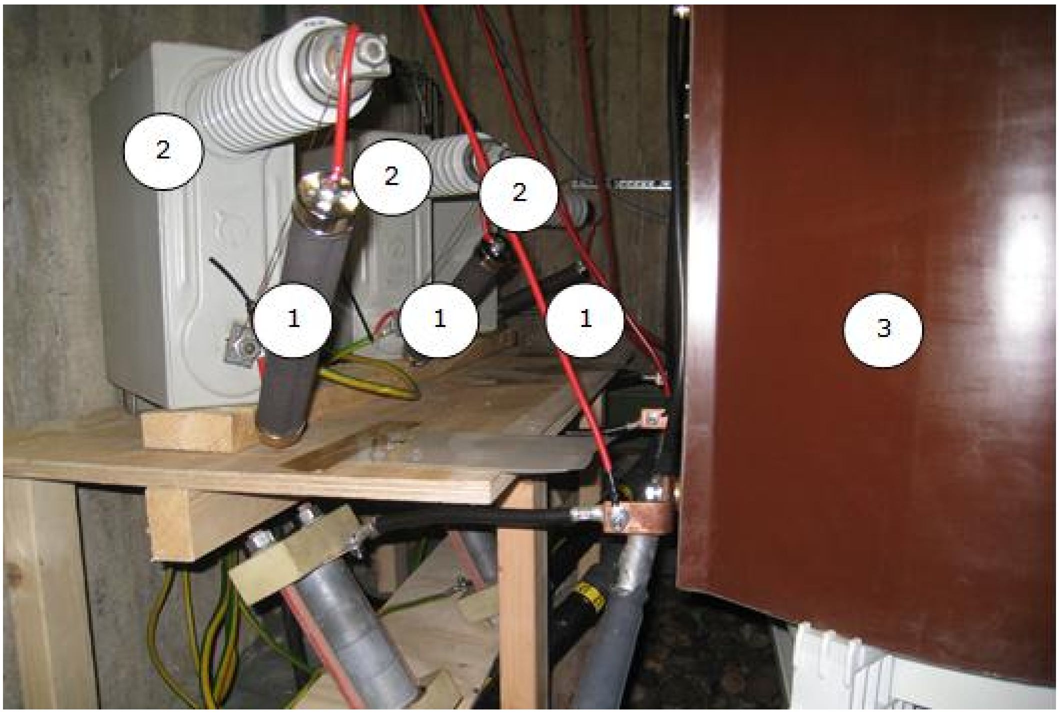

Figure 11 RC-protections of 3 x 20 Ohm resistors (1) and 3 x 83 nF surge capacitors (2) are installed at terminals of dry transformer TX1 (3)

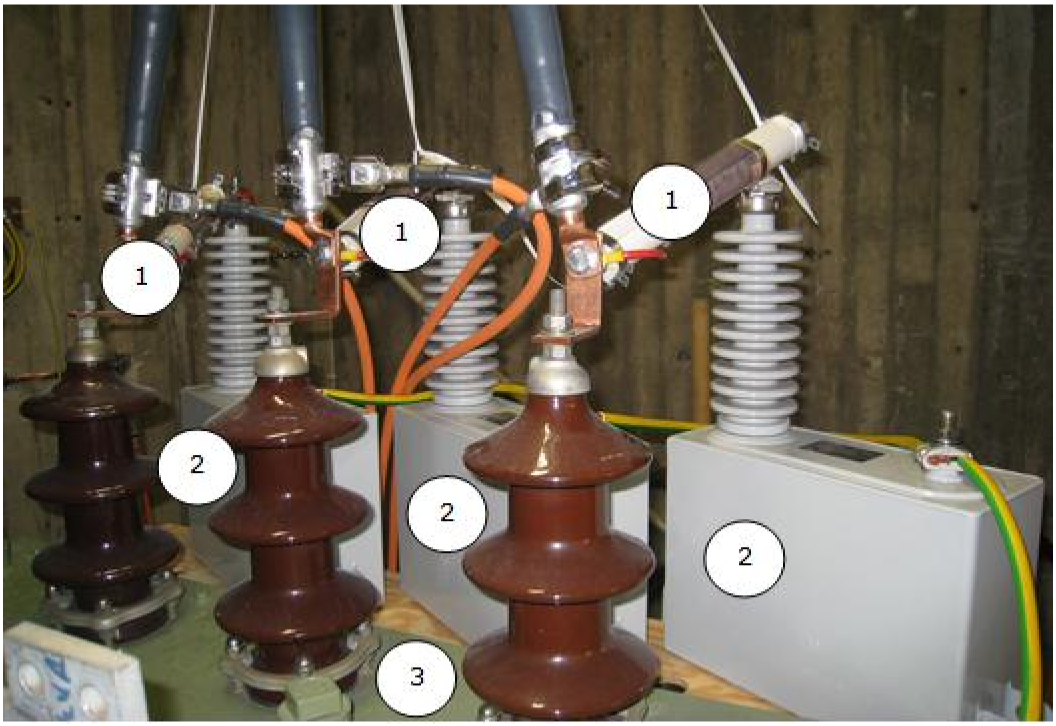

Figure 12 RC-protections of 3 x 30 Ohm resistors (1) and 3 x 130 nF surge capacitors (2) are installed at terminals of transformer TX2 (3)

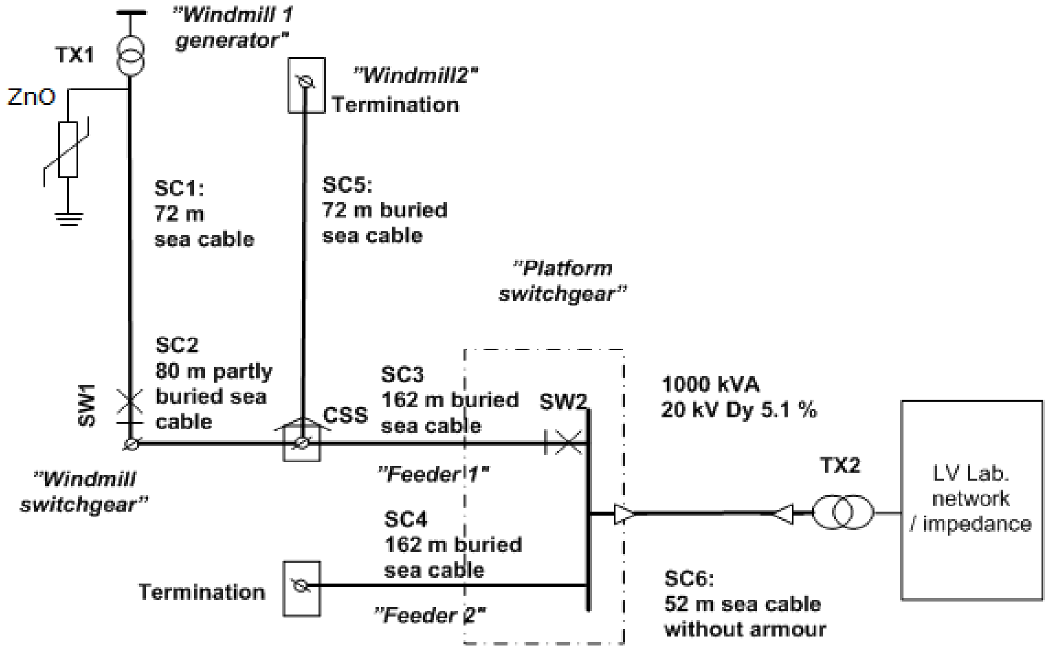

Figure 13 Surge arresters installations

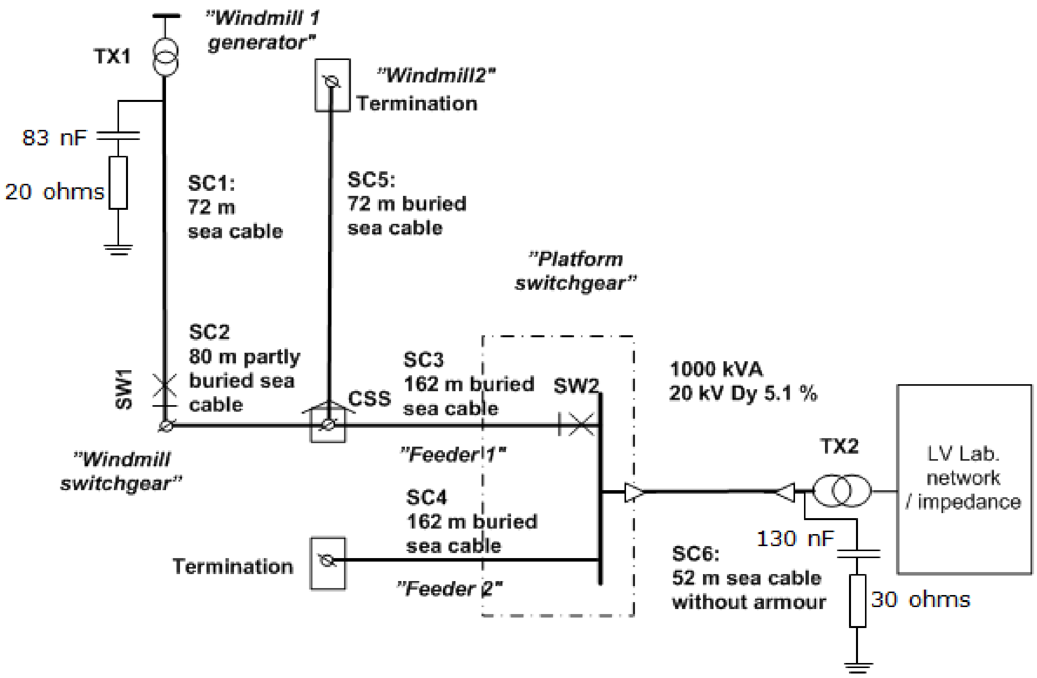

Figure 14 RC protections installations (surge arresters are also installed in this case that RC-protections are installed, however for better visibility the surge arresters are not drawn)

3 Experimental results and analysis

3.1 List of cases

Experiments presented in this chapter are conducted during Vindforsk III project. This project included various experiments with different layouts, surge arrester levels, loads and mitigation devices. Two different layouts have been used in experiments. Layout 1 includes all cables and equipment shown in Figure 14. Layout 2 has lines SC4 and SC5 disconnected. The surge arresters are installed as shown in Figure 13. All the cases except the last four are performed with three ZnO surge arresters, where the voltage is clamped at about 30 kV. The last four cases are done with four ZnO arresters where the voltage is clamped at about 40 kV. The last two cases are performed in order to make a comparison with some results obtained in Vindforsk II. The last two cases are only simulated. The experiment with a 17mH load could not have been performed due to a high current in the inductor. A 17mH load is used in order to obtain the same current level through the breaker as it was in the Vindforsk II project.

Table 1: List of cases

Case ID	Loading	Circuit Breaker Operation	Layout	Arrester Status	Protection
1.1a	No load	Closing	2	3ZnO	
1.1b	No load	Opening	2	3ZnO	
1.3a	No load	Closing	1	3ZnO	RC
1.3a	No load	Opening	1	3ZnO	RC
1.4a	inductive - 94mH	Closing	1	3ZnO	RC
1.4b	inductive - 94mH	Opening	1	3ZnO	RC
1.5a	inductive - 94mH	Closing	2	3ZnO	
1.5b	inductive - 94mH	Opening	2	3ZnO	
1.5.3a	inductive - 94mH	Closing	1	3ZnO	
1.5.3b	inductive - 94mH	Opening	1	3ZnO	
1.5.3ax	inductive - 94mH	Closing	1	4ZnO	
1.5.3bx	inductive - 94mH	Opening	1	4ZnO	
1.5.4cx (simulation)	inductive - 17mH	Opening	1	4ZnO	

3.2 Breaker rate of rise of dielectric strength

Transient overvoltages caused by circuit breaker opening were studied under full load conditions. The full load condition was performed both experimentally and in simulations by connecting an inductor with a 94mH inductance on the high-voltage side of the transformer TX1.
The breaker used in the Vindforsk III is placed in a ring main unit (RMU) and differs significantly from the breaker (VCB) used in the Vindforsk II project. The new breaker is designed for operation at 20kV, and its rate of rise of dielectric strength (RRDS) is much faster compared with the previously used 10kV breaker. A comparison between the RMU and the VCB is presented in Figure 15.

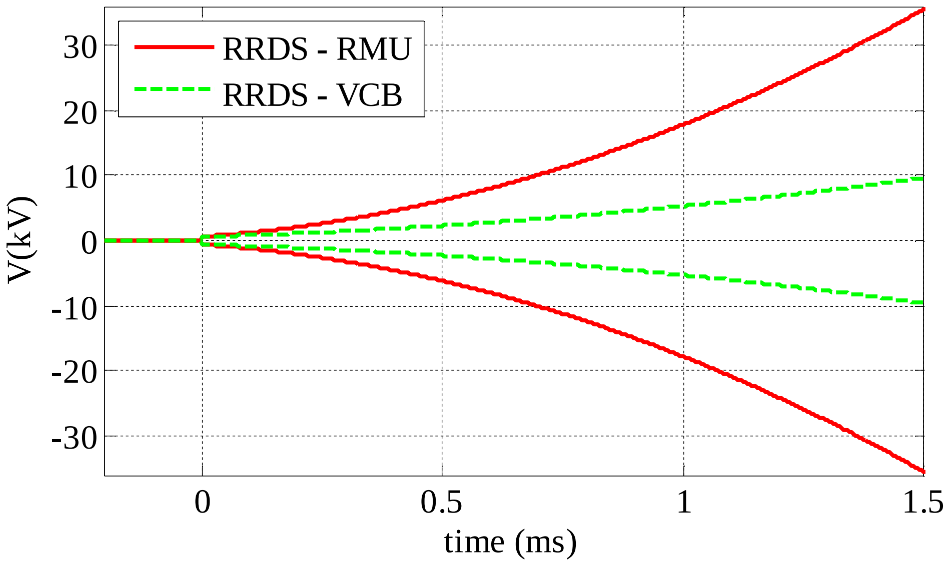

Figure 15 Comparison of rate of rise of dielectric strength (RRDS)

3.2.1 No-load case, layout 2 without RC protection

The no-load case without any protection is performed in the layout with disconnected SC4 and SC5 cables. This is the same cable setup as it was used in the Vindforsk II project.

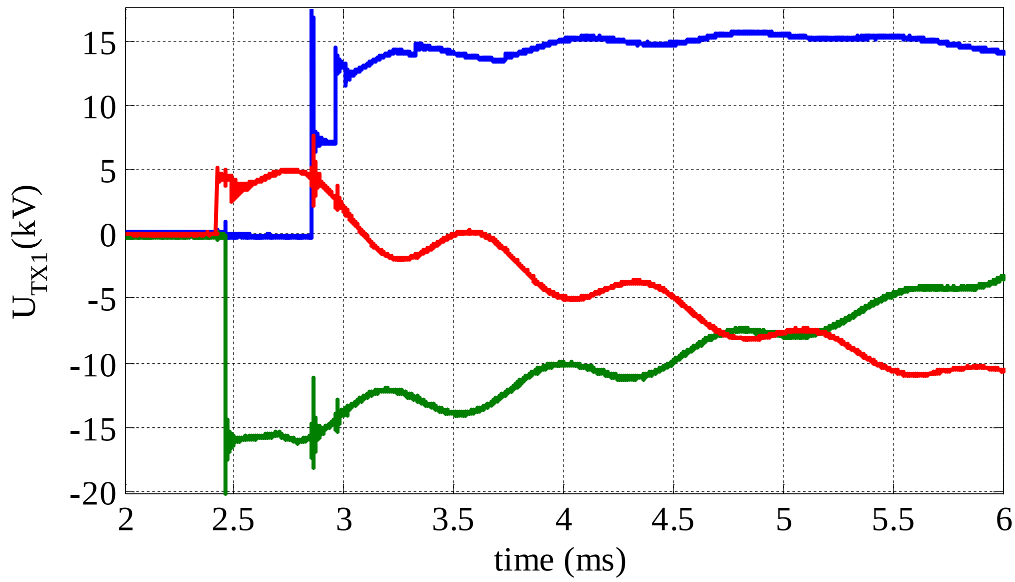

Figure 16 Voltage at transformer TX1 - no-load, layout 2, closing

Figure 16 shows the voltage at transformer TX1 recorded during the closing transient. This plot shows three prestrikes with a voltage magnitude of about 1pu. The magnitude of the strikes is comparable to magnitudes of the voltage strikes recorded in the Vindforsk II project test setup. However, the rise time of the strikes is much shorter compared to strikes obtained with an oil insulated transformer.

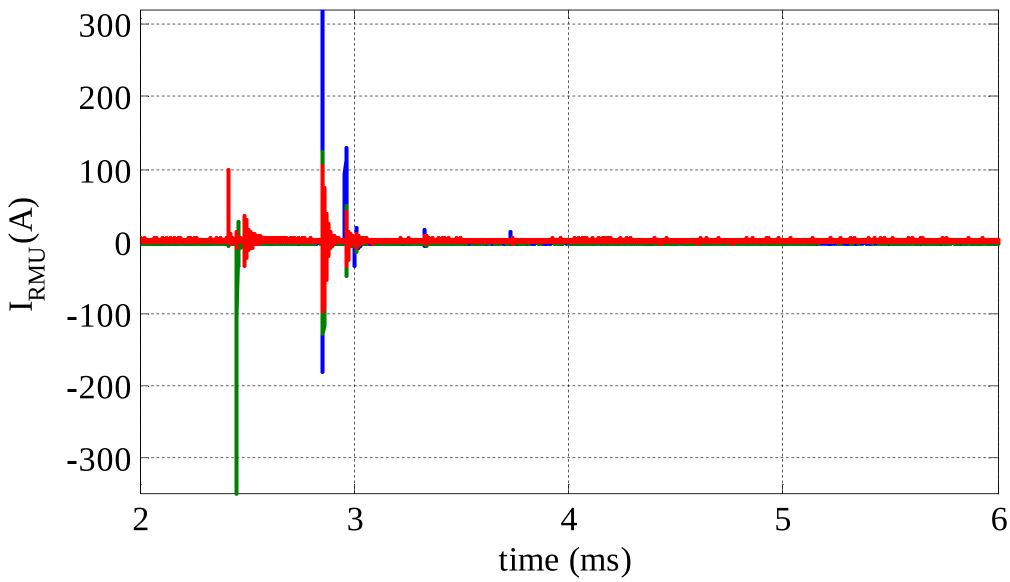

Figure 17 Current through RMU - no-load, layout 2, closing

Figure 17 presents the current through the RMU during a closing operation of the breaker. A current burst appears at each voltage strike.

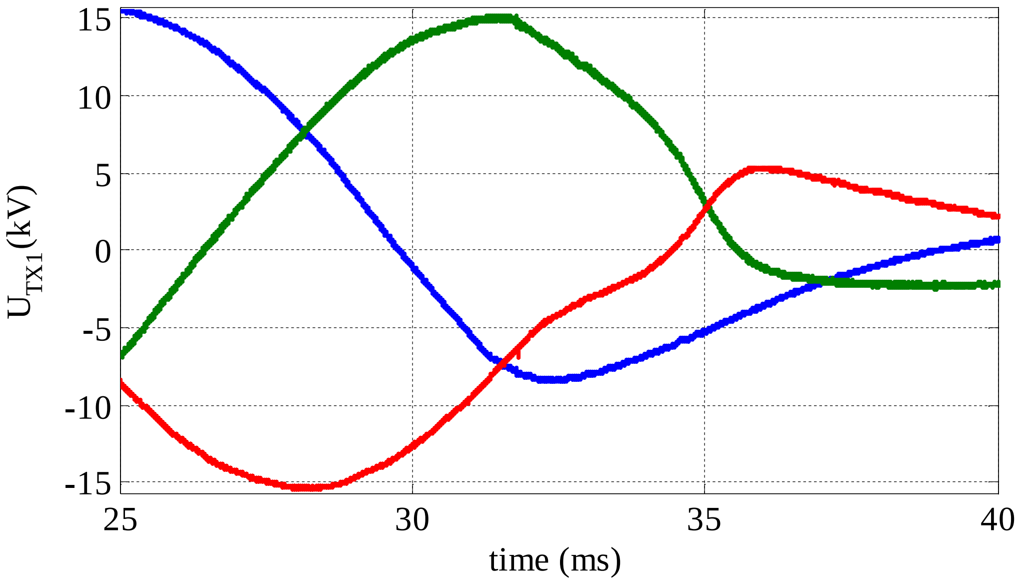

Figure 18 Voltage at transformer TX1 - no-load, layout 2, opening

Figure 18 shows the voltage at transformer TX1 during the breaker opening transient. Since a very low current is interrupted, the transient recovery voltage is too slow to reach the dielectric strength of the gap of the breaker. Therefore, no restrikes are recorded. This is quite opposite to what was recorded with the oil insulated transformer and a slower vacuum breaker during the Vindforsk II project. Due to a slower breaker, a few restrikes of a low magnitude were recorded.

3.2.2 No-load case, layout 1 with RC protection

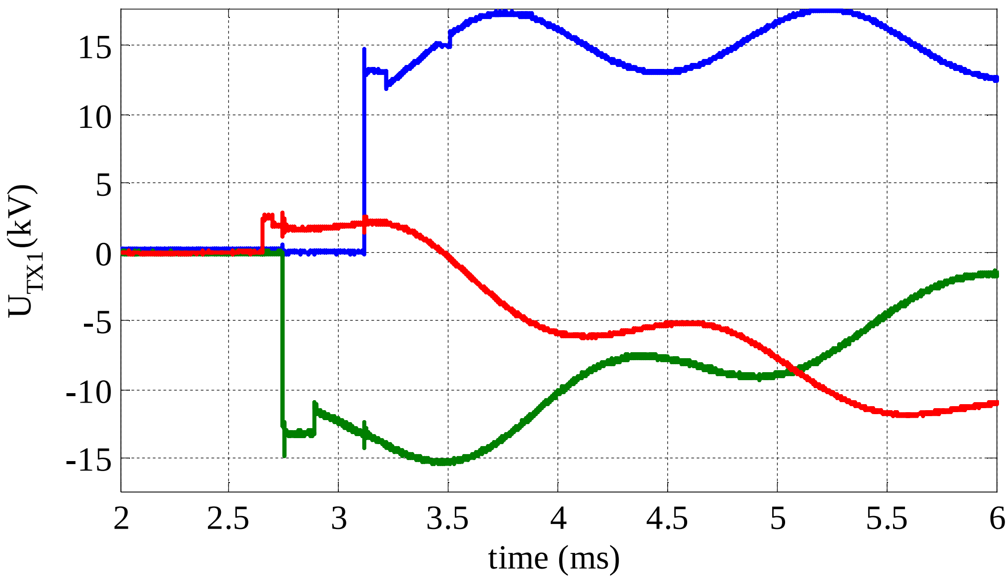

Figure 19 Voltage at transformer TX1 - no-load, layout 1, RC protection, closing

Figure 19 shows the voltage transient during the breaker closing. In this setup, the full cable layout is used (layout 1) with RC protection at transformers TX1 and TX2. Due to RC protection, oscillations after prestrikes are damped quite quickly. The magnitude of the voltage strikes is at the same level as in the previous case, while the rise time is increased.

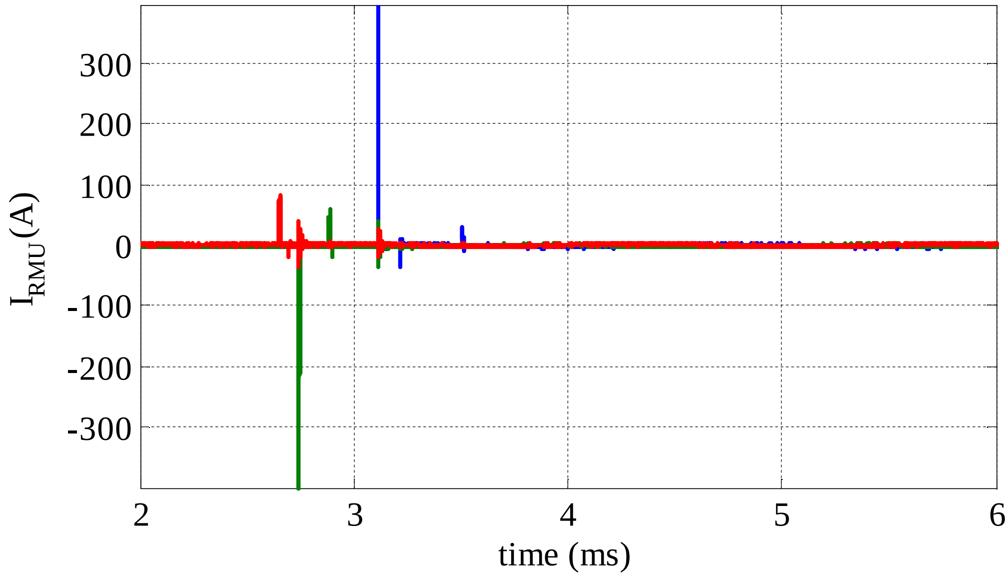

Figure 20 Current through RMU - no-load, layout 1, RC protection, closing

The current bursts presented in Figure 20 are very similar to the previous case. Current peaks are about 400A. The significant difference is that the current oscillations are damped quite quickly.

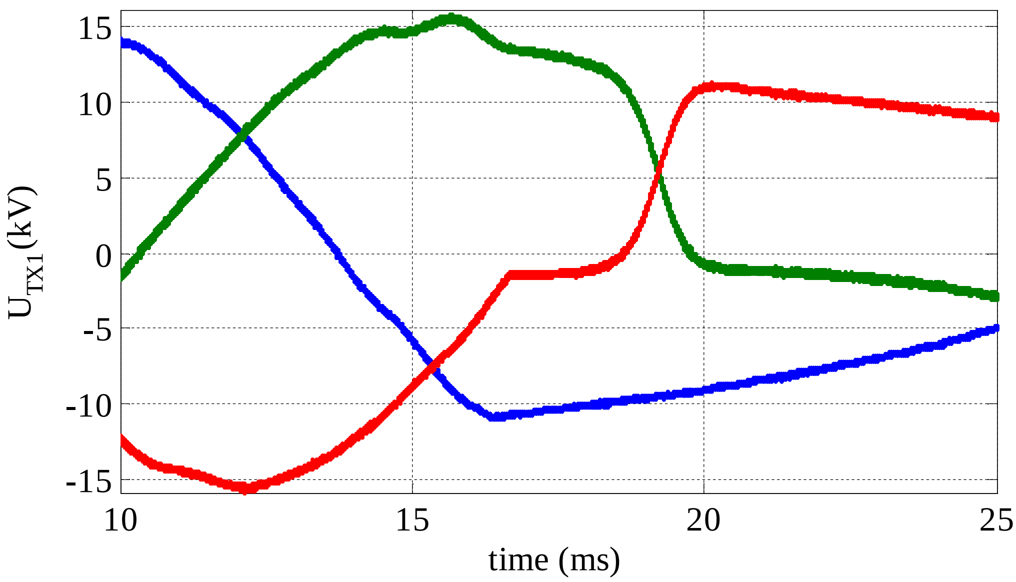

Figure 21 Voltage at transformer TX1 - no-load, layout 1, RC protection, opening

Similarly to the previous case, no restrikes are observed in Figure 21. This is due to a low current and a quicker breaker. A low di/dt gives a slow rise to the recovery voltage that simply can't reach the breakdown level of the gap between the contacts of the breaker.

3.2.3 Inductive load case (94mH), layout 1 with RC protection

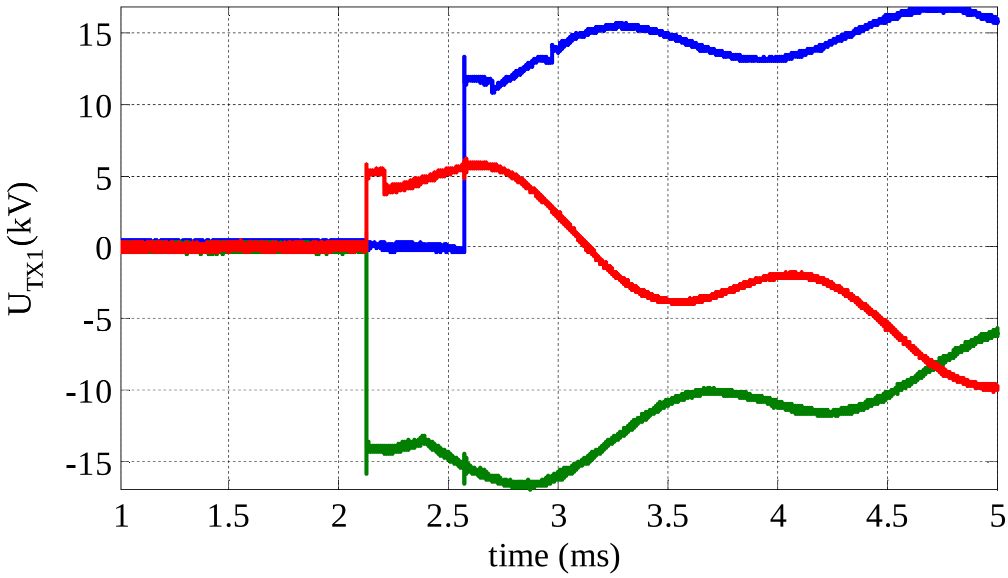

Figure 22 Voltage at transformer TX1 - inductor 94mH, layout 1, RC protection, closing

Figure 22 shows a voltage transient during the closing operation of the breaker. Voltage strikes of a low magnitude are recorded. The response looks almost identical to the response recorded without any load and with the RC protection.

Although the load is added in the setup the connection transients didn't change. An identical test during the Vindforsk II project produced somewhat different results. Although the initial prestrikes are similar, the oil insulated transformer with the slower vacuum breaker used in the Vindforsk II produced even some additional restrikes during the bouncing of the breaker's contacts.

Figure 23 presents current transients during the same switching event. A current of about 400 A is obtained. As it was shown in the previous case with the RC protection, the current is interrupted at the first zero crossing and the current oscillations are damped very well.

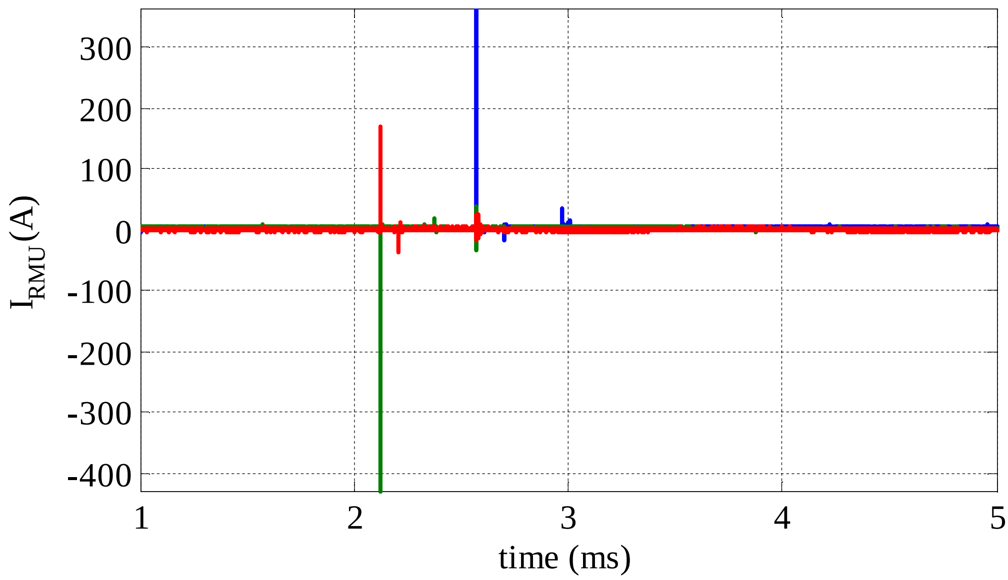

Figure 23 Current through RMU - inductor 94mH, layout 1, RC protection, closing

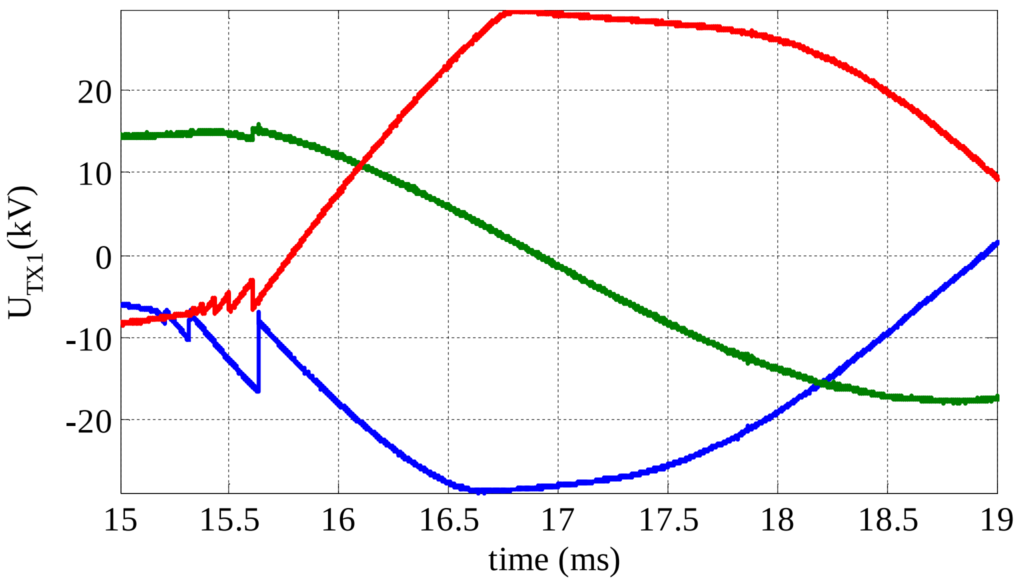

Figure 24 Voltage at transformer TX1 - inductor 94mH, layout 1, RC protection, opening

Figure 24 shows voltage restrikes recorded at transformer TX1 during the breaker opening operation. In this case, an RC protection is used. Only a few restrikes are recorded during this event. The main reason for this is a low current that is interrupted during the switching. The peak current for a load of 94mH is about 3.5A, which is a chopping current level. Due to a low current, the current is chopped at the very instant when the contacts start to separate. Consequently, the current is chopped at a lower level, which gives a slower rise of the transient recovery voltage than the worst case scenario.

Furthermore, the RC protection prevents wave reflections and damps high frequency oscillations that appear after strikes. As shown in Vindforsk II, this significantly reduces the number of restrikes.

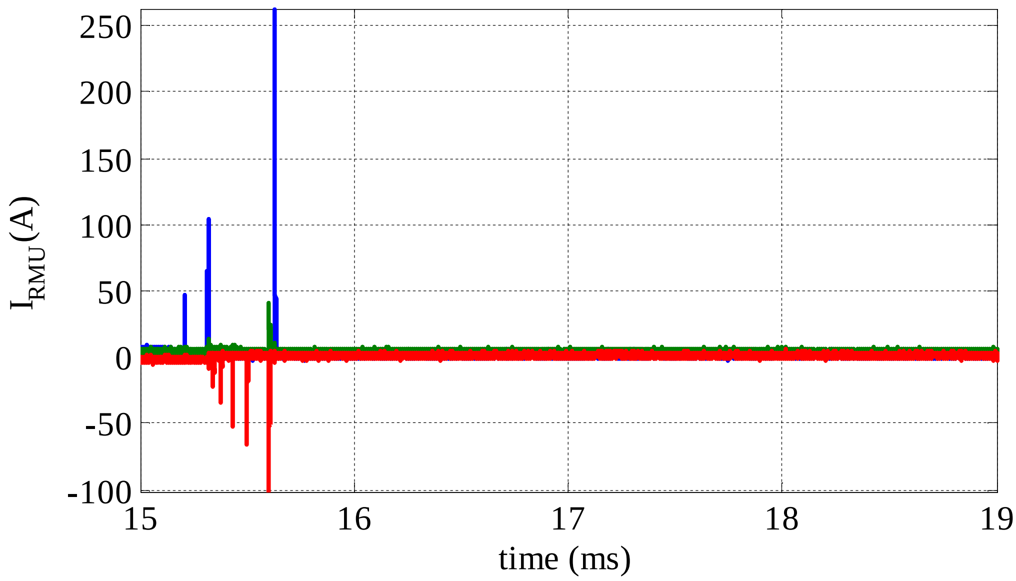

Figure 25 Current through RMU - inductor 94mH, layout 1, RC protection, closing

Current transient during the same switching event is observed in Figure 25. The current magnitude is directly proportional to the magnitude of the breakdown voltage. Therefore, the magnitude is somewhat lower than in the cases of breaker closing. The RC protection prevents current oscillations and only single current spikes are recorded.

3.2.4 Inductive load case (94mH), layout 2 without RC protection

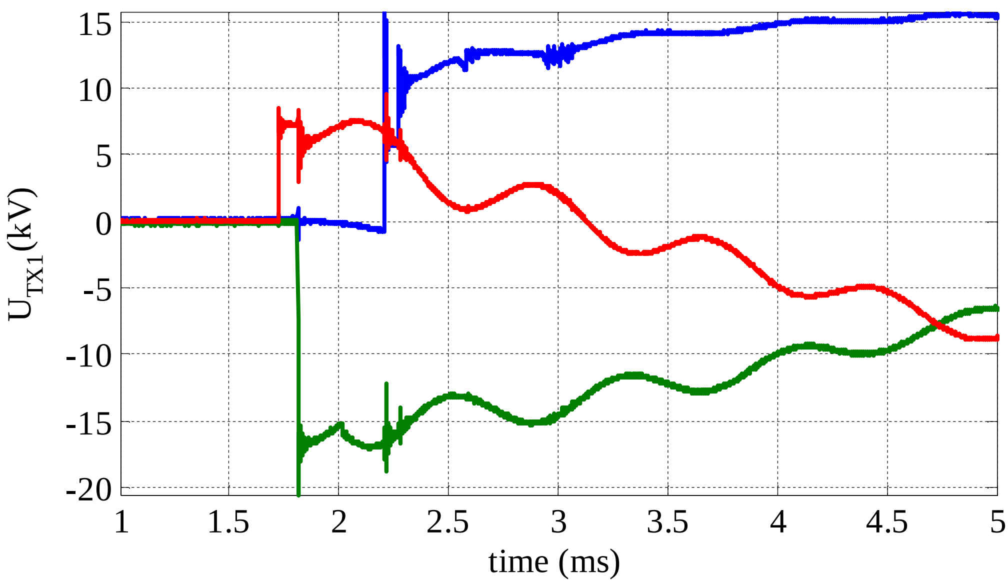

Figure 26 Voltage at transformer TX1 - inductor 94mH, layout 2, closing

Figure 26 shows another voltage transient during closing of the breaker. Prestrikes are recorded in each phase. The obtained results are similar with other cases without RC protection. Oscillations are observed after each strike.

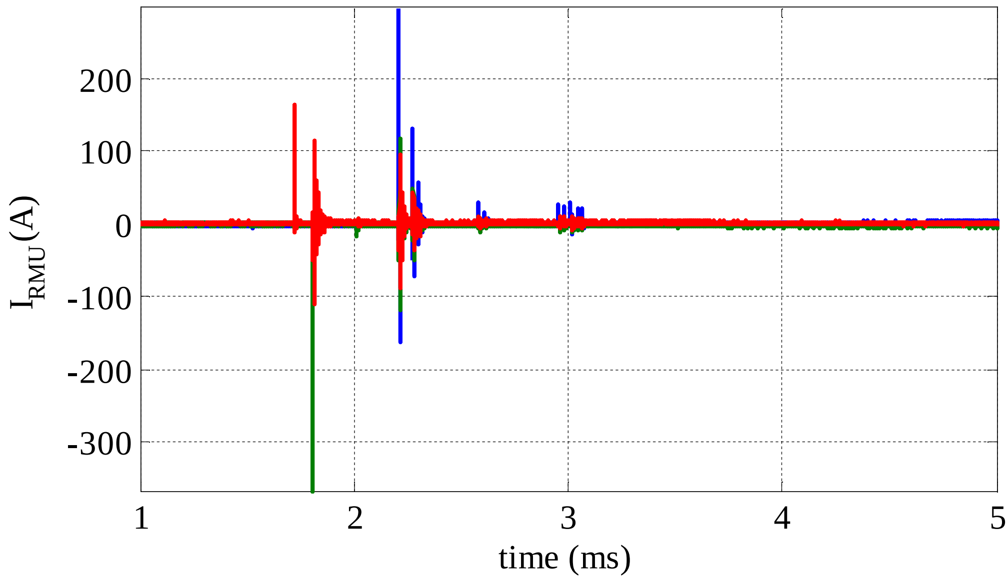

Figure 27 Current through RMU - inductor 94mH, layout 2, closing

Figure 27 presents current during closing of the breaker. A peak current of about 380A is measured. Since there are not any additional damping components, high frequency oscillations are observed during the current bursts.

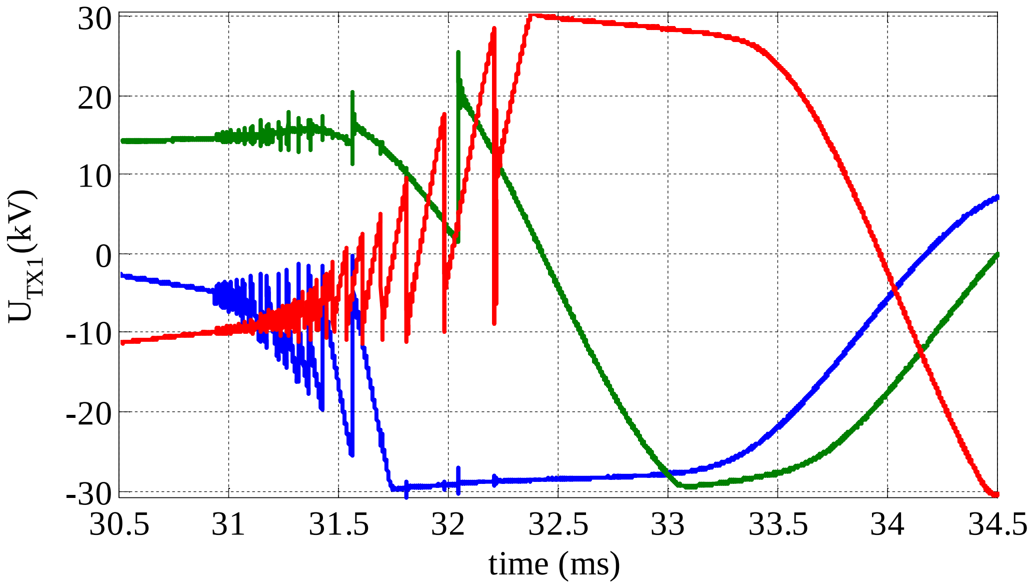

Figure 28 Voltage at transformer TX1 - inductor 94mH, layout 2, opening

Figure 28 shows a voltage transient during an opening operation of the breaker. Since no RC protection is used, a large number of restrikes are recorded. The number of restrikes and their magnitude is not as severe as it may be. The reason for that is a low current which does not provide very fast rising of the transient recovery voltage.

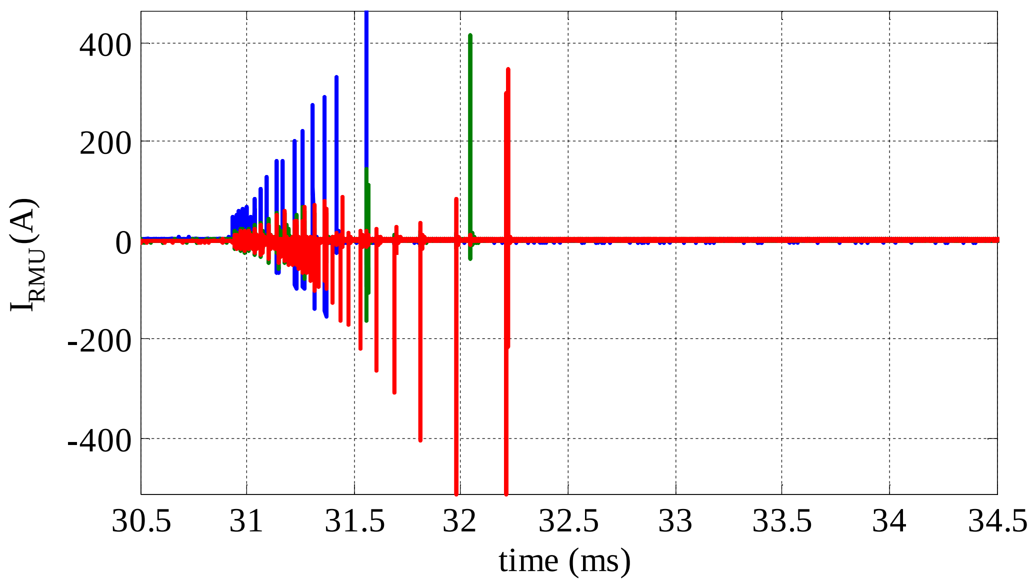

Figure 29 Current through RMU - inductor 94mH, layout 2, opening

Figure 29 shows the current transient during the same event. Due to a higher breakdown voltage, the peak current reaches a level of about 500A. Current bursts are recorded with multiple zero crossings. The frequency of these oscillations is equal to the resonant frequency between the cable and the transformer.

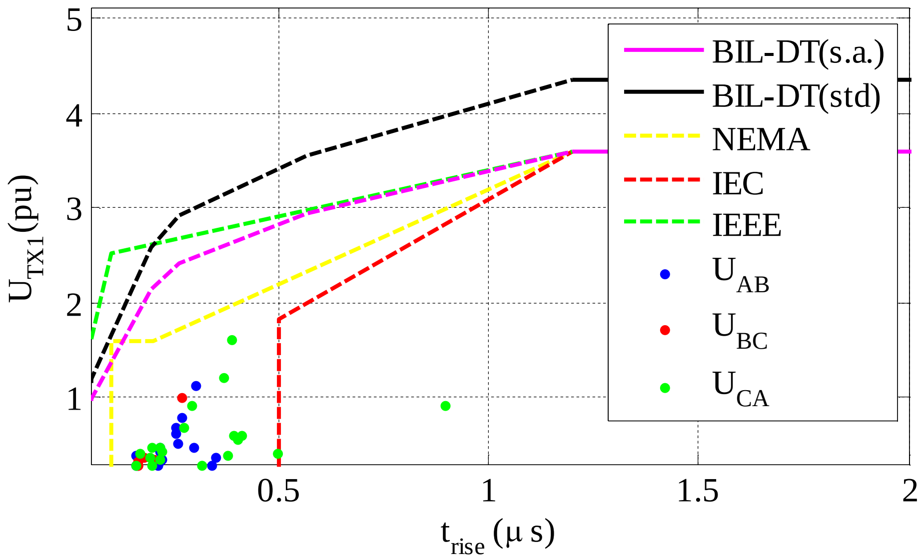

Figure 30 Voltage strikes recorded at transformer TX1 - inductor 94 mH, layout 2, opening

Figure 30 presents voltage strikes in a scatter plot. This scatter plot is used to observe if a voltage strike above the critical level is obtained. Critical levels are obtained with different standards for large motors [20]-[22]and standards for dry-type distribution transformers [24]. In addition, standards for dry-type transformers are extended into region of voltage strikes with rise times below 1.2μs using measurements presented in [12]. It is shown that the obtained voltage strikes are below the critical level and the standards except the IEC standard. The IEC standard is defined for transients faster than 500ns. A case setup with the breaker at the transformer will give much faster transients with rise times of about 50-100ns.

3.2.5 Inductive load case (94mH), layout 1 without RC protection

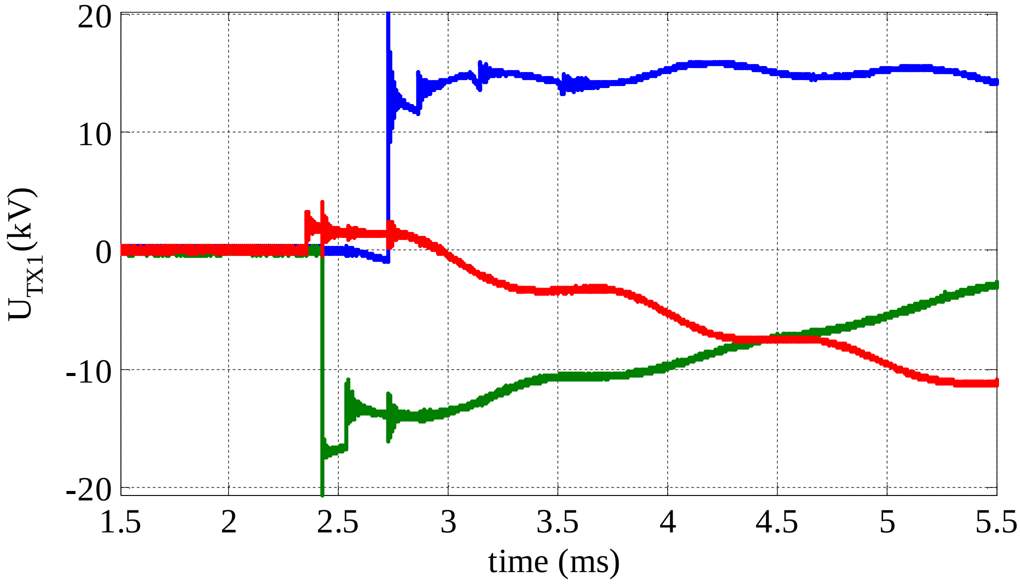

Figure 31 Voltage at transformer TX1 - inductor 94 mH, layout 1, closing

Figure 31 shows a voltage transient during closing of the breaker. Prestrikes are observed in each phase. A similar pattern of voltage prestrikes is obtained with other connection transients.

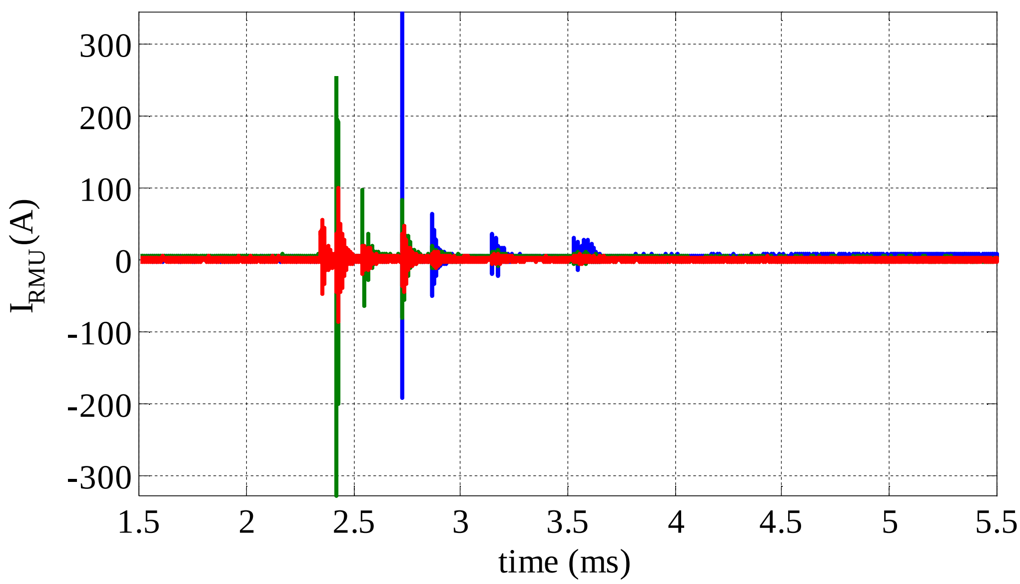

Figure 32 Current through RMU - inductor 94 mH, layout 1, closing

Figure 32 shows current transients during the same operation. A peak current of about 350A is obtained. Without the additional damping of the RC snubber, the high frequency current oscillations are observed after each prestrike.

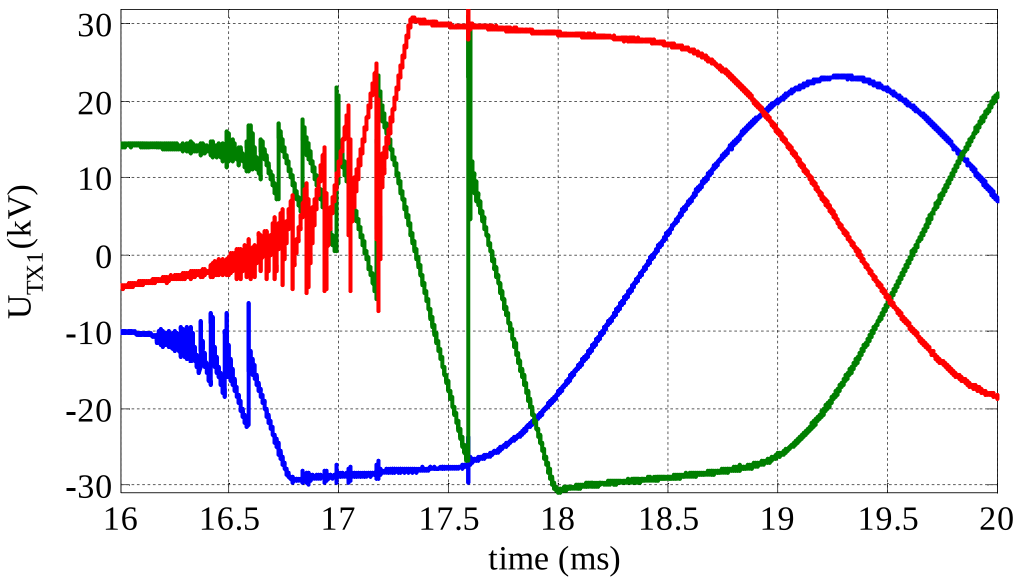

Figure 33 Voltage at transformer TX1 - inductor 94 mH, layout 1, opening

Voltage transients obtained during the opening of the breaker are presented in Figure 33. The result is similar to the opening of the breaker in layout 2 configuration. Similar magnitudes of voltage restrikes are obtained. Again, this does not represent the worst case scenario due to a low current.

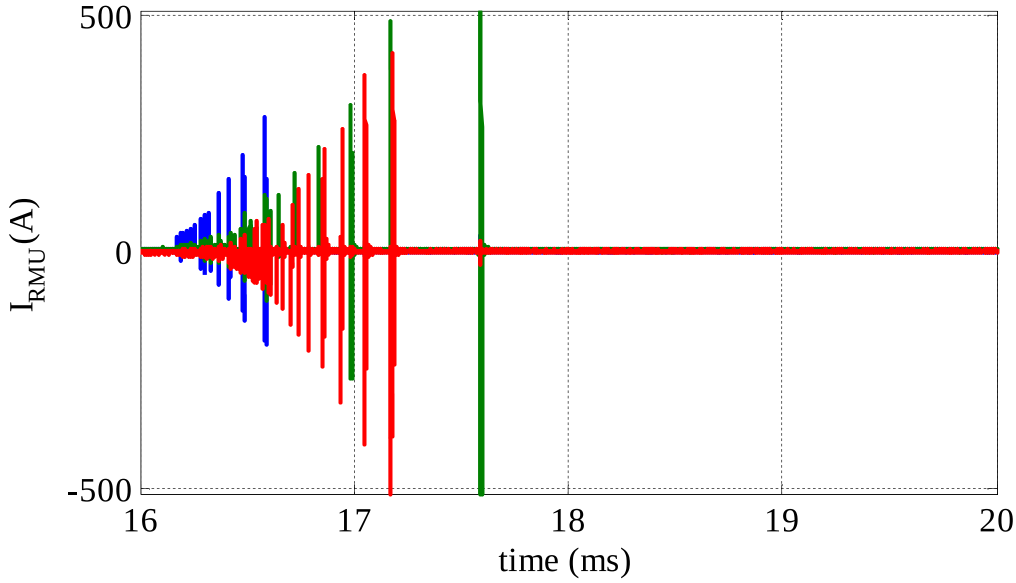

Figure 34 Current through RMU - inductor 94 mH, layout 1, opening

The current transients shown in Figure 34 are very similar to the current transients in Figure 29. A peak current of about 510A is obtained. Again, multiple current zero crossings are observed.

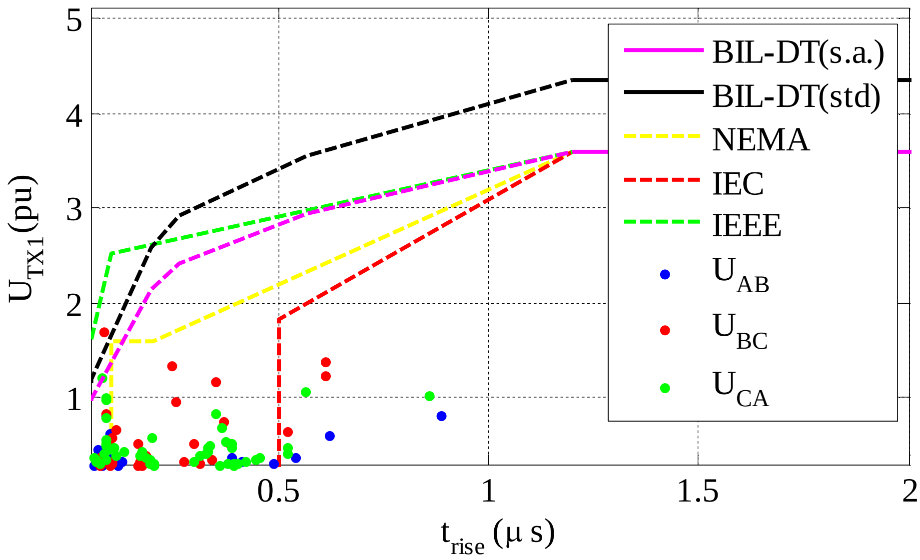

Figure 35 Voltage strikes recorded at transformer TX1 - inductor 94 mH, layout 1, opening

Figure 35 shows voltage restrikes in a scatter plot. In this case, somewhat faster strikes are recorded. Although the maximum voltage of 1.8pu is recorded, due to its very short rise time, this voltage strike is considered to be above the critical voltage level. It is considered to be above the critical voltage level by all the standards except the IEEE standard. Although the load of 94mH cannot produce the worst case scenario, the recorded voltage restrikes reveal that obtained voltage strikes are above the critical voltage level.

Figure 36 shows a voltage transient during closing of the breaker. In this case, the surge arresters clamp the voltage at about 40kV due to an additional ZnO block. However, the increased surge arrester level does not influence the voltage transient during the closing of the breaker.

3.2.6 Inductive load case (94mH), layout 1 without RC protection and increased surge arrester voltage level

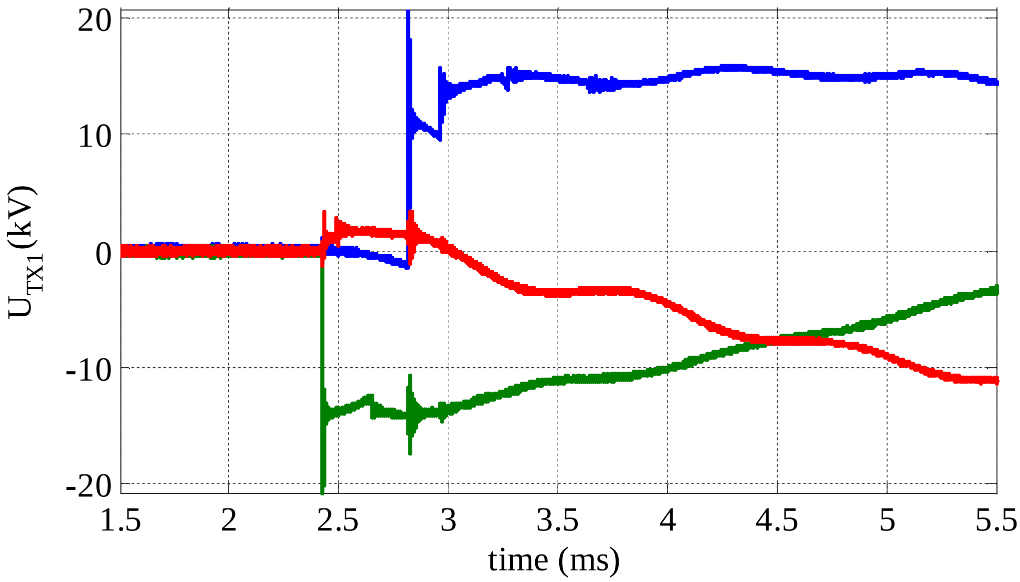

Figure 36 Voltage at tr. TX1 - inductor 94 mH, layout 1, 4xZnO, closing

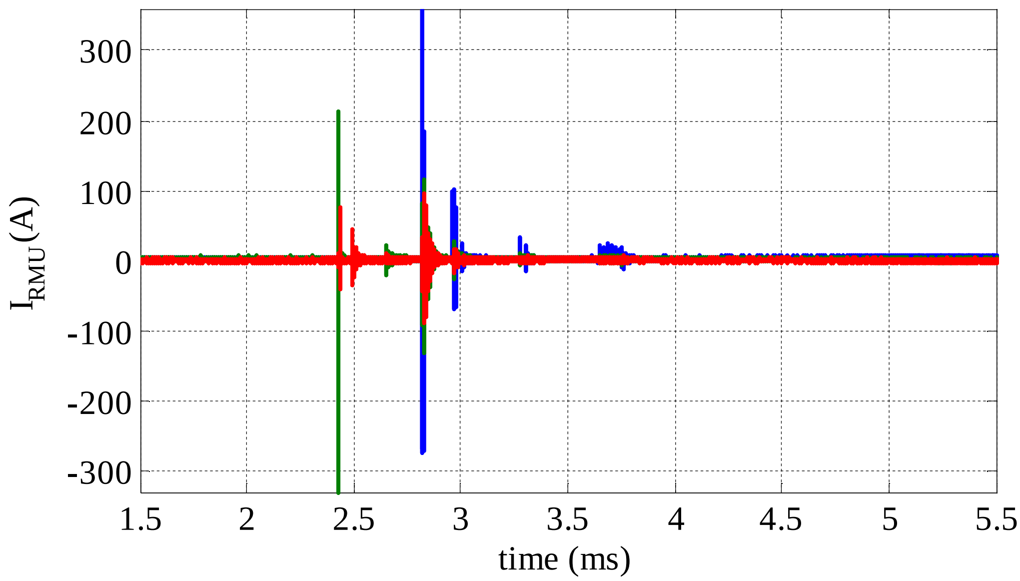

Figure 37 Current through RMU - inductor 94 mH, layout 1, 4xZnO, closing

Figure 37 shows current transients during the closing of the breaker. A peak current of about 350 A is recorded. Multiple current zero crossings are observed as well.

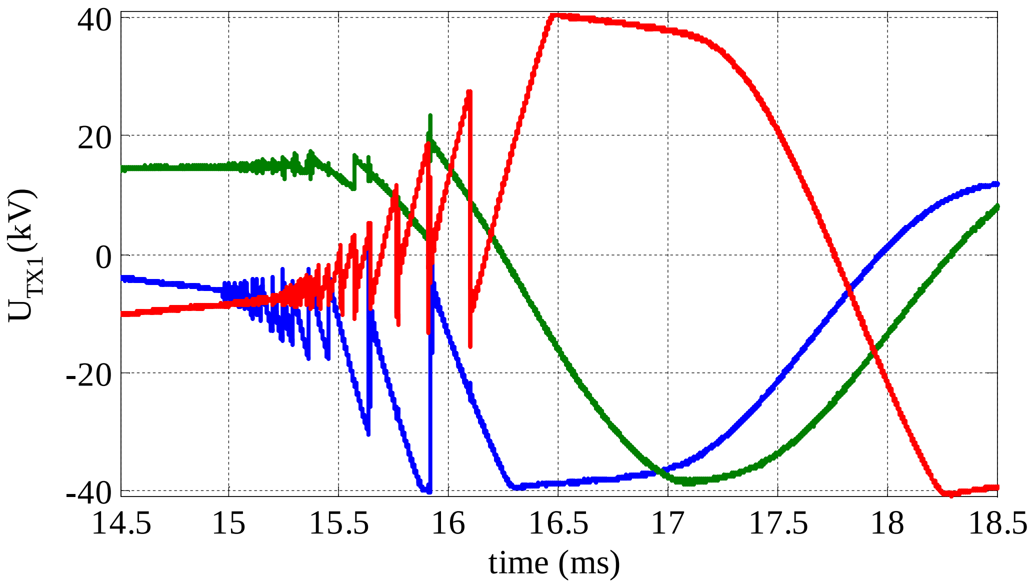

Figure 38 Voltage at transformer TX1 - inductor 94 mH, layout 1, 4xZnO, opening

The influence of the increased surge arrester level is shown in Figure 38. It can be observed that the voltage is clamped at about 40kV. Consequently, higher voltage strikes are obtained compared to previous cases with 3xZnO setup. However, this does not represent the worst case scenario due to interruption of low current. This case can be directly compared in terms of the surge arrester protection with the case with the oil-insulated transformer studied in the Vindforsk II. However, a mismatch in the load current, does not reveal a true severity of the case with the dry-type transformer.

Higher breakdown voltages produce current bursts with higher current peaks. In this case, the peak current of about 800A is recorded, which is shown in Figure 39. Due to a higher current level, a higher number of the current zero crossings is observed.

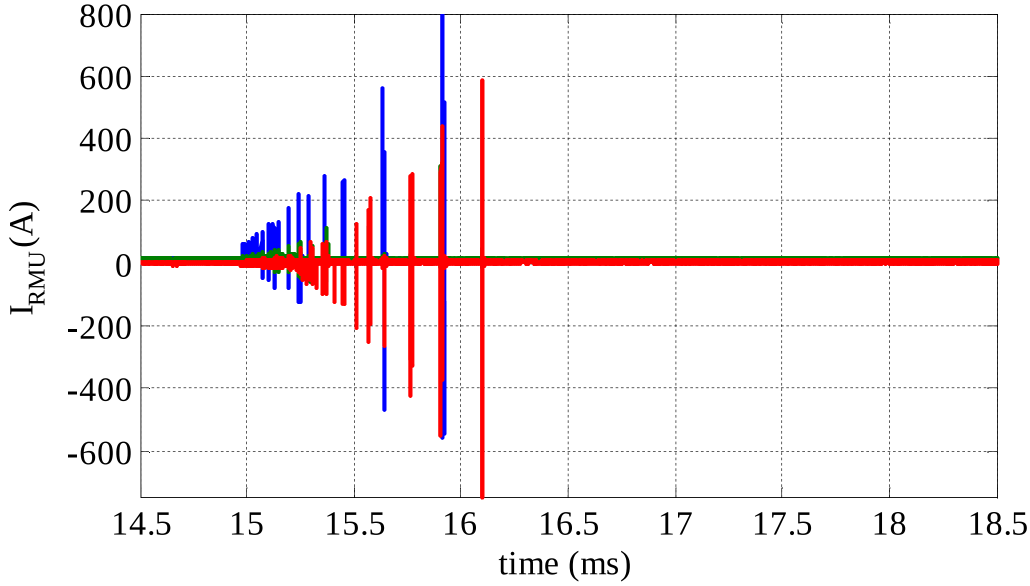

Figure 39 Current through RMU - inductor 94 mH, layout 1, 4xZnO, opening

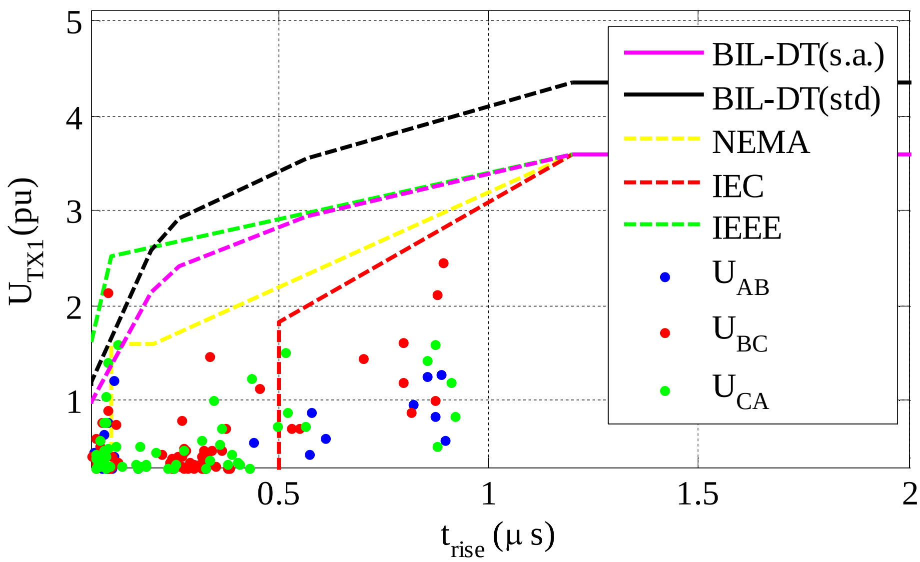

Figure 40 Voltage strikes recorded at transformer TX1 - inductor 94 mH, layout 1, 4xZnO, opening

Voltage strikes can be observed in Figure 40. It can be noted that the voltage level of the restrikes is increased compared to the case with only three ZnO-blocks. Now, the voltage strikes that exceed the critical voltage level are observed in phases BC and CA, and the highest recorded voltage is a 2.1pu, 100ns voltage strike, recorded between lines B and C. This is a clear evidence of appearance of severe voltages during switching of breakers.

3.2.7 Inductive load case (17mH), layout 1 without RC protection and increased surge arrester voltage level

It was not possible to run tests in the lab environment with the higher current level which would be required to obtain the worst case scenario, as it was obtained in the Vindforsk II project. For comparison with the Vindforsk II project, a simulation with a 17mH inductor is performed. This load gives identical current through the breaker. For the worst case scenario, the arcing time of the breaker is set to be very short. In fact, the breaker contacts were set to open at the moment when the current reaches the chopping level of about 3.5 A. Consequently, the transient recovery voltage rises very quickly, producing voltage strikes soon after the opening of the contacts.

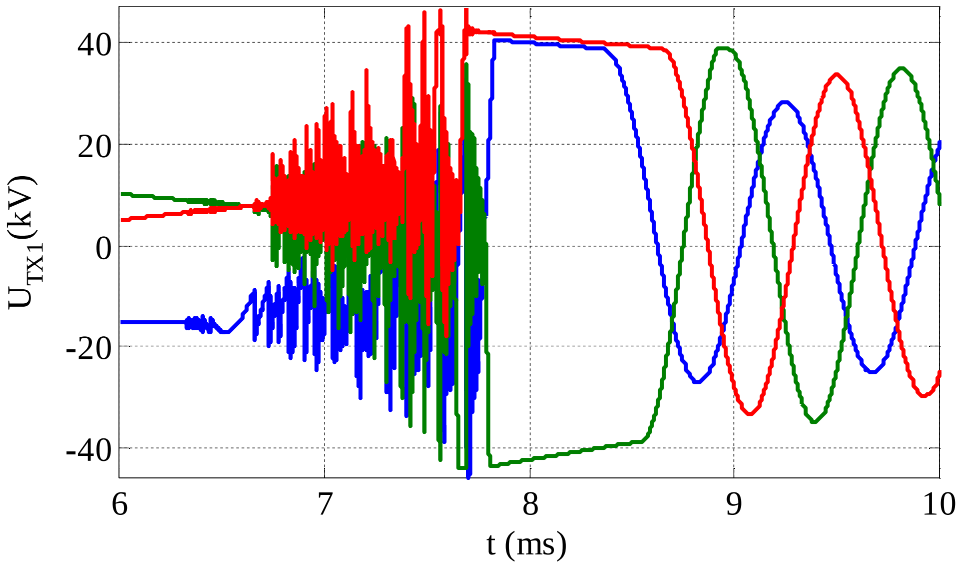

Figure 41 Voltage at transformer TX1 - inductor 17 mH, layout 1, 4xZnO, opening

Figure 41 shows the voltage transient during the opening of the breaker. Due to higher current, voltage strikes reached a very high level.

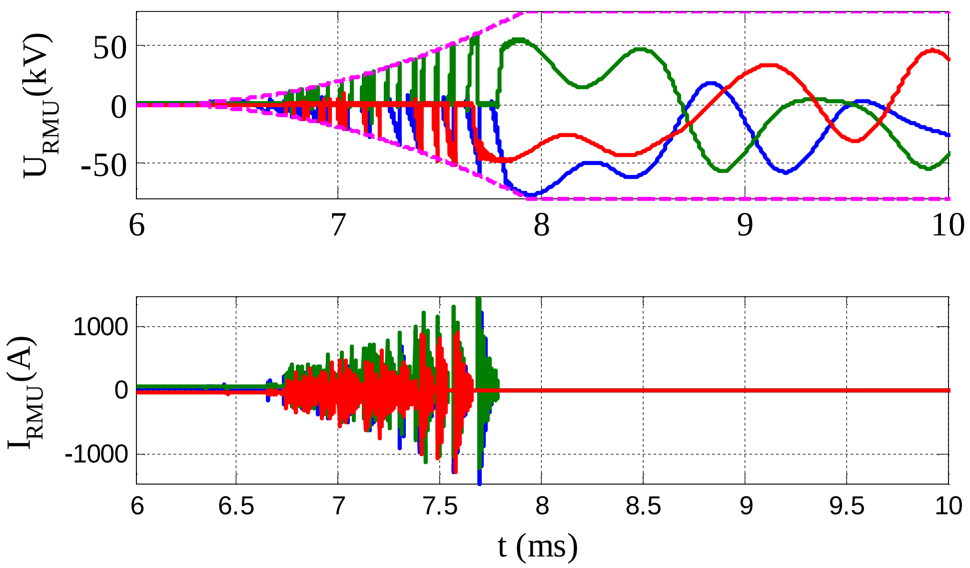

Figure 42 Voltage and current at RMU- inductor 17 mH, layout 1, 4xZnO, opening

Figure 42 shows the voltage and the current at the breaker. Due to high magnitude of voltage strikes, the maximum current is about 1200A.

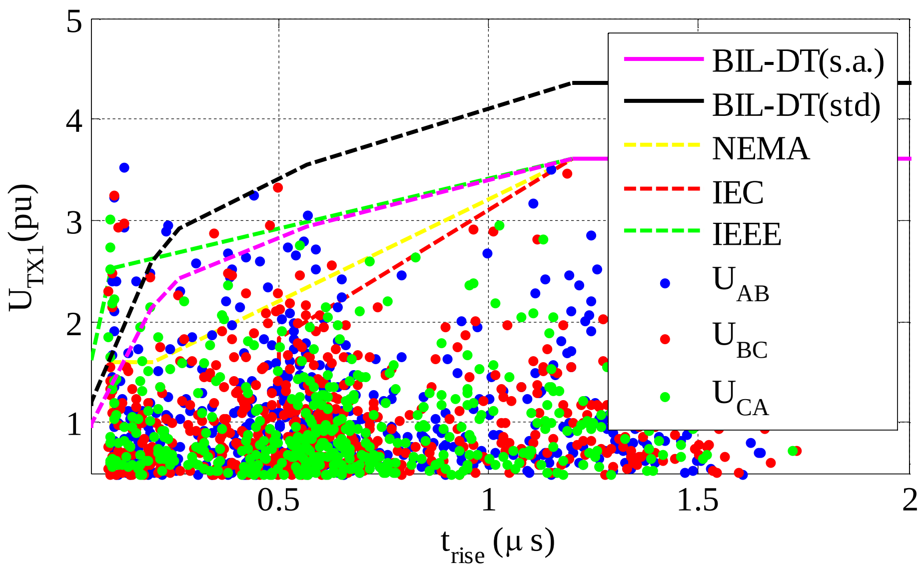

Figure 43 Voltage strikes recorded at transformer TX1- inductor 17 mH, layout 1, 4xZnO, opening

Figure 43 shows that the voltage strikes exceeded the critical voltage level in all phases. Furthermore, the most critical voltage recorded in phase AB has a magnitude of about 3.6pu and the rise time of about 120ns. This voltage strike produces severe turn-to-turn voltages that can damage the transformer’s insulation.

4 Models validation using experimental data

4.1 Methods for investigating transients in large wind farms

Table 2 presents the Comparison of using field installation measurement, laboratory experiment and computer simulation for investigating transient phenomena in large wind farms. Characterization of the transients occurring due to switching operation is best to obtain from field measurements, since it would represent real apparatus exposed in real operational systems – thus real-life conditions are recorded. However, several difficulties are attached to the field measurements:

- Parameters in a certain installation defined by the apparatus, circuit fixed to a real life condition so that they are not flexible to vary during measurement, e.g. to gather additional data, to confirm certain impact of changing apparatus parameters, etc.
- It is difficult to record all necessary parameters to reproduce the exact conditions, and correspondingly to isolate specific condition, mainly due to limitation on space and time for installing necessary measurement devices as well as due to commercial aspects (insurance and warranties) and risks involved
- Intermittency in some of the phenomena to measure. A fault, for example is an intermittent phenomenon in when and where it happens. It is difficult to predict exactly when and where it might happen – in fact it should be avoided at first place – and place accurate measurement and setup around it.

On the other hand, computer simulation offers all flexibility against field measurement. Computer simulation means very flexible parameters variation, easy repeatability and specific isolation of transient cases, measurement device and time flexibility and practicality no issue on risk imposed to commercial aspects or intermittency. Computer simulation however, does not work with real apparatus. Therefore the main issue is to validate the models used in the simulation as best as possible to represent real apparatus, circuit and phenomena.

In laboratory environment, it may be difficult to realize a down-scaled test circuit that still is representative of the actual real-life conditions. However, by realizing such test circuit it would give full flexibility to change parameters, define different test scenarios, and even test contingencies and faults, which are practically impossible to test in a real system. More important, the laboratory test results are a valuable mean to validate computer models. Thus, a combination of laboratory measurements and computer simulations can - to large extent - provide comprehensive understanding of transients due to interaction with different electrical apparatus as well as the impact on particular objects within a large wind farm. The latter is the goal of Chapter 5.

Table 2 Comparison of using field installation measurement, laboratory experiment and computer simulation for investigating transient phenomena in large wind farms

	Field Installation	Laboratory Experiment	Computer Simulation
Real apparatus	++	+	-
Parameter flexibility	-	+	++
Repeatability & specific isolation	-	+	++
Measurement device/time flexibility	-	+	++
Risk imposed to commercial	-	+	++
"Intermittency"	-	+	++

4.2 PSCAD Validation

The goal of this work is to combine the use of computer simulations (i.e. PSCAD simulations) as a complement to the laboratory measurements. For this purpose, a PSCAD model will be developed to represent the circuit with the laboratory setup. The developed model is then calibrated to the results obtained from the laboratory experiments. Eventually, the calibrated PSCAD model will be used as a virtual expansion of the wind cable laboratory, so that ultimately it can be used for more flexible parametric simulations as well as simulations in large wind farms. A remark should be made here that due to best availability of the test data, the validation has been focused on the use of laboratory test results obtained in the 2007-2008 laboratory campaign [1].

4.2.1 PSCAD Simulation as Virtual Expansion of the Wind Cable Laboratory

A large number of transient cases were investigated in the wind cable laboratory and analysis was made with good agreements. The experiments confirm the consistent occurrence of transient overvoltages. Selected scenarios with different surge protection devices have been performed in the laboratory, and it has been found that all surge protection methods tested, namely the surge capacitors and RC-protections, show some transient mitigation effects [1].

Compared to computer simulations, laboratory experiments have the main advantage that measurements are obtained from real apparatus. The test object can then be considered accurate to high details, something which is quite difficult to model within computer simulations. On the other hand, although to some extent laboratory experiments are flexible to test different components, layout circuits and parameters, practically – and especially economically – the flexibility of laboratory experiments has limitations in compared to computer simulations.

During the measurements campaign performed in [1] some of these limitations have been observed and analyzed, and will be presented in the following sections.

4.2.2 PSCAD Models

The PSCAD model has been developed to represent the laboratory circuit shown in Figure 3. The main components of the model are explained below.

Vacuum Breaker Model

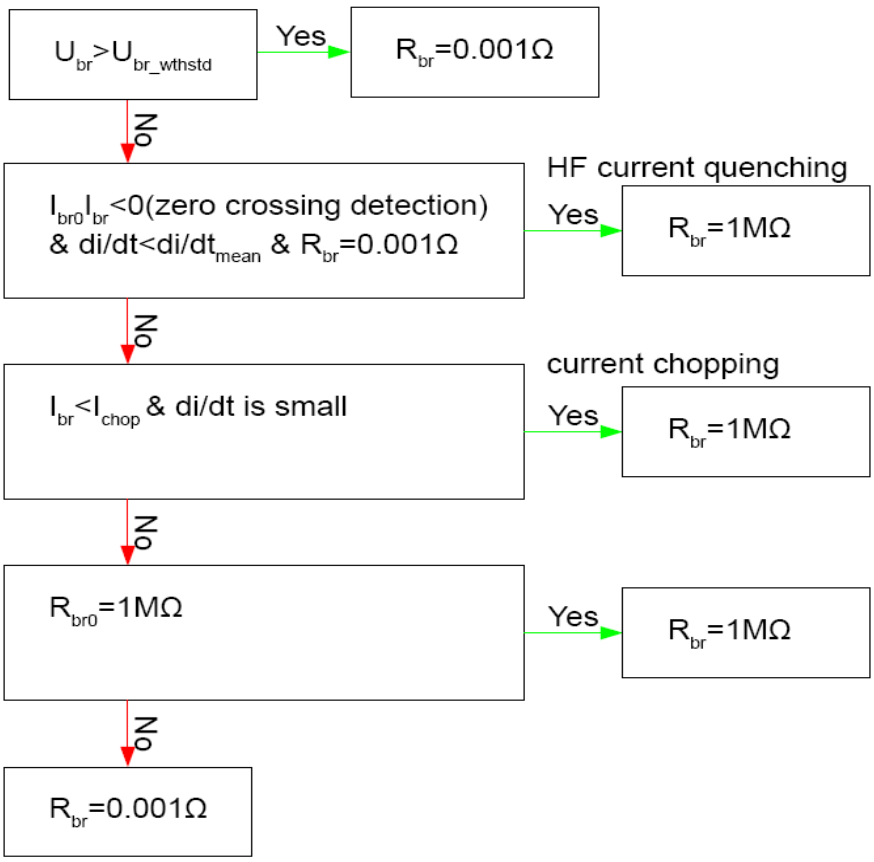

Figure 44 Vacuum breaker interruption diagram

Cables

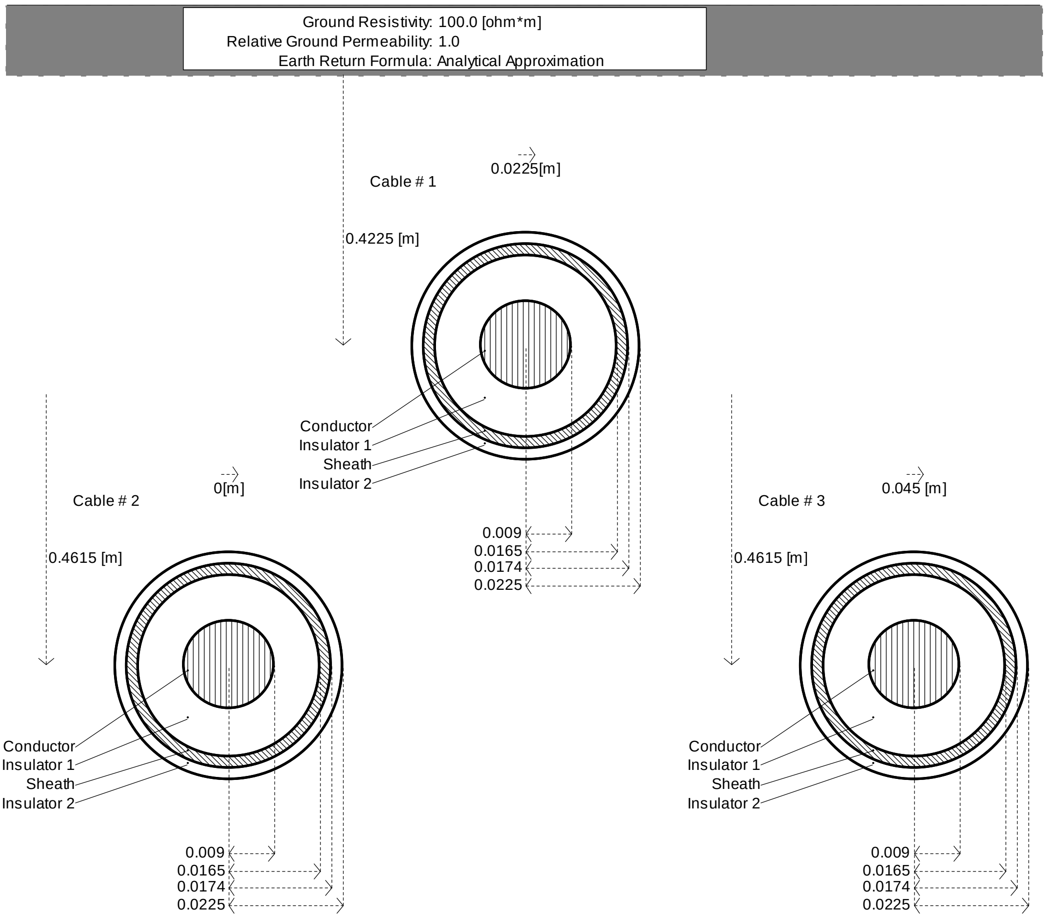

Figure 45 XLPE Cable 240 mm2

Transformers

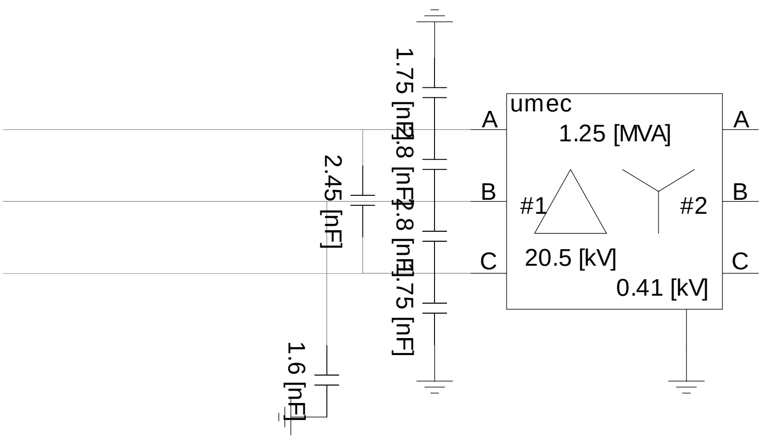

Figure 46 Transformer TX1

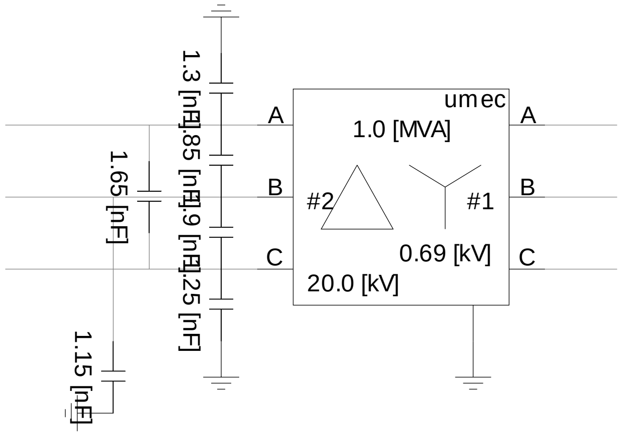

Figure 47 Transformer TX2

4.2.3 Basic experimental cases

Theoretically, there are four basic situations of switching operation in a cable system, namely: (1) closing at no load, (2) opening at no load, (3) closing with loading and (4) opening with loading, so simulations are focused on these basic cases as to fairly compare them with the experimental results. It is important to point out that opening with load is an extreme case which is provoked in the laboratory in order to reproduce and test worst-case scenarios, however it will probably not represent normal operation in a wind park, where it should not be regarded as normal practice to open a breaker or switch with fully loaded transformer on the wind turbine side. Furthermore, even when the breaker is opening an inductive load, this will not necessarily result in multiple re-ignitions due to the stochastic behavior of the breaker:
If the switching is not controlled to occur in a specific time or condition, it is purely stochastic whether any of the phase currents will be at the chopping level while the contacts starts to separate, which is the condition for re-ignitions to occur.

When the four possible switching operations mentioned in the previous paragraph were tested in the wind cable systems laboratory, the results of voltages measured at transformer TX1 terminals were obtained as shown in Figure 48 to Figure 51. Some remarks can still be made. Figure 48 shows the closing of the breaker at no load. The switching time is adjusted so that the withstand voltage of the breaker reaches the maximum rated peak voltage when the voltage is at its maximum at one phase. If that condition is fulfilled, the pre-strike current is at its maximum value, and additional pre-strikes will produce the maximum transient overvoltages. In Figure 49, the switching time of the opening operation for the no load case is chosen so that the no load current in one phase is at its maximum when the breaker starts separating the contacts. Since the no-load current represents the magnetizing current of the transformer, the current lags 90^{o} and the voltage re-strikes are superimposed on the fundamental frequency voltage while at its maximum. Figure 50 shows the closing of the breaker at inductive load. The switching time is adjusted as it is in case 1. In Figure 51, opening of the breaker with inductive load is shown. The breaker switching instant in this case is chosen so that the phase current in one phase is at the current chopping level when the contacts starts to separate. This ensures that the transient recovery voltage will reach the breaker withstand voltage very short time after the contact separation producing a re-strike. It takes much longer time for the breaker to build up the withstand voltage to the level higher than the transient recovery voltage produced by re-strikes compared to the no-load case. This increases the magnitude and the number of re-strikes compared to the no-load case. It can be observed that the voltage over the transformer TX1 is limited by the surge arresters to the level of 20 kV.

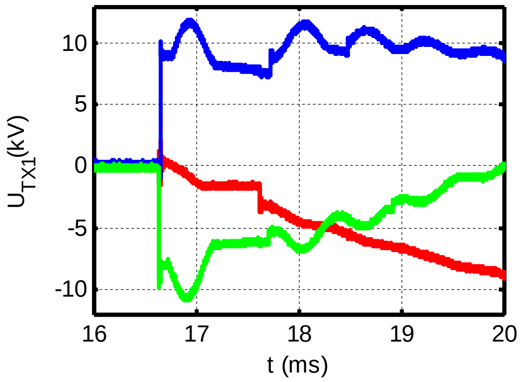

Figure 48 Closing the breaker at no load (case 1)

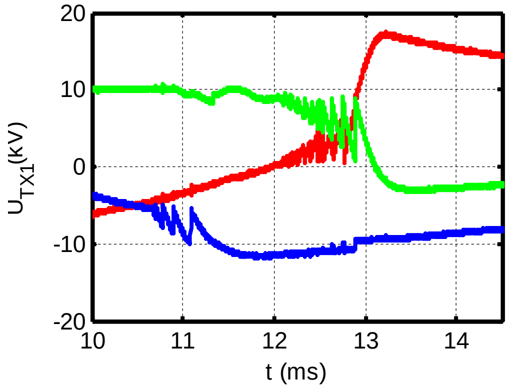

Figure 49 Opening the breaker at no load (case 2)

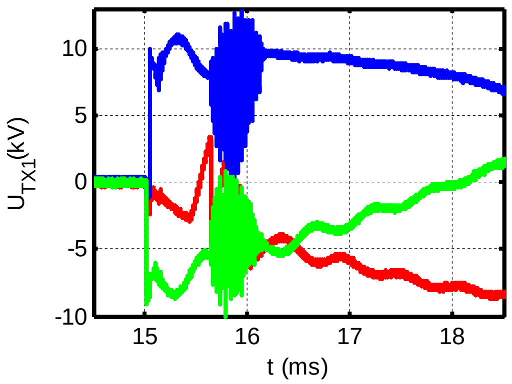

Figure 50 Closing the breaker with inductive load connected at transformer TX1 (case 3)

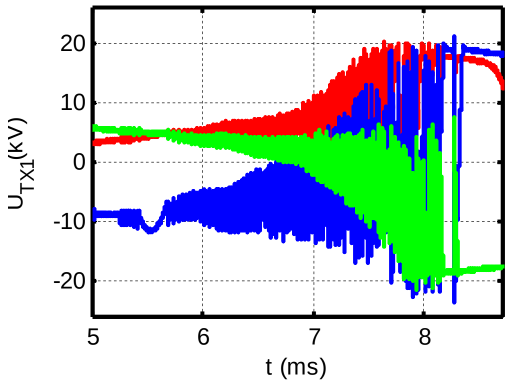

Figure 51 Opening the breaker with inductive load connected at transformer TX1 (case 4)

Strikes resulting from breaker operation depend to a large extent on the time instant of opening and closing of the contacts of the breaker [4-5]. In this experiment the opening and the closing of the breaker are performed in such a way that the worst case scenario is likely to be achieved. It was assessed that the time instant of opening and closing of the breaker contacts results in the voltage transient of the highest magnitude. Moreover, the breaker used in the experiment has also stochastic and probabilistic characteristics (e.g. probability of arc quenching, etc.). To take this into account, after the switching time instant resulting in the highest/steepest voltage transient is obtained for each test case, 2-4 extra shots are additionally performed with the exact same instant time. Transients resulting from a typical test sequence are quantified in terms of number of re-ignitions, the magnitude and the rise-time of voltage step for further analysis and clear comparison to simulations.

4.2.4 Verification to computer simulation results

The laboratory setup model was made using PSCAD/EMTDC. The cable model for the high frequency simulations is developed using the frequency dependent (phase mode) cable model available in the PSCAD/EMTDC master library. Models of other components such as the breaker and the transformer are either built using the FORTRAN code or by modifying the existing PSCAD/EMTDC models.

The transformer model is developed by modification of the existing PSCAD/EMTDC by addition of transformers stray capacitances on the high voltage side of the transformer. This method gives very accurate results for a high frequency phenomenon such as surges generated by a breaker switching in a system consisting of cables and transformers.

The breaker model is developed using a PSCAD/EMTDC feature for the development of user defined models. The breaker model is deterministic and does not include the stochastic behaviour of the arc interruption and vacuum breakdown. However, the model includes modelling of the most important breaker phenomena such as the breaker voltage withstand, the current chopping, virtual current chopping and the high frequency current quenching capability.

The simulation results are presented in Figure 52-Figure 55. Although the models used for simulations are somewhat simplified, obtained results match very well to the measurements if the critical properties of the surge voltages such as the magnitude, rise-time and the repetitiveness are compared.

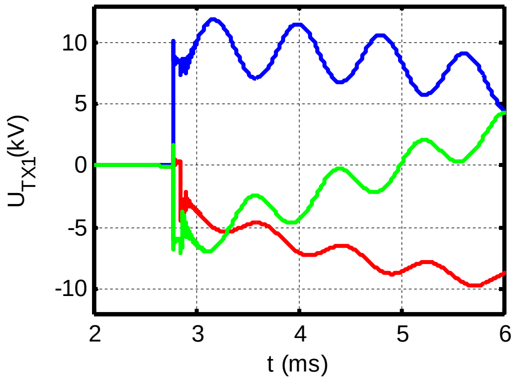

Figure 52 Closing the breaker at no load (case 1) - SIMULATION

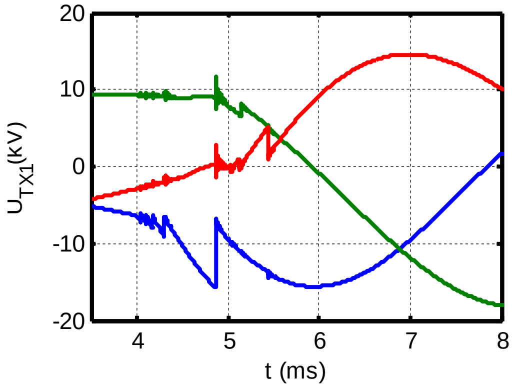

Figure 53 Opening the breaker at no load (case 2) - SIMULATION

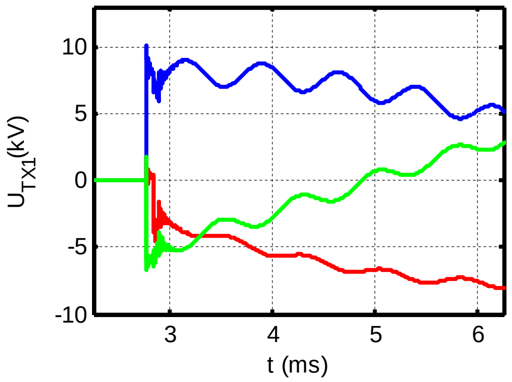

Figure 54 Closing the breaker with inductive load connected at transformer TX1 (case 3) - SIMULATION

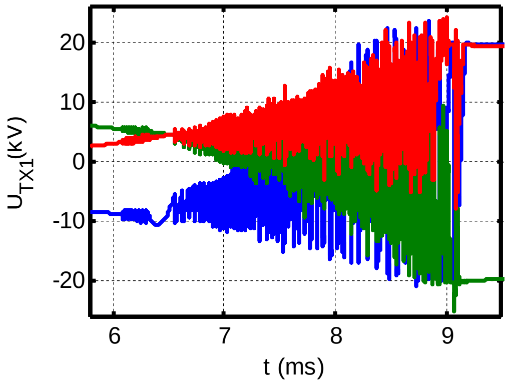

Figure 55 Opening the breaker with inductive load connected at transformer TX1 (case 4) - SIMULATION

4.3 Conclusions

This work concludes that the models developed have been successfully calibrated to represent the laboratory measurements and allow for the use of computer simulation with confidence, as a virtual expansion of the wind cable laboratory as well as for expanded investigations of transient phenomena in large wind farms such as those presented in the following Chapters 5 and 6

5 Simulation of transient phenomena in large wind farms

In this Chapter, several phenomena of transients in large wind farms are investigated. Investigation is performed by means of computer simulation models which are validated using laboratory experimental data.

5.1 Multiple reflection and refraction

The objective was to investigate the effect of the multiple reflection points and occurrence of constructive interference in the transient overvoltage construction during the collection grid energizing, and see if it can create a potentially harmful situation to the transformers installed at the towers' top. The voltage peaks will be compared to the Basic Impulse Level recommended by IEEE Standards [23] and [24].

5.1.1 Reflection and refraction effect in the collection grid

When the interest is to study the transient behavior of the system, the cable's representation by its lumped components is not enough. Instead, in order to take into account the voltage and current travel times through the conductor, its distributed parameters such as series inductance and shunt capacitance per meter must be used. The proportion between voltage and current during a transient is given by the cable *characteristic impedance* (also known as *surge impedance*), calculated as following (with L representing the series distributed inductance [H/m] and C the shunt distributed capacitance [F/m]):

$$Z_0 = \sqrt{\frac{L}{C}}\ \Omega \qquad (1)$$

Every time a travelling wave reaches a discontinuity on the conductor's surge impedance (that can be a connection with a different cable, or with more than one cable – this last one called *derivation point*), some adjustments take place in order to respect the voltage and current proportion in all the branches involved, and the continuity of these elements at the junction. This way, it's said that part of the energy travels through the new surge impedance, called the *refracted wave*, and part of it is reflected back through the previous surge impedance (the *reflected wave*). The proportion between the incident, the reflected and refracted waves is a function of the ratio between the involved surge impedances.

Reflection Coefficient

The Reflection Coefficient rules the proportion between the incident and the reflected waves. It is given by equation (2), where Z_A stands for the surge impedance that carries the incident wave, and Z_B is the new surge impedance (that will conduct the refracted wave). If the discontinuity is a derivation point, Z_B will be calculated as the parallel association of all surge impedances of the cables connected to the point, except for Z_A.

$$\alpha = \frac{Z_B - Z_A}{Z_B + Z_A} \qquad (2)$$

Note that, for one specific discontinuity configuration, each possible incoming direction of the incident wave results in a different value of α.
The value of α varies from -1 to 1 (see figure 1). It is -1 when Z_B=0 (a short circuit), or when there is a voltage control at the node (for example, a voltage source). The opposite case (α=1) is when the voltage wave reaches an open circuit, or an unloaded transformer's terminals.

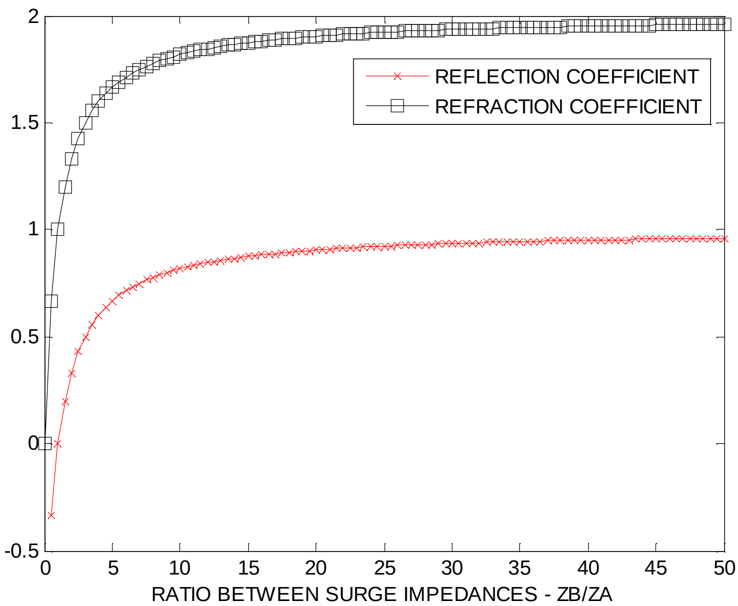

Figure 56 Reflection and refraction coefficients for a voltage wave as a function of the ratio between the surge impedances involved

Refraction Coefficient

The refraction coefficient rules the proportion between the incident and the refracted waves. It is given either by equation (3) or by equation (4), with Z_A and Z_B being the same as in equation (2).

The consideration about the direction of the incoming wave for a given discontinuity about α is also valid for β (there is one value of refraction coefficient for each incoming direction of the travelling wave).

$$\beta = \frac{2 \cdot Z_B}{Z_B + Z_A} \qquad (3)$$

$$\beta = \alpha + 1 \qquad (4)$$

This way, in a short circuit case (α = -1), as there is no proper conductor connected, there is no refracted wave either (β=0). On the other hand, for Z_B greater than Z_A, β is greater than 1, increasing as the circuit gets closer to an open circuit ($\beta=\infty$). This means that, depending on the cables connection, it is possible for the refraction phenomena to act as amplification for the transient voltage.

Wave form construction

Applying the reflection and refraction theory to the simple circuit shown in Figure 57, it can be seen how the transient overvoltage wave form is constructed by the multiple reflections in the branches 2 and 3. The travelling wave speed is given by equation 5, with μ_r and ε_r referring to the cable's insulation material. In this case, the speed considered was 200 m/µs.

$$v = \frac{3 \cdot 10^8}{\sqrt{\mu_r \cdot \varepsilon_r}} \quad (m/s) \qquad (5)$$

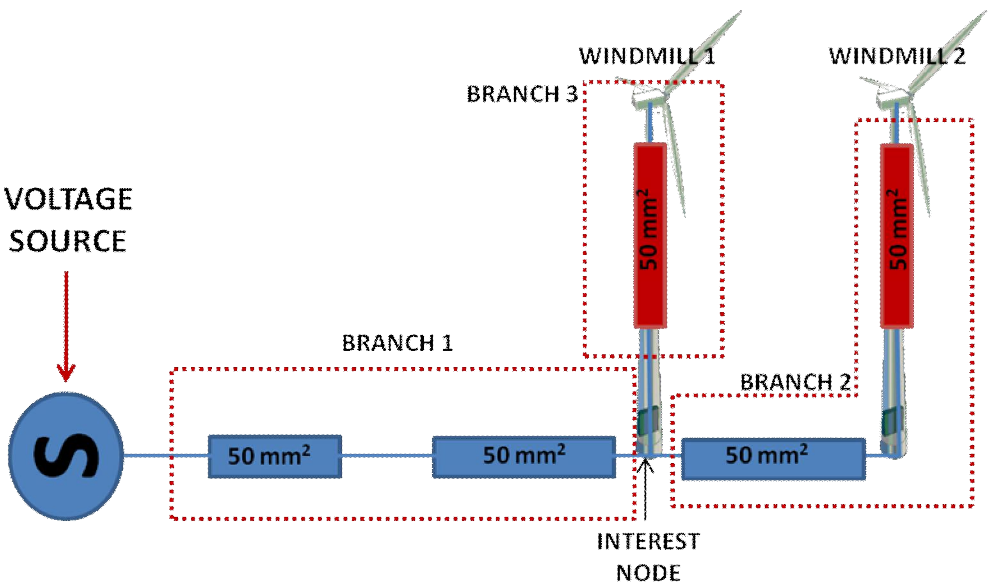

Figure 57 Simple circuit for multiple reflection analysis

Even if the voltage source is a 50 Hz sinusoidal signal (200 ms period), for the transient period (only a few µs), it behaves like a battery. As all the cables involved have the same cross section, the reflection coefficient at the interest node is the same for all possible incoming direction. Finally, as the energizing moment is under analysis, the transformers at the towers' top are all unloaded, and behave like open circuits ($\alpha=1$). Detail parameters for Figure 57 are shown in below Table 3 to Table 5

Table 3 Reflection and refraction coefficients at interest node

Incoming Direction	α	β
Windmill 1	-1/3	2/3
Windmill 2		
Voltage Source		

Table 4 Branches reflection coefficient

Circuit Point	α
Voltage Source	-1
Windmill 1	1
Windmill 2	1

Table 5 Branches length and travel time (V = 200 m/µs)

Branch	*Length (m)*	*Travel Time (µs)*
Branch1	900	4.5
Branch2	880	4.4
Branch3	80	0.44

When the source is connected to the non-energized circuit, a voltage wave will start to travel towards the interest node. Once it reaches the discontinuity point, the reflected wave will start travelling in the source's direction, and will be reflected back and forth at Branch1. Simultaneously, the refracted waves will be also reflected several times at branches 2 and 3.

Figure 58 shows the result of the multiple reflections at Branch1, as Figure 59 and Figure 60 show the reflections at Branches 2 and 3, respectively. Table 6 and Table 7 show the voltage values construction, where T is the travel time for the correspondent Branch (see Table 5).

Table 6 Voltage wave consecutive reflections at branch 1

time	Travelling Wave Magnitude [p.u.]	Travelling Wave Direction	Voltage at Node [p.u.]
0<t<T	1	⟶	0
T<t<2*T	-1/3	⟵	2/3
2*T<t<3*T	1/3	⟶	2/3
3*T<t<4*T	-1/9	⟵	2/3+(1/3)*(2/3)=8/9
4*T<t<5*T	1/9	⟶	8/9
5*T<t<6*T	-1/27	⟵	8/9+(1/9)*(2/3)=26/27

Table 7 Voltage wave consecutive reflections at branches 2 and 3

time	Travelling Wave Magnitude [p.u.]	Travelling Wave Direction	Voltage at Node [p.u.]
0<t<T	1	⟶	0
T<t<2*T	2/3	⟶	2/3
2*T<t<3*T	2/3	⟵	2/3
3*T<t<4*T	-2/9	⟶	2/3+(2/3)*(2/3)=10/9
4*T<t<5*T	-2/9	⟵	10/9
5*T<t<6*T	2/27	⟶	10/9+(-2/9)*(2/3)=26/27

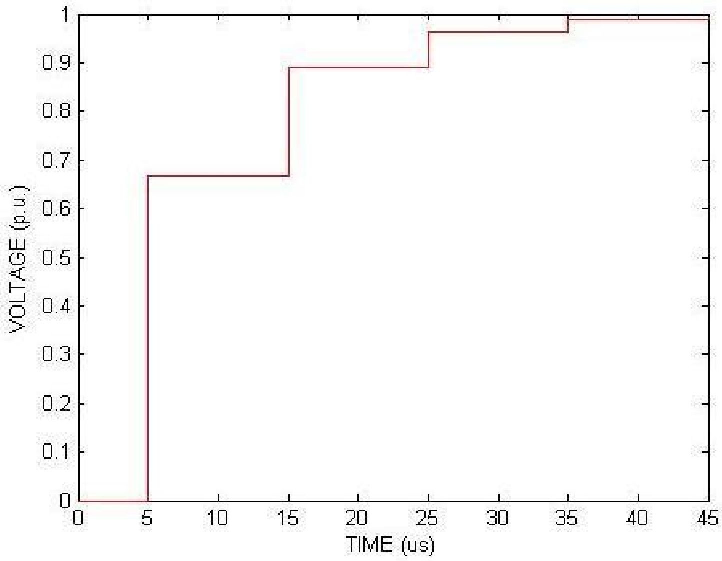

Figure 58 Multiple reflections at Branch1 contributing for the voltage wave form construction. T=4.5 µs

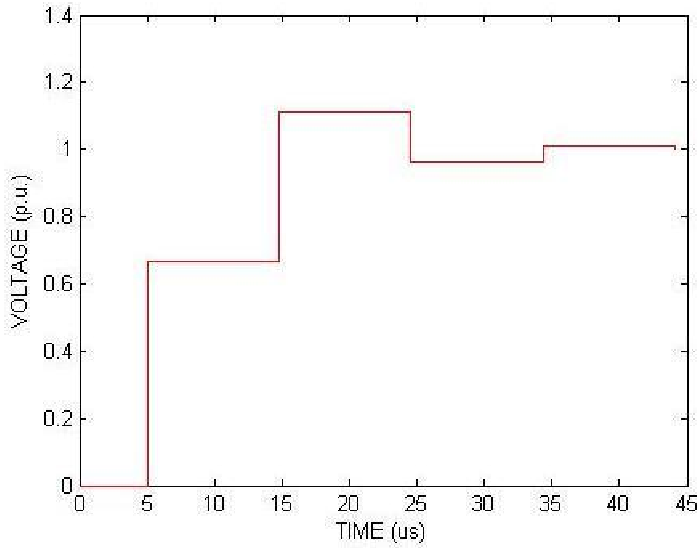

Figure 59 Multiple reflections at Branch2 contributing for the voltage wave form construction. T=4.4 µs

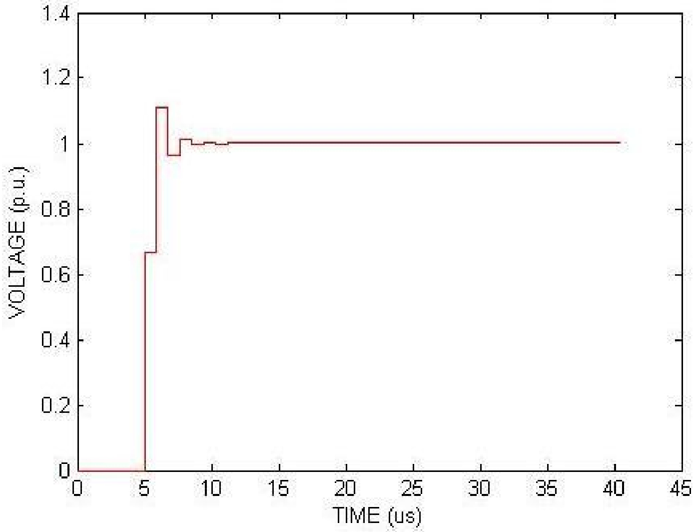

Figure 60 Multiple reflections at Branch3 contributing for the voltage wave form construction. T=0.44 µs

Figure 61 shows combined effect at the node of interest (see Figure 57)of the individual multiple reflections shown in Figure 58, Figure 59 and Figure 60.

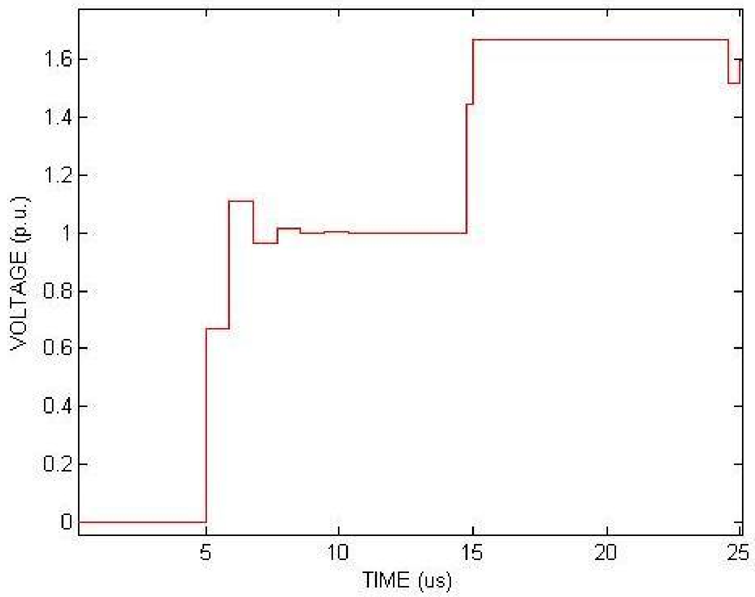

Figure 61 Voltage wave form construction at the node of interest (see Figure 57) by the sum of multiple reflections at Branches 1, 2 and 3

Multiple Reflections x Consecutive Refractions

For any transient, the traditional Offshore Wind Parks configurations (refer to Figure 63 and Figure 64) consist in a lot of reflection points and possibilities of construction interference. Also, although in these cable grids the travelling wave speed is smaller than in overhead lines (see equation 5), the short distances involved results in very short travel times and smaller attenuation due to cable's losses. In addition, during the energizing period, as the tower top transformers are unloaded, they behave like an open circuit, reflecting 100% of any voltage travelling wave that reaches its terminals back to the collection grid.

Depending on the cables' connection configuration, the refraction phenomenon is also capable of amplifying the voltage travelling wave. However, as in the collection grids most of the discontinuity points are in fact derivations (a connection of more than 2 cables together), the ratio between the resulting surge impedances required for the amplification to take place ($Z_B > Z_A$) rarely happen.

This way, as the possibility of constructive interference occurrence, the multiple reflections and the unloaded transformers contribute to increase the voltage peak during the transient, the consecutive refractions (with $\beta < 1$) has a damping effect when the travelling wave goes through the feeder. Figure 8 illustrates this effect in a feeder with 4 windmills.

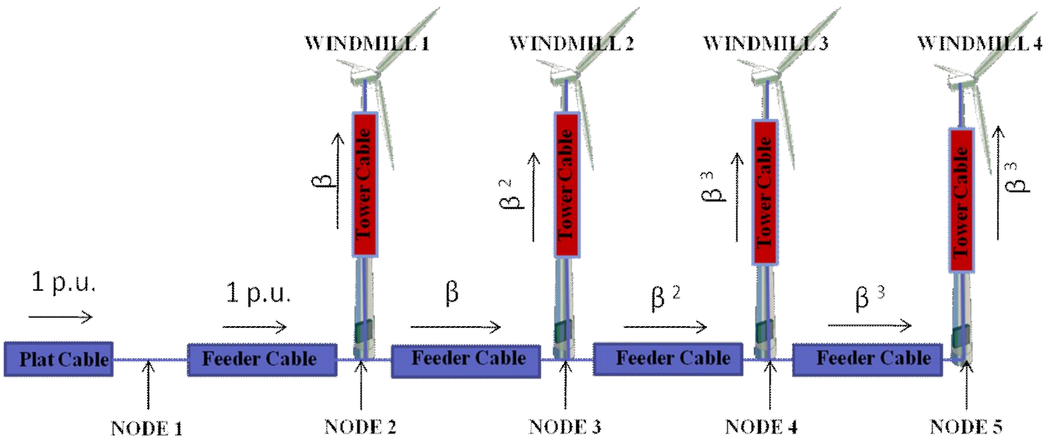

Figure 62 Damping effect of the consecutive refractions in a feeder with 4 windmills

5.1.2 Layouts studied

In this work two basic layouts were studied, with different number of windmills each, as shown in Figure 63 and Figure 64. The generators' nominal power considered was 2 MVA, and the collection grid voltage level 36 kV. The cables were chosen according to the information at ABB XLPE Cable Systems User's Guide [25]. The voltage wave initiation occurred at TX2 terminals.

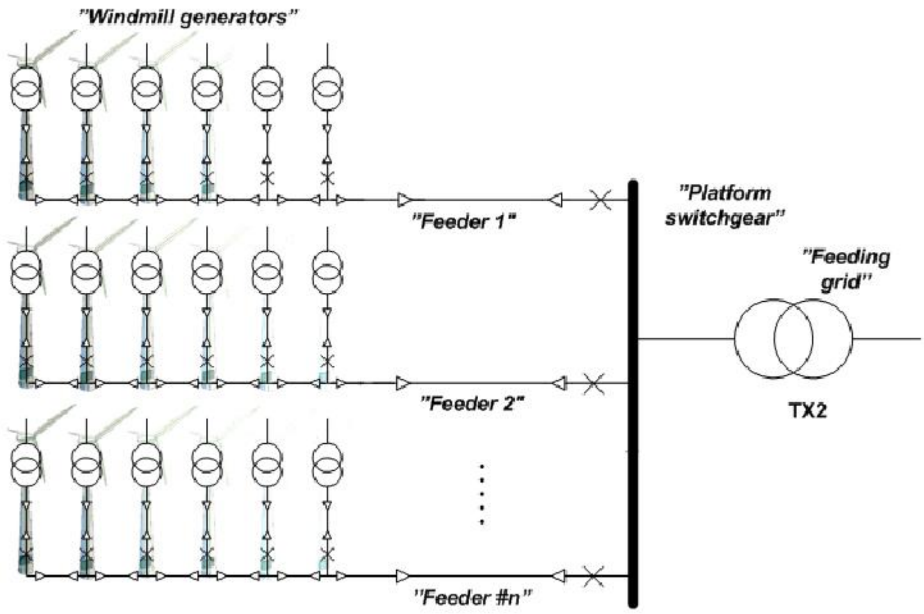

Figure 63 Long feeder layouts

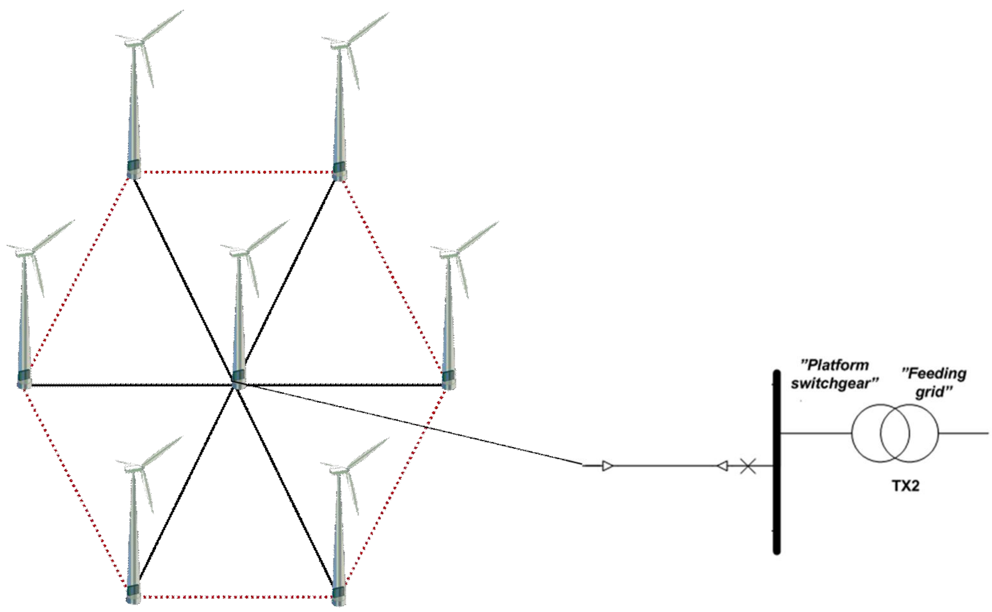

Figure 64 Star symmetries

Furthermore, the two basic layouts are expanded into situations with only 1 feeder with 4 to 9 windmills, to bigger cases with up to 9 feeders considered. Details of the cases studied are listed in Table 8. The first six cases in are derived from layout of Figure 63 and the last two cases are derived from layout of Figure 64.

Table 8 Cases studied

Case ID	Description
F1_W4	1 FEEDER WITH 4 WINDMILLS
F4_W4	4 FEEDERS WITH 4 WINDMILLS EACH
F1_W6	1 FEEDER WITH 6 WINDMILLS
F6_W6	6 FEEDERS WITH 6 WINDMILLS EACH
F1_W9	1 FEEDER WITH 9 WINDMILLS
F9_W9	9 FEEDERS WITH 9 WINDMILLS EACH
STAR_7	7 WINDMILLS, CABLES CONNECTED AS STAR GRID
STAR_9	9 WINDMILLS, CABLES CONNECTED AS STAR GRID

5.1.3 Coefficients calculation

All the cases described in Table 8 were studied: the cables cross section was selected according to the current conducting capacity [25] and the reflection and refraction coefficients were calculated at all the nodes. Some of the results are shown in the next tables.

Table 9 Cable characteristics – some cases

Cable	*Length*	*Cross Section*	Z_0
Tower – all cases	80 m	50 mm^2	40 Ω
Platform – Case F1_W4	100 m	50 mm^2	40 Ω
Platform – Case F4_W4	100 m	500 mm^2	16.9 Ω
Platform – Case F6_W6	100 m	2x630 mm^2	7.65 Ω
Platform – Case STAR_7	3000 m	120 mm^2	30.3 Ω
Feeder – Case F1_W4	800 m	50 mm^2	40 Ω
Feeder – Case F4_W4	800 m	50 mm^2	40 Ω
Feeder – Case F6_W6	800 m	95 mm^2	33.3 Ω
Feeder – Case STAR_7	800 m	120 mm^2	30.3 Ω

Table 10 Reflection and refraction coefficients – CASE F1_W4

Incomming Direction	*Platform Swithgear*	*Tower Bottom 1-3*	*Tower Bottom 4*
Platform	α=0	α=-1/3	α=0
	β=1	β=2/3	β=1
Windmill	--	α=-1/3	α=0
		β=2/3	β=1
Feeder end	α=0	α=-1/3	--
	β=1	β=2/3	

Table 11 Reflection and refraction coefficients – CASE F4_W4

Incomming Direction	*Platform Swithgear*	*Tower Bottom 1-3*	*Tower Bottom 4*
Platform	α=-0.26	α=-1/3	α=0
	β=0.74	β=2/3	β=1
Windmill	--	α=-1/3	α=0
		β=2/3	β=1
Feeder end	α=-0.57	α=-1/3	--
	β=0.42	β=2/3	

Table 12 Reflection and refraction coefficients– CASE F6_W6

Incomming Direction	*Platform Swithgear*	*Tower Bottom 1-5*	*Tower Bottom 6*
Platform	α=-0.16	α=-0.29	α=0.09
	β=0.84	β=0.71	β=1.09
Windmill	--	α=-0.42	α=-0.09
		β=0.58	β=0.91
Feeder end	α=-0.81	α=-0.29	--
	β=0.19	β=0.71	

Table 13 Reflection and refraction coefficients – CASE STAR_7

Incomming Direction	*Central Node*
Plaftorm Cable	α=-0.68
	β=0.32
Any Windmill	α=-0.76
	β=0.24

5.1.4 Simulation Results

The cases described in Table 8 were simulated using the software PSCAD. The switch was closed at the voltage peak in Phase C (t=3ms), so the worst case would be experienced. According to the incidence time of the main voltage steps (or the delay between then) and its sign (positive when the voltage increases and negative when it decreases), it was possible to know the origin of the reflected wave. This way, the coefficients calculations shown in Section 5.1.3 were validated. The transient's voltage peaks measured at the towers' top transformers terminals for some cases are listed below.

<u>Case F1_W4</u>

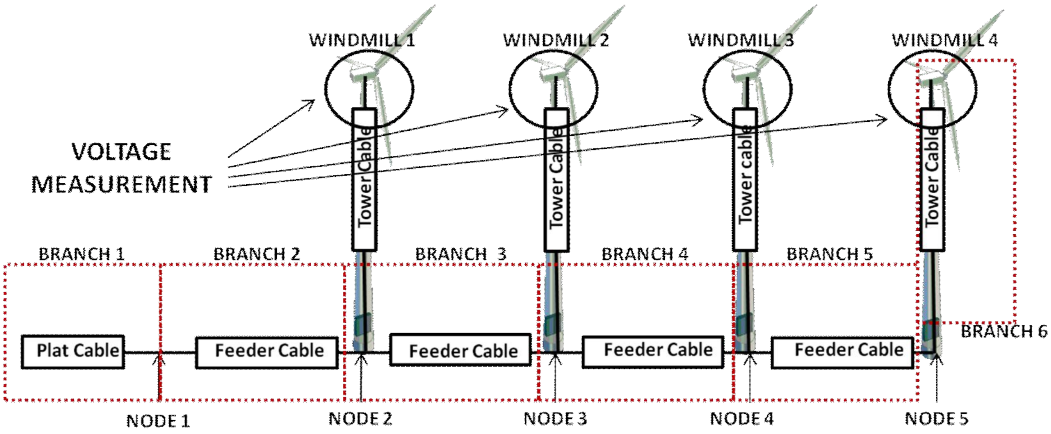

Figure 65 Case F1_W4 simulation configuration

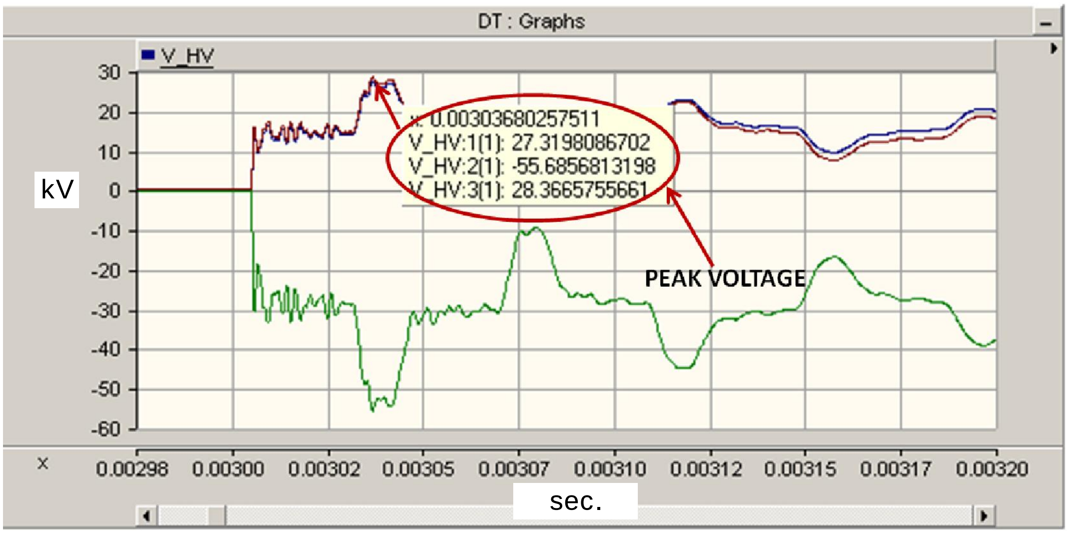

Figure 66 Voltage transient at transformer terminals, tower 1

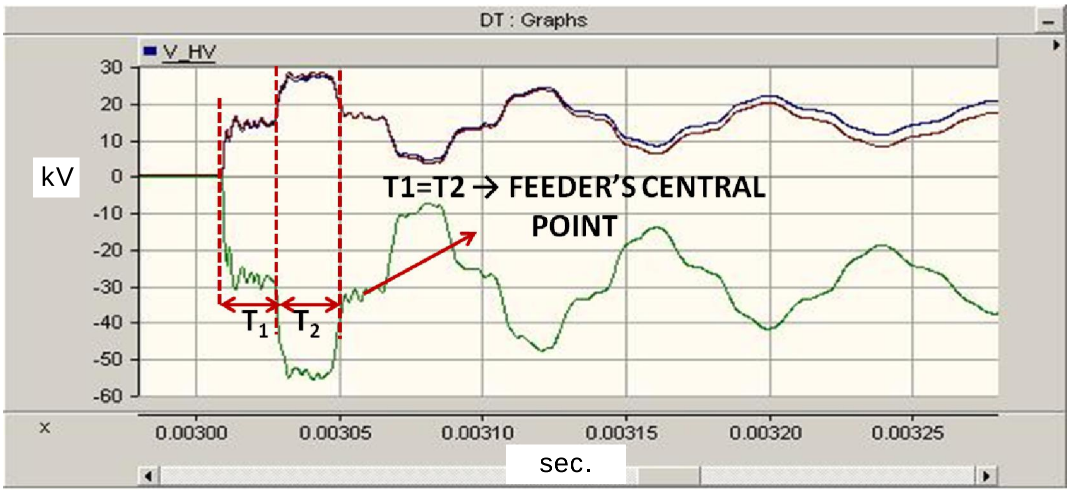

Figure 67 Voltage transient at transformer terminals, tower 2

Referring to Figure 66, there is a main voltage step 5 µs after the breaker closure, exactly the time needed to the travelling wave to cross the platform cable and the tower cable. The next significant voltage step, with positive sign, happens 25 µs after the first one, meaning that it was reflected at the last tower's top. But according to Table 10, the refraction coefficient at every tower bottom for this configuration β is 2/3, and the travelling wave originated at the platform is refracted 6 times during its travel to the feeder end and back (Figure 62), an equivalent damping of more than 90%. The reason why this voltage step can be seen at the first tower transformer terminals is that, despite the damping that results from the refraction phenomena at every tower bottom, there is also the occurrence of constructive interference in all these points, increasing the magnitude of the resultant voltage travelling wave.

After 10 µs delay there is a negative voltage step, resultant of the voltage travelling wave reflected at the voltage source's terminals, where the reflection coefficient α is -1. This cycle is repeated until the voltage transient vanishes, that happens in less than 50 µs. The reflections at the tower cable result in the higher frequency (and smaller magnitude) oscillations (period of 1 µs). The dynamic for the other towers are the same. The only difference is the time delay between these main voltage steps, once they refer to the relative position of the tower between the voltage source and the feeder end.

The voltage peaks experienced for each transformer are summarized on Table 14.

Table 14 Voltage peaks at transformer terminals – CASE F1_W4

	Phase A	*Phase B*	*Phase C*
Windmill 1	27.20 kV	28.23 kV	-55.43 kV
Windmill 2	26.81 kV	27.94 kV	-54.74 kV
Windmill 3	27.08 kV	28.35 kV	-55.43 kV
Windmill 4	26.25 kV	27.73 kV	-56.98 kV

Case F4_W4

The dynamic of the transient propagation in this case is very similar to the F1_W4 case. As the travelling wave comes always from the platform and all the feeders are identical, the voltage transients experienced in the first feeder are the same experienced by the others. The reflection and refraction coefficients are summarized in Table 11, and the voltage peaks experienced for each transformer are summarized on Table 15.

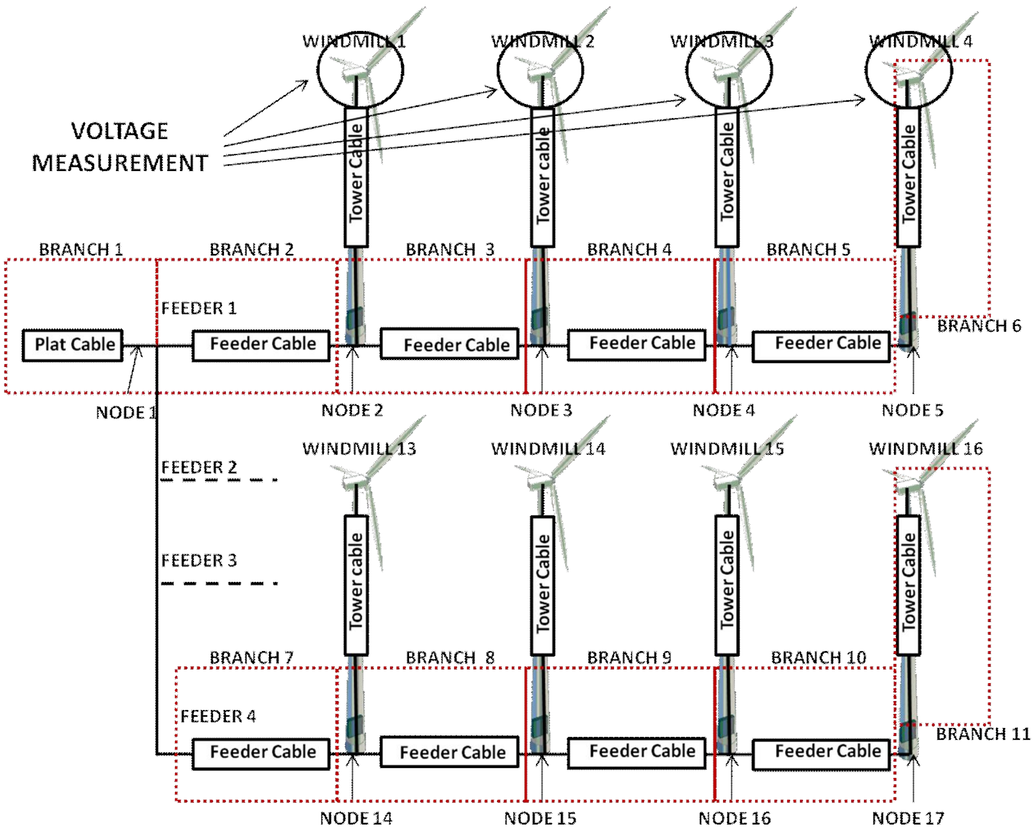

Figure 68 Case F4_W4 simulation configuration

Table 15 Voltage peaks at transformer terminals – CASE F4_W4

	Phase A	*Phase B*	*Phase C*
Windmill 1	26.72 kV	27.67 kV	-54.40 kV
Windmill 2	26.96 kV	28.00 kV	-54.97 kV
Windmill 3	27.28 kV	28.00 kV	-55.28 kV
Windmill 4	27.69 kV	28.29 kV	-55.99 kV

Case F6_W6

The dynamic of the transient propagation in this case is very similar to the previous ones. The reflection and refraction coefficients are summarized in Table 12, and the voltage peaks experienced for each transformer are summarized on Table 16.

Table 16 Voltage peaks at transformer terminals – CASE F6_W6

	Phase A	*Phase B*	*Phase C*
Windmill 1	25.79 kV	26.44 kV	-52.24 kV
Windmill 2	26.25 kV	26.82 kV	-53.07 kV
Windmill 3	26.49 kV	26.96 kV	-53.45 kV
Windmill 4	26.73 kV	27.08 kV	-53.82 kV
Windmill 5	26.82 kV	27.04 kV	-53.86 kV
Windmill 6	27.19 kV	27.32 kV	-54.52 kV

Case STAR_7

In this case, the central point is the node where the travelling waves being reflected at all 7 feeders can be added due to the physical symmetry. However, as the refraction coefficient β (Table 13) is very low, the voltage transients' multiplication at this point is still not enough to create a peak voltage higher than the BIL recommended by IEEE Standard [24]. The wave form of the voltage transient experienced by transformers at windmills 1-6 is shown in Figure 68, and the voltage peaks in each transformer are summarized on Table 17.

Table 17 Voltage peaks at transformer terminals – CASE STAR_7

	Phase A	*Phase B*	*Phase C*
Windmills 1-6	30.02 kV	30.19 kV	-60.21 kV
Windmill 7	29.64 kV	29.83 kV	-59.47 kV

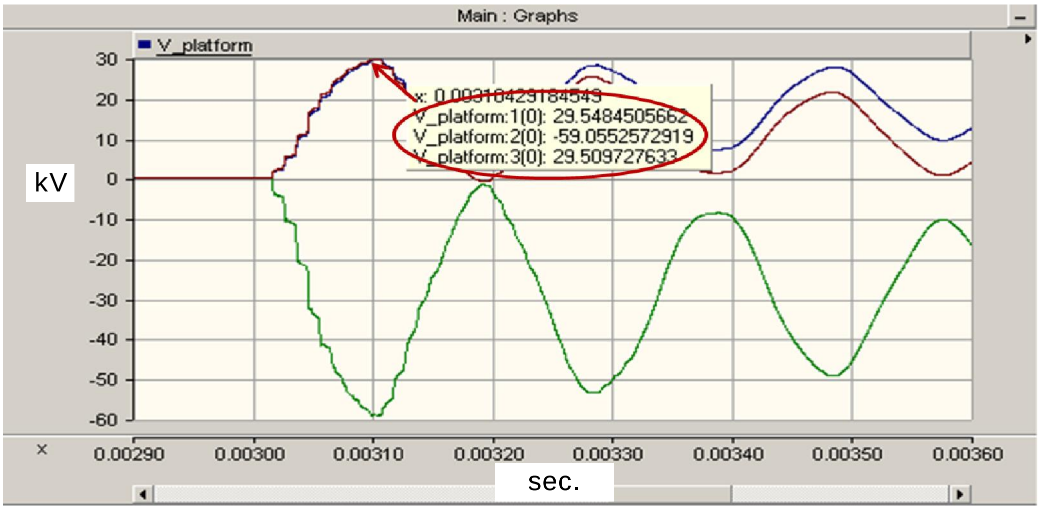

Figure 69 Voltage transient at transformer terminals, towers 1-6

5.1.5 Conclusions

Investigation on multiple reflections and refractions found that in cable grid configuration with a lot of reflection and refraction points and interference occurrence at every tower bottom (or at the central node for the star configurations), an overvoltage is not built up to a level much higher than original voltage source magnitude. This happens because the usual connection of the cables and its typical surge impedance values results in refraction coefficients most of the times smaller than 1, many times even around 0.5, making the damping effect very significant due to consecutive refractions. This way, while at one side the multiple reflections and occurrence of constructive interference increase the transient's voltage peak, the refraction coefficient smaller than 1 turns the consecutive refractions into a significant damping, acting on the opposite side.

Therefore, when the voltage source causing transient is in a magnitude of 1 pu, e.g. during energizing the grid, while at one side the multiple reflections and occurrence of constructive interference increase the transient's voltage peak, the refraction coefficient being smaller than 1 turns the consecutive refractions into a significant damping effect, acting on the opposite side. The result is overvoltage levels occur lower than recommended by the Basic Impulse Level test in IEEE Standard [23] and [24].

5.2 Transient phenomena and effectiveness of surge mitigation devices in large wind park

As mentioned in Section 4.1, the wind cable laboratory circuit had limitation for studying the impact of surge mitigation devices in large wind park. Therefore, once the models validation was done as presented in Section 4.2, the transient phenomena and effectiveness of surge mitigation devices in large wind park were studied using PSCAD/EMTDC, as it will be presented in the following Sections.

Two relatively large wind parks of 40 MW and 100 MW installed capacity were studied. Simulations are focused on the use of different choke concepts to mitigate transient in large wind farms [27]-[29]. As a remark , the focus on choke concepts were made with consideration that mitigation effectiveness of other conceptual methods were tested and analysed already in [1] as well as in Chapter 3.

5.2.1 Simulation Setup

A wind park model was developed with PSCAD representing a radial wind-collection grid with 4 feeders and 5 wind mills (wind turbine generators) in each feeder, thus 20 wind mills in the whole wind park. The collection grid was designed to operate at medium voltage level (30 kV-rms) and the wind park was connected to the grid at high voltage level 150 kV-rms. The system frequency was 50 Hz.

Figure 70 shows how the point of common coupling (PCC) was modelled and Figure 71 shows the layout of the wind collection grid.

Two wind park sizes were modelled in this work, namely (1) 40 MW wind park and (2) 100 MW wind park. In the 40 MW wind park, each wind turbine generator shown in Figure 71 is equipped with a 2 MW generator (thus total 20 x 2 MW = 40 MW), while in the 100 MW wind park, each wind turbine generator shown in Figure 71 is equipped with a 5 MW generator (thus total 20 x 5 MW = 100 MW). The models of the 2 MW and 5 MW wind generator installed in the wind mill are shown respectively in Figure 72 and Figure 73. A remark can be made here that Figure 72 and Figure 73 show the case when the transformer in the wind mill is installed at the nacelle (the generator and the wind transformer are connected via an LV cable).

<u>Point of common coupling (PCC)</u>

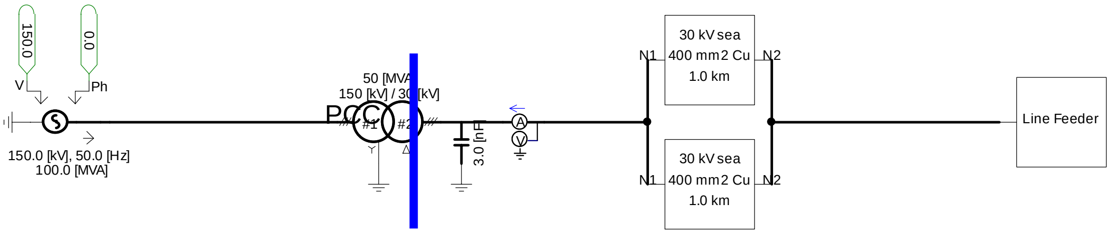

Figure 70 Point of common coupling (PCC)

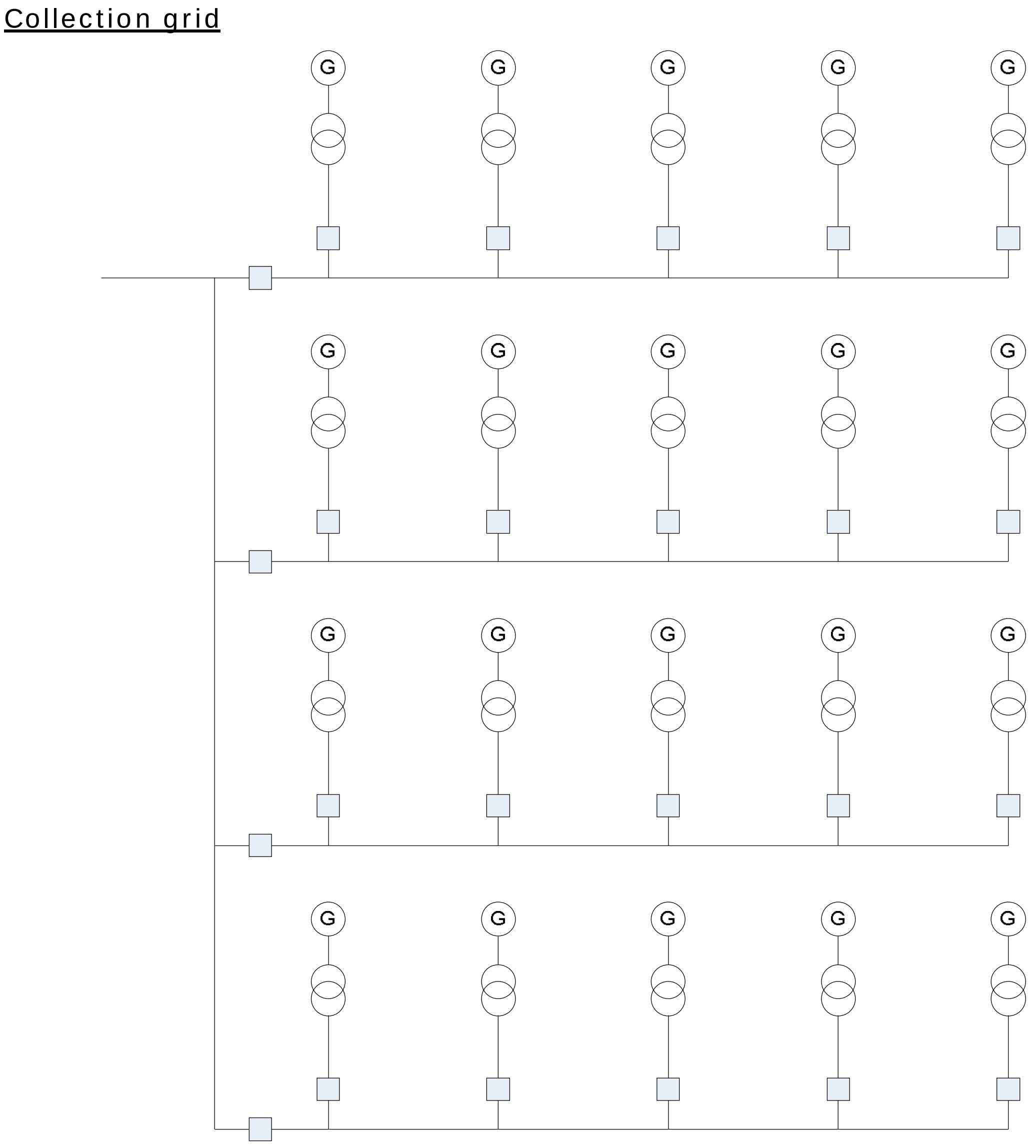

(a)

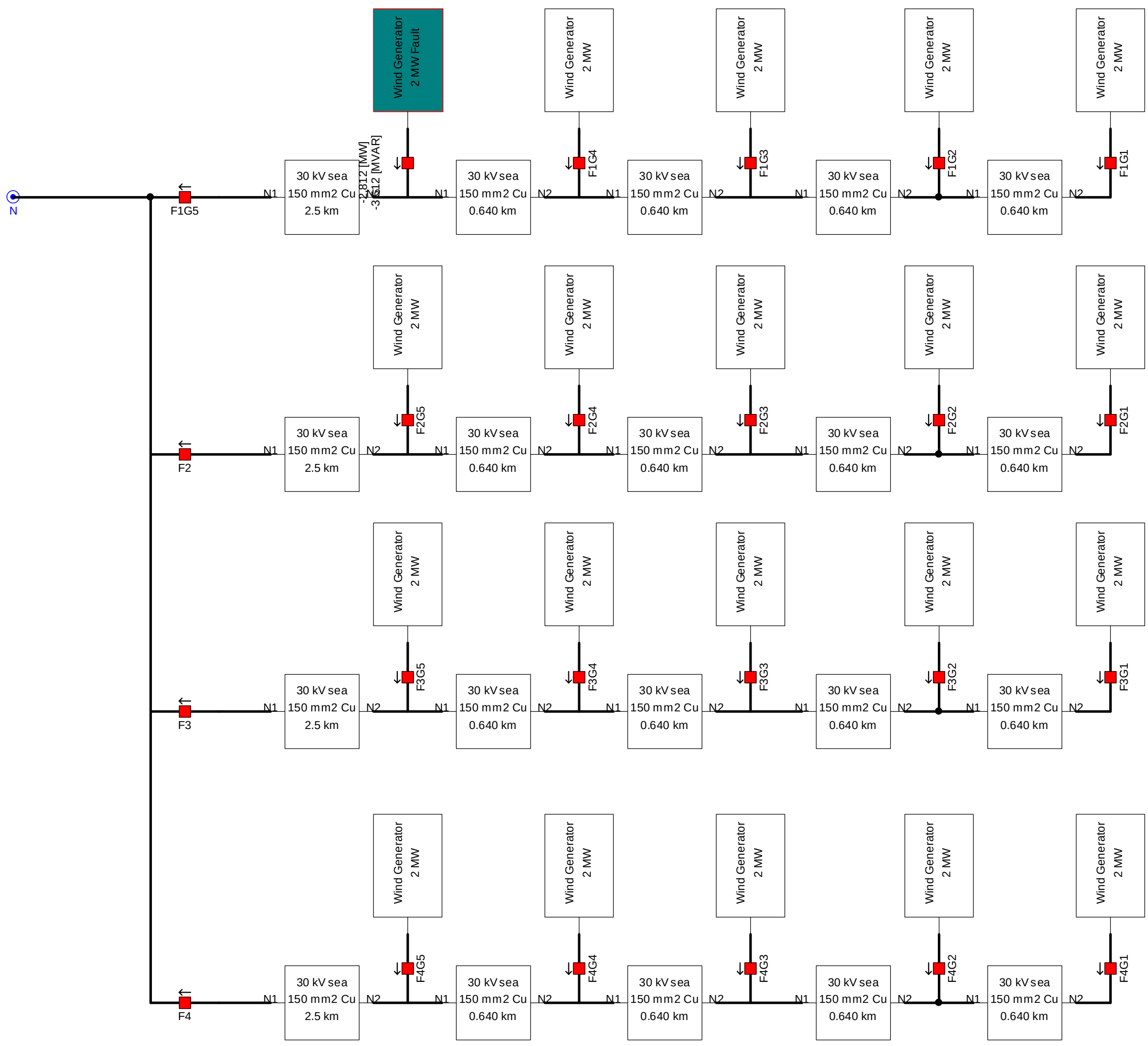

Figure 71 Wind collection grid layout: Wind park illustration (a) and Wind park with parameters written in PSCAD (b)

2 MW Wind Turbine Generator in 40 MW Wind Park

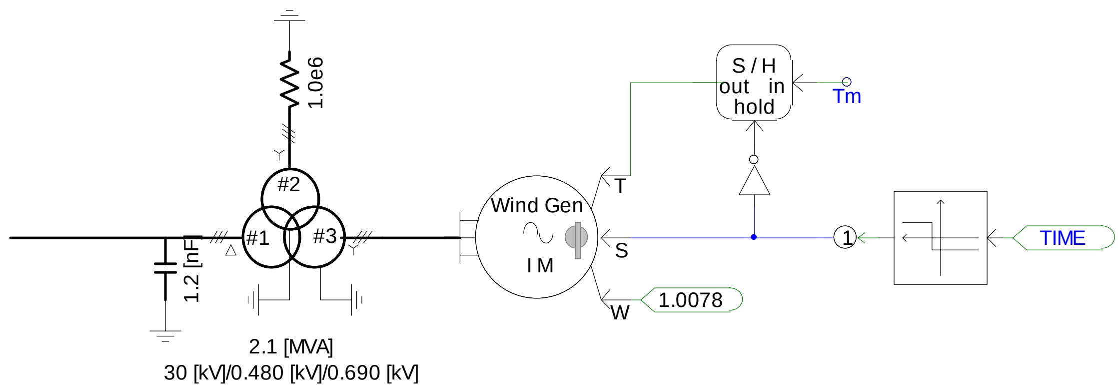

Figure 72 2 MW wind turbine generator in 40 MW wind park

5 MW Wind Turbine Generator in 100 MW Wind Park

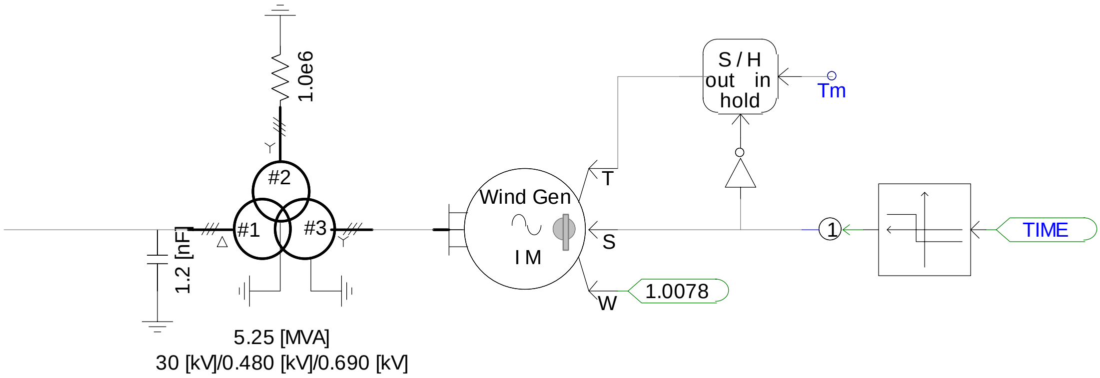

Figure 73 5 MW wind turbine generator in 100 MW wind park

5.2.2 Simulation scenarios

Several simulation scenarios were developed to investigate the effectiveness of the mitigation methods against electrical transients. The relevant simulation scenarios are discussed as follow:

Wind turbine layouts

Two wind turbine layouts are considered as:

1. The wind transformer is placed in the nacelle and the breaker is at the bottom of the wind mill tower, see Figure 74.
2. Both the wind transformer and the breaker are placed at the bottom of the wind mill tower, see Figure 75.

Remarks can be made that the circuit breaker is connected at point “N” in Figure 74 and Figure 75, moreover, a short medium voltage cable (5 m) connects the wind transformer and the circuit breaker in the wind turbine layout 2 (Figure 75).

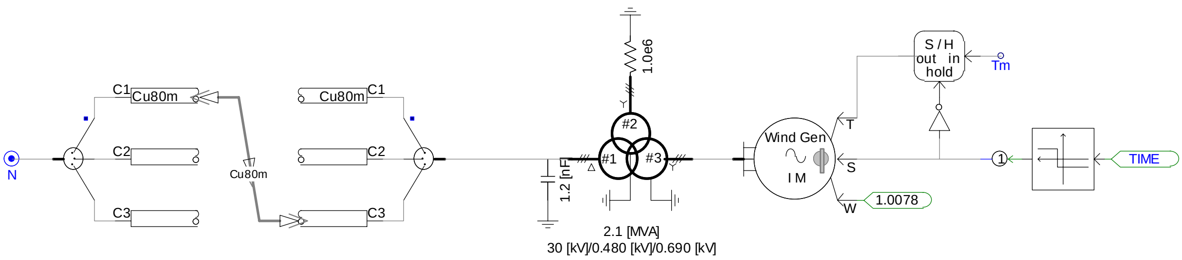

Figure 74 Wind turbine layout 1

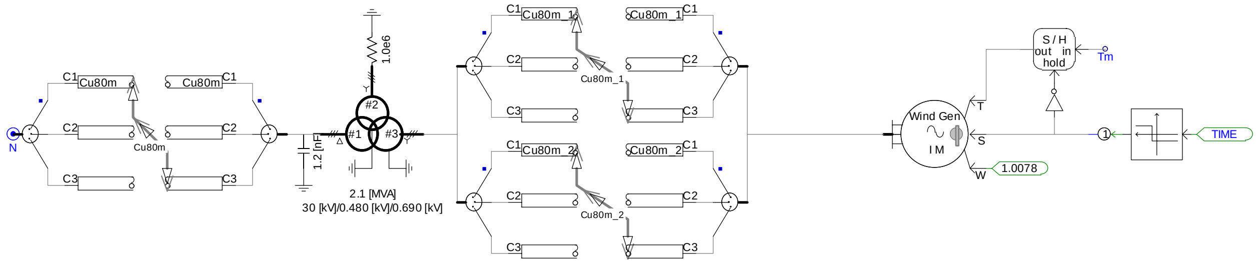

Figure 75 Wind turbine layout 2

Breaker operation

Two breaker operations were considered:

1. Opening the circuit breaker at full load (full power generation), see Figure 76.
2. Opening the circuit breaker to clear three-phase fault at wind generator terminal, see Figure 77.

A remark should be made that an algorithm has been developed within this simulation assuming that the breaker is always opening at the "worst case", i.e. when the current chopping level is at the highest value.

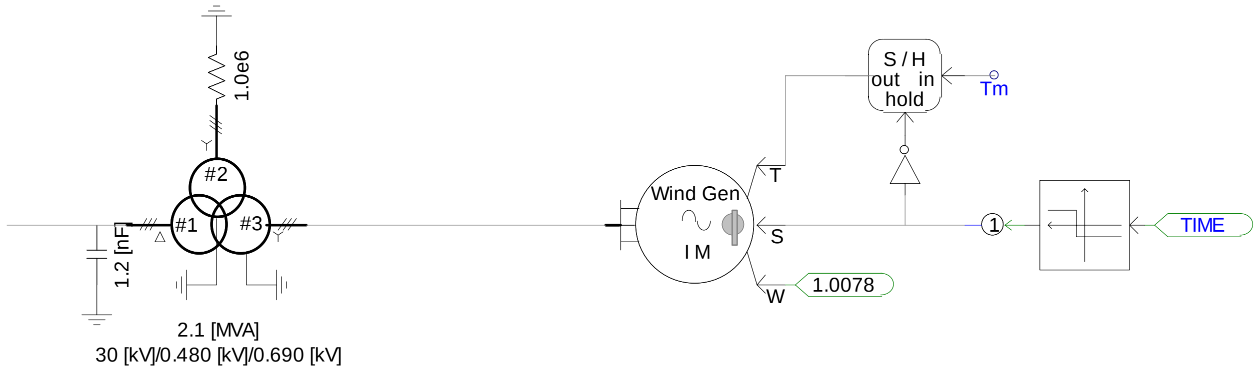

Figure 76 Opening the circuit breaker at full power generation

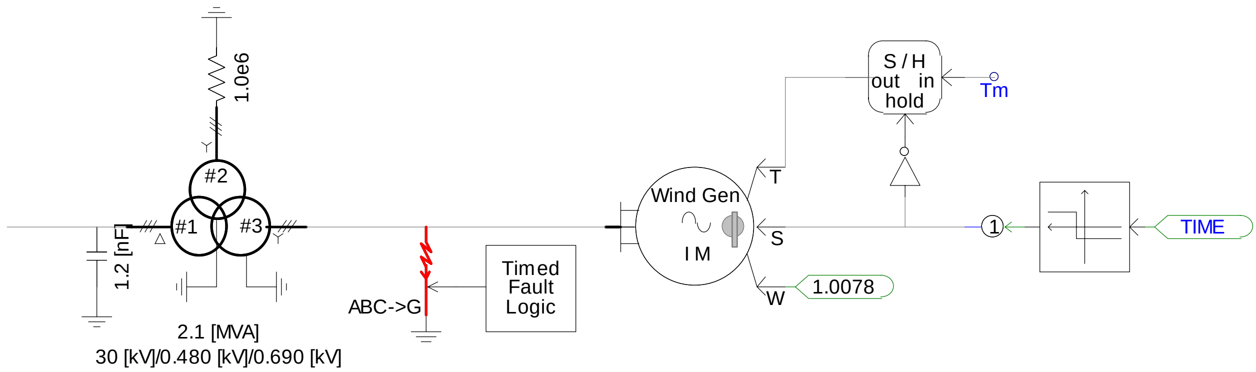

Figure 77 Opening the circuit breaker to clear three-phase fault at wind generator terminal

Wind turbine location

Two wind mills (wind turbine generators) of interest are considered based on the location in the feeders within the wind collection grid:

1. First wind turbine in the feeder, see the green block in Figure 78.
2. Last wind turbine in the feeder, see the green block in Figure 79.

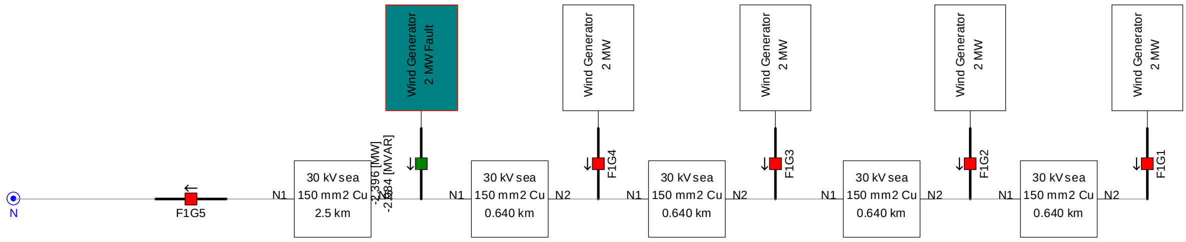

Figure 78 First wind turbine in the feeder

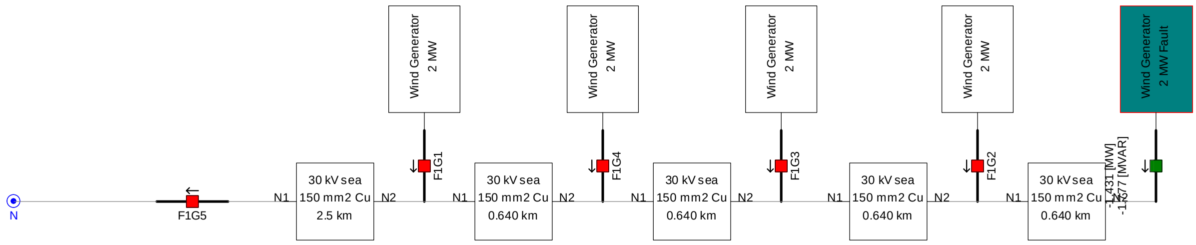

Figure 79 Last wind turbine in the feeder

Switching location

Two switching locations are considered:

1. Switching breaker at wind mill (wind turbine generator, RMU), see Figure 80 (the breaker pointed by the arrow in the figure).
2. Switching breaker at PCC platform, see Figure 81 (the breaker pointed by the arrow in the figure).

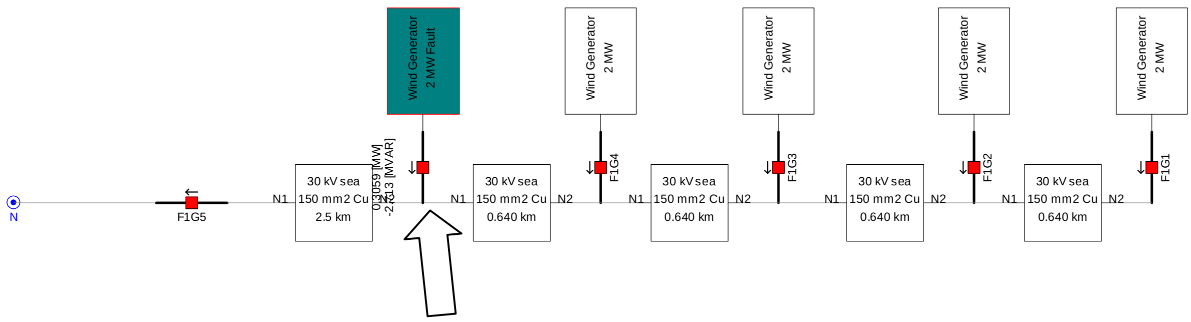

Figure 80 Switching breaker at wind mill (wind turbine generator, RMU)

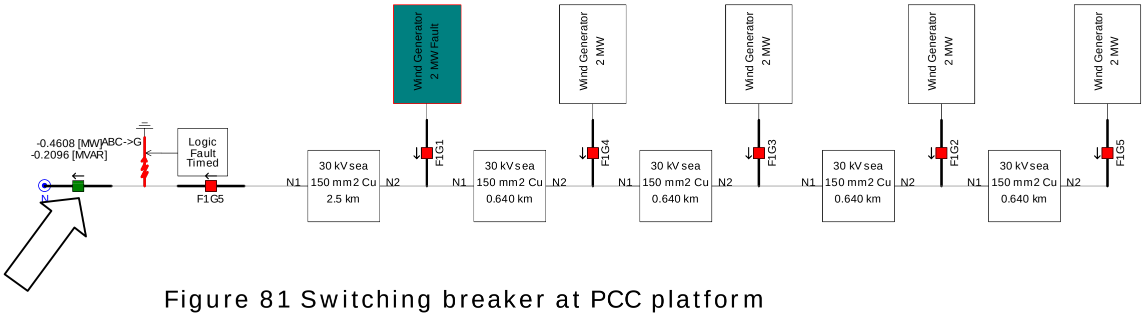

Figure 81 Switching breaker at PCC platform

5.2.3 Surge mitigation methods using choke concepts

A large number of simulation cases were investigated based on the simulation

- Smart Choke, see Figure 82.
- Smart Choke with 10 nF surge capacitor, see Figure 83.
- Simple Choke, see Figure 84.
- Simple Choke with 10 nF surge capacitor, see Figure 85.

To be implemented at the circuit breaker terminals (RMU), see Figure 86

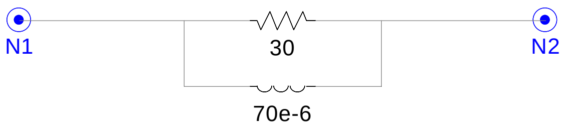

Figure 82 Smart Choke

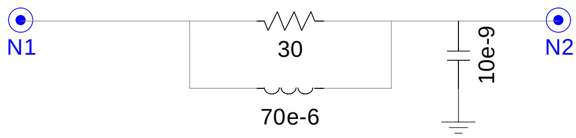

Figure 83 Smart Choke with 10 nF surge capacitor

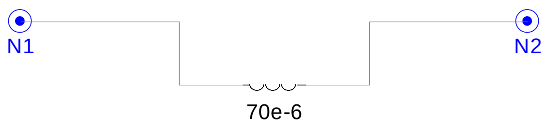

Figure 84 Simple Choke

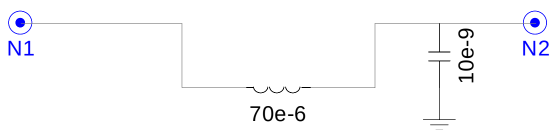

Figure 85 Simple Choke with 10 nF surge capacitor

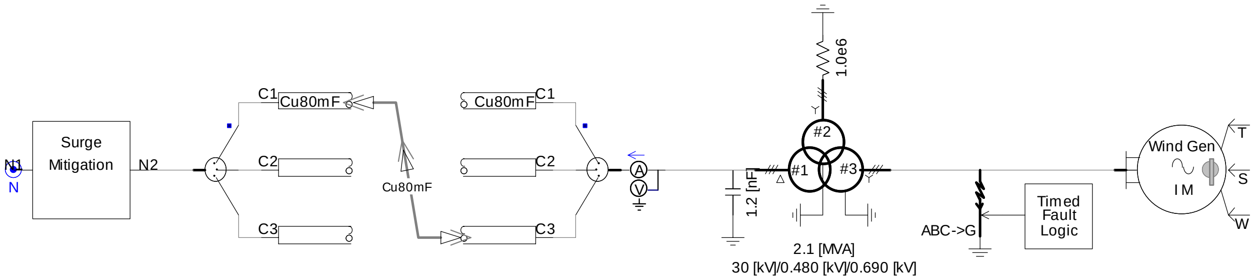

Figure 86 Implementing surge mitigation device at the circuit breaker terminals (connected to point "N")

5.2.4 Test cases

Based on simulation scenarios defined in Section 5.2.2, five group of cases can be further defined as the test cases. These groups of test cases are listed in Table 18 to Table 22.

<u>Group cases A</u>

Table 18 lists the cases simulated for the purpose of studying transient characteristics within a typical wind park. Based on simulations done within this group of cases, a worst case will be selected as a base for further simulations of electrical transient in larger wind park where the impact of surge mitigation devices will be investigated.

Table 18 Group cases A

Group Cases A	*To study transient characteristics within a typical wind park, then selected one transient case to simulate further with larger wind park and to simulate the impact of surge mitigation device.*					
Case ID	Wind park size	Wind transformer layout	Capacitor installed at generator	Opening breaker at	Wind turbine in focus in feeder	Switching at
Case_40V_N_FL_1	40 MW	At nacelle	No	Fault at gen terminal	First wind turbine	RMU
Case_40V_N_FL_5	40 MW	At nacelle	No	Fault at gen terminal	Last wind turbine	RMU
Case_40V_N_OL_1	40 MW	At nacelle	No	Full load	First wind turbine	RMU
Case_40V_N_OL_5	40 MW	At nacelle	No	Full load	Last wind turbine	RMU
Case_40V_Y_FL_1	40 MW	At nacelle	Yes	Fault at gen terminal	First wind turbine	RMU
Case_40V_Y_FL_5	40 MW	At nacelle	Yes	Fault at gen terminal	Last wind turbine	RMU
Case_40V_Y_OL_1	40 MW	At nacelle	Yes	Full load	First wind turbine	RMU
Case_40V_Y_OL_5	40 MW	At nacelle	Yes	Full load	Last wind turbine	RMU

Group cases B

Table 19 lists the cases simulated for the purpose of studying transient characteristics within 40 MW with transformer at nacelle, and compares the transient characteristics with and without surge mitigation devices.

Table 19 Group cases B

Group Cases B	*To study transient characteristics within 40 MW with transformer at nacelle, and compare the transient characteristics with and without surge mitigation devices.*					
Case ID	Wind park size	Wind transformer layout	Capacitor installed at generator	Opening breaker at	Wind turbine in focus in feeder	Switching at
Case_40V_N_OF_1	40 MW	At nacelle	No	Fault at gen terminal	First wind turbine	RMU
Case_40V_N_OF_S3	40 MW	At nacelle	No	Fault at gen terminal	First wind turbine	RMU
Case_40V_N_OF_S4	40 MW	At nacelle	No	Fault at gen terminal	First wind turbine	RMU
Case_40V_N_OF_S5	40 MW	At nacelle	No	Fault at gen terminal	First wind turbine	RMU
Case_40V_N_OF_S6	40 MW	At nacelle	No	Fault at gen terminal	First wind turbine	RMU

Group cases C

Table 20 lists the cases simulated for the purpose of studying transient characteristics within 40 MW with transformer at bottom of wind turbine tower and compares the transient characteristics with and without surge mitigation devices.

Table 20 Group cases C

Group Cases C	*To study transient characteristics within 40 MW with transformer at bottom of wind turbine tower and compare the transient characteristics with and without surge mitigation devices.*					
Case ID	Wind park size	Wind transformer layout	Capacitor installed at generator	Opening breaker at	Wind turbine in focus in feeder	Switching at
Case_40S_N_OF_1	40 MW	At bottom of tower	No	Fault at gen terminal	First wind turbine	RMU
Case_40S_N_OF_S3	40 MW	At bottom of tower	No	Fault at gen terminal	First wind turbine	RMU
Case_40S_N_OF_S4	40 MW	At bottom of tower	No	Fault at gen terminal	First wind turbine	RMU
Case_40S_N_OF_S5	40 MW	At bottom of tower	No	Fault at gen terminal	First wind turbine	RMU
Case_40S_N_OF_S6	40 MW	At bottom of tower	No	Fault at gen terminal	First wind turbine	RMU

Group cases D

Table 21 lists the cases simulated for the purpose of studying transient characteristics within 100 MW, and compares the transient characteristics with and without smart choke[2].

Table 21 Group cases D

Group Cases D	*To study transient characteristics within 100 MW, and compare the transient characteristics with and without smart choke.*					
Case ID	Wind park size	Wind transformer layout	Capacitor installed at generator	Opening breaker at	Wind turbine in focus in feeder	Switching at
Case_100V_N_OF_1	100 MW	At nacelle	No	Fault at gen terminal	First wind turbine	RMU
Case_100V_N_OF_1_S3	100 MW	At nacelle	No	Fault at gen terminal	First wind turbine	RMU

Group cases E

Table 22 lists the cases simulated for the purpose of studying transient characteristics with switching operations at the platform. [?]

Table 22 Group cases E

Group Cases E	*To study transient characteristics with switching action at breaker platform*					
Case ID	Wind park size	Wind transformer layout	Capacitor installed at generator	Opening breaker at	Wind turbine in focus in feeder	Switching at
Case_40V_N_OF_P	40 MW	At nacelle	No	Fault at platform terminal	First wind turbine	Platform
Case_40V_N_OF_P_S3	40 MW	At nacelle	No	Fault at platform terminal	First wind turbine	Platform

[2] Results obtained from simulations on group cases B and C suggest that smart-choke can mitigate transients large wind park due to clearing of the fault at wind generator terminals. Therefore in the further group cases D and E, only smart-choke is simulated as the surge mitigation device.

5.2.5 Simulation results

The characteristics of electrical transients in large wind park were investigated by means of simulations on the test cases in the group cases A. Due to limited space in this report, detail results of the simulations are presented in separate supplement to this report [26]. However, some highlights can be made based on the transient overvoltage quantification[3] as follows:

- Opening the breaker at full generation capacity results in less transient overvoltages than opening the breaker to clear faults at the generator terminals.
- Installing surge capacitors at generator may help reducing the transient overvoltages, although it is less obvious in the case of clearing faults.
- Transient overvoltages obtained during operating a breaker at the first wind mill in a feeder may be higher than during operating a breaker at the last wind mill in the feeder.

Based on these findings, it was decided from this point forward that simulations in the latter group cases B-E will be concentrated on opening the breaker for clearing fault at the generator terminals of the first wind mill in a feeder. The four surge mitigation methods considered in Section 5.2.3 were simulated, firstly within the 40 MW wind farms (groups cases B and D), and later the most effective surge mitigation device is simulated within the 100 MW wind farms as well as within the operation of the breaker at the wind farm platform.

Detailed simulation results, as well as the transient overvoltage quantification, are presented in supplement to this report [26]. From the results obtained from the simulations however, some highlights can be listed as follow:

- Plain Smart Choke and Smart Choke with 10 nF surge capacitor are the most effective mitigation methods both for the layout where the wind transformer is implemented at the nacelle as well as for the layout where the wind transformer is implemented at the bottom of the wind mill tower. The effectiveness is observed when the simulation results with Smart Choke or Smart Choke with 10 nF surge capacitor is compared to the base case (when no surge mitigation device is applied).
- However, it is observed that implementing Smart Choke alone, without the additional small surge capacitor is already effective to mitigate the effect of transient overvoltages that would be resulted from opening breaker to clear fault i.e. when no other surge mitigation device is used.
- Simple Choke and Simple Choke with 10 nF surge capacitor are quite effective for mitigating overvoltage transients in a layout where the wind transformer is implemented at the nacelle. However they are not effective when implemented in a layout where the wind transformer is

[3] The transient overvoltages quantification method [1] is applied and expanded on each of the simulation data of the voltages at the wind transformer terminals.

implemented at the bottom of the wind mill tower. In such a case, resonant phenomena were observed.

- As a remark, the effectiveness of Smart Chokes for mitigation of transient overvoltages can be explained by the fact that the Smart Choke the resistor part has a damping effect on the current oscillation after the breaker contact opening point in such a way that the high frequency zero crossing current is prevented., while the transient recovery voltage is still low (building up). The following current interruption occurs on condition that the breaker withstand voltage is sufficiently high compared with the transient recovery voltage, in order to prevent further re-ignitions. The complementary case is when the transient recovery voltage exceeds the withstand voltage causing re-ignitions, see Figure 87

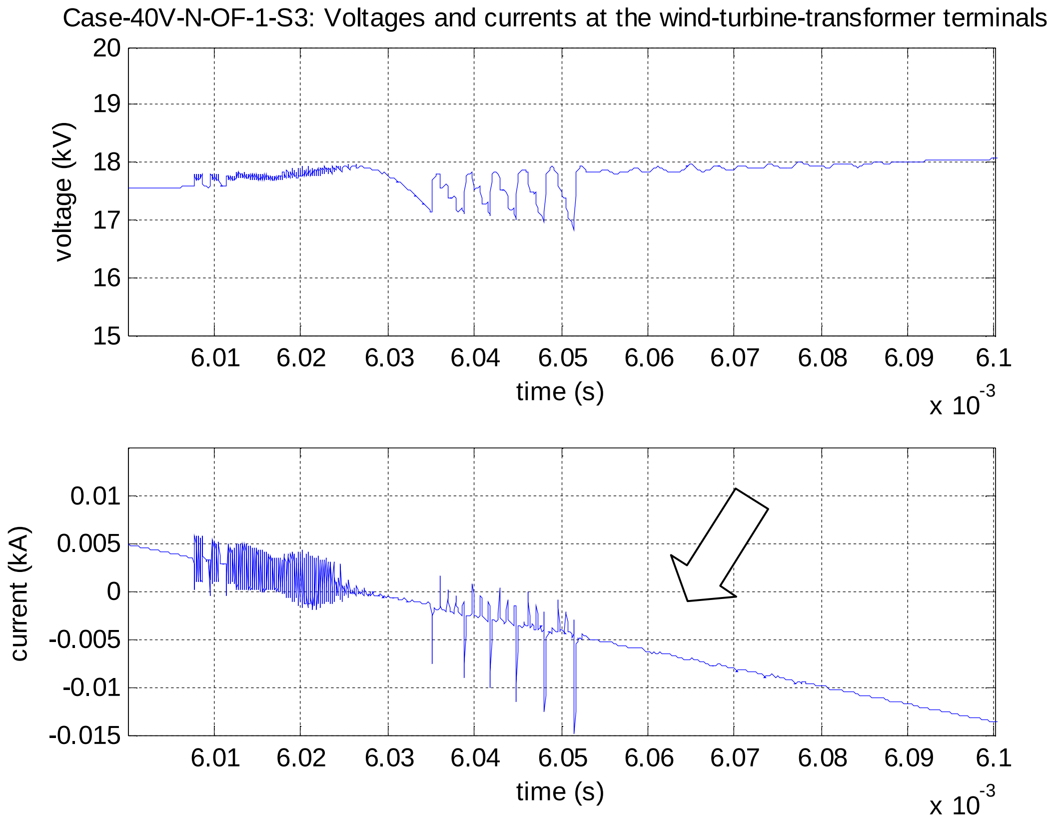

Figure 87 Prevented high frequency currents to cross the zero value

6 Conclusions and future works

This work - High Frequency Transients in Large Wind Farm: Advanced Measurement and Characterization done in 2010-2011 with support from Elfrosk program Vindforsk III, project V-326, together with the earlier work of cable system transient study done in 2007-2008 under support of Elforsk program Vindforsk II, project V-110 [1] confirms the existence of transient overvoltage phenomena in a cable system.

- Both experimental results and extended simulation study results confirm voltage transients casused by interaction between different apparatus with specific circuits conditions and and parameters (electrical and mechanical characteristics).
- Repetitive voltage transients with higher time derivatives than standard lightning impulse test have been recorded, analyzed and confirmed with different (real) apparatus (transformers: oil type, dry type, breakers) and test setup (voltage levels, surge arrester protection levels).
- Exsisting standard lightning impulse tests do not consider repetitive voltage transients with steep fronts but with magnitudes lower than the anticipated risk levels.
- Surge arresters always limit the maximum voltage magnitude but voltage steps with a magnitude twice the protective level can occur while the voltage swing within a band in magnitude below the surge arrester protection level, i.e. from negative to positive polarity.
- Surge capacitors and the RC-protection show mitigation effects although not removing the repetitive transients completely.

Furthermore, results from the laboratory experiments (2007-2008 as well as 2010-2011) have been used to validate computer simulation models developed within this project. The models were successfully calibrated to represent the laboratory measurements. Therefore, the models allow for the use of computer simulation with confidence as a virtual expansion of the wind cable laboratory as well as for expanded investigations of transient phenomena in large wind farms, such as multiple reflection and refraction as well as the impact of transient mitigation methods in large wind parks are performed using the same validated models with higher degree of confidence.

Investigation on multiple reflections and refractions found that in a cable grid configuration with a lot of reflection and refraction points and interference occurrence at every tower bottom (or at the central node for the star configurations), an overvoltage is not attenuated to a level much higher than the original voltage source magnitude. This is because the usual connection of the cables and its typical surge impedance values results in refraction coefficients mainly smaller than 1.0, commonly even around 0.5, gives a significant damping effect due to consecutive refractions. This way, while at one side the multiple reflections and occurrence of constructive interference increase the transient’s voltage peak, a refraction coefficient smaller than 1.0

turns the consecutive refractions into a significant damping effect, acting on the opposite side.

When investigation on characteristics of electrical transients in large wind farm by means of simulations was performed on two relatively large wind parks of 40 MW and 100 MW installed capacity, the following general phenomena were observed:

- Opening the breaker at full generation results in less transient overvoltages then opening the breaker to clear faults at the generator terminals.
- Installing surge capacitors at the generator may help reducing the transient overvoltages, although less obvious in the case of clearing faults.
- Transient overvoltages obtained during operating a breaker at the first wind mill in a feeder may be higher than during operating a breaker at the last wind mill in a feeder.

Furthermore, as a compliment to previous study [1] as well as in Chapter 3 of this report where mitigation effectiveness of other conceptual methods – except the choke concept – were tested and analysed, simulations of large wind farms were performed with focus on the use of various choke concepts to mitigate transients, where the effectiveness of these choke concepts are shown. As a remark, the effectiveness of Smart Chokes for mitigation of transient overvoltages can be explained by the fact that the Smart Choke the resistor part has a damping effect on the current oscillation after the breaker contact opening point in such a way that the high frequency zero crossing current is prevented., while the transient recovery voltage is still low (building up). The following current interruption occurs on condition that the breaker withstand voltage is sufficiently high compared with the transient recovery voltage, in order to prevent further re-ignitions. The complementary case is when the transient recovery voltage exceeds the withstand voltage causing re-ignitions.

It is not within the scope of this work to determine what is a dangerous (respectively, a safe) level of steepness of transient overvoltages. Nevertheless, the understanding transient characteristics is required for dimensioning related components, insulation coordination of the components within large cable-based systems as well as implementation of effective mitigation and prevention methods.

7 References

[1] M. Reza, H. Breder, "Cable System Transient Study". Vindforsk V-110, Elfrosk report 09:05, January 2009. Available online at: http://www.elforsk.se/Global/Vindforsk/Rapporter%20fran%20Vindforsk%20II/09_05_rapport.pdf

[2] Erik Persson, "Transient Effect in Application of PWM Inverters to Induction Motors," *IEEE Transaction on Industry Applications*, vol. 28, no. 5, pp. 1095-1101, Sep./Oct. 1992.

[3] S.M.Wong, L.A.Snider, E.W.C.Lo, ''Overvoltages and reignition behavior of vacuum circuit breaker,'' *International Conference on Power Systems Transients - IPST 2003 in New Orleans, USA*, 2003.

[4] P.Picot, 'Vacuum switching,'' *Cahier technique Schneider Electric*, no. 198, pp. 4, March 2000.

[5] A. Mazur, I. Kerszenbaum, and J. Frank, ''Maximum insulation stresses under transient voltages in the HV barrel type winding of distribution and power transformers,'' *IEEE Transaction on Industry Applications*, Vol. 24, pp. 427-433, May-June 1988.

[6] D. Paul, ''Failure Analysis of Dry-Type Power Transformer,'' *IEEE Transaction on Industry Applications*, Vol. 37 No. 3, May-June 2001.

[7] M. Olsen, ''Failure Analysis of Siemens Geafol Cast-resin Transformer,'' Danish Technological Institute, Technical Report No. 1154834-1, May 2003

[8] D.D. Shipp, T.J. Dionise, V. Lorch, B.G. MacFarlane, ''Transformer Failure Due to Circuit-Breaker-Induced Switching Transients,'' *IEEE Transaction on Industry Applications,* Vol. 47 No. 2 pp. 707-718 March-April 2011.

[9] D.J.Clare, ''Failures of encapsulated transformers for converter winders at Oryx Mine,'' Electron Magazine, pp. 24-27, March. 1991.

[10] CIGRE working group A2-A3-B3.21, ''Electrical Environment of Transformers; Impact of fast transients,'' *ELECTRA*, 208, February 2005.

[11] W. H. Bartley, ''An Analysis of Transformer Failures, Part 2 - Causes, Prevention and Maximum Service Life,'' *The Locomotive, The Full Story,* 1997.

[12] T. Abdulahovic, "Analysis of High-Frequency Electrical Transients in Offshore Wind Parks", Chalmers University of Technology, Dissertation ISBN/ISSN: 978-91-7385-598-3, Gothenburg, 2011.

[13] B.K. Gupta, B.A.Lloyd, D.K. Sharma, ''Degradation of Turn Insulation in Motor coils Under Repetitive Surges,'' *IEEE Transaction on Energy Conversion,* Vol.5 No. 2, June 1990.

[14] G.C. Stone, R.G. Van Heeswijk, R. Bartnikas, ''Investigation of The Effect of Repetitive Voltage Surges on Epoxy Insulation,'' *IEEE Transaction on Energy Conversion,* Vol. 7 No. 4 December 1992.

[15] W. Sweet, ''Danish wind turbines take unfortunate turn,'' *Spectrum, IEEE,* vol. 41, Issue 11, pp. 30-34, Nov. 2004.

[16] J.Larssen, H.Soerensen, E.Christiansen, S. Naef,P.Völund, ''Experiences from Middelgrunden 40 MW Offshore Wind Farm,'' *Copenhagen Offshore Wind*, , 26-28 Oct. 2005.

[17] B. K. Gupta, N. E. Nilsson, D. K. Sharma, ''Protection of Motors Against High Voltage Switching Surges,'' *IEEE Transaction on Energy Conversion*, Vol. 7 No. 1, March 1992

[18] Turn Insulation Capability of Large AC Motors, EPRI Project RP 2307-1, *Final Report, EPRI EL-5862*, Vol. 1 and 2, July 1988.

[19] B. K. Gupta, B. A. Loyd, S. R. Campbell, D. K. Sharma, N. E. Nilsson, ''Turn Insulation Capability of Large AC Motors, Part 1/Surge Monitoring,'' *IEEE Transaction on Energy Conversion*, EC-2 No. 4, December 1987, pp 658-665.

[20] ''IEEE Guide for Testing Turn Insulation of Form-Wound Stator Coils for Alternating-Current Electric Machines,'' *IEEE Std 522-2004 (Revision of IEEE Std 522-1992)*, 2004.

[21] National Electrical Motor Association Standards, NEMA Standard MG1.20-2006.

[22] ''Rotating Electric Machines, Part 15: Impulse voltage withstand levels of rotating a.c. machines with form-wound coils,'' *IEC 34-15*, 1995.

[23] General Requirements for Liquid Immersed Distribution, Power and Regulating Transformers, IEEE Standard. C57.12.00-2006.

[24] General Requirements for Dry Type Ventilated Distribution, Power and Regulating Transformers, IEEE Standard. C57.12.01-2005.

[25] ABB, “XLPE Cable Systems, User’s Guide", ABB Power Technologies AB High Voltage Cables, Karlskrona.

[26] M. Reza, K. Srivastava, T. Abdulahovic, A. Marinopoulos, H. Breder, “High Frequency Transients in Large Wind Farm - Advanced Measurement and Characterization”. Elforsk rapport V-326 – Supplement. Submitted for publication in January 2012.

[27] W. Piasecki, M. Florkowski, M. Fulczyk, P. Klys, E. Stryken, P. Gawas, ”Surviving a strike”. ABB Review, No. 1, Vol 11, pp. 69-72.

[28] M. Glinkowski, W. Piasecki, M. Florkowski, M. Fulczyk, F. Arauzo, “SmartChoke- protecting power equipment from fast transients”, IEEE PES Transmision and Distribution Conference Chicago,USA, 2008

[29] W. Piasecki, M. Ostrogórska, M. Florkowski, M. Fulczyk, P. Kłys, “dU/dt protection for distribution transformers”, Int. Conf. on Power Systems Transients IPST’2009, Kyoto

8 Attachment A: Selected photographs from laboratory setup

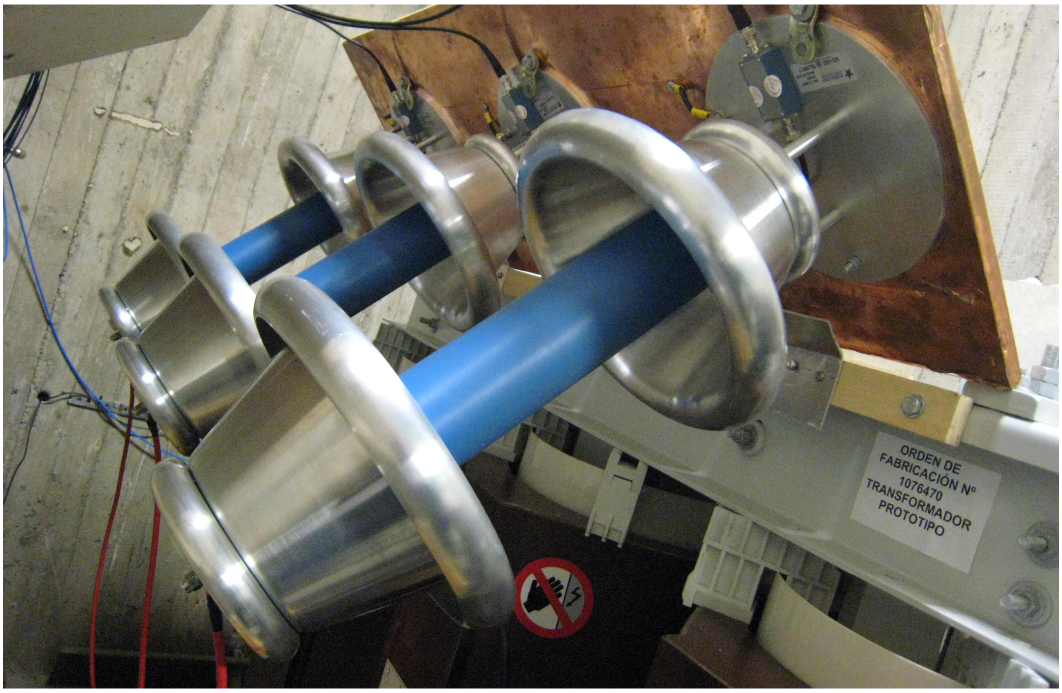

Figure 88 Voltage dividers (North-Star) installed at transformer terminal

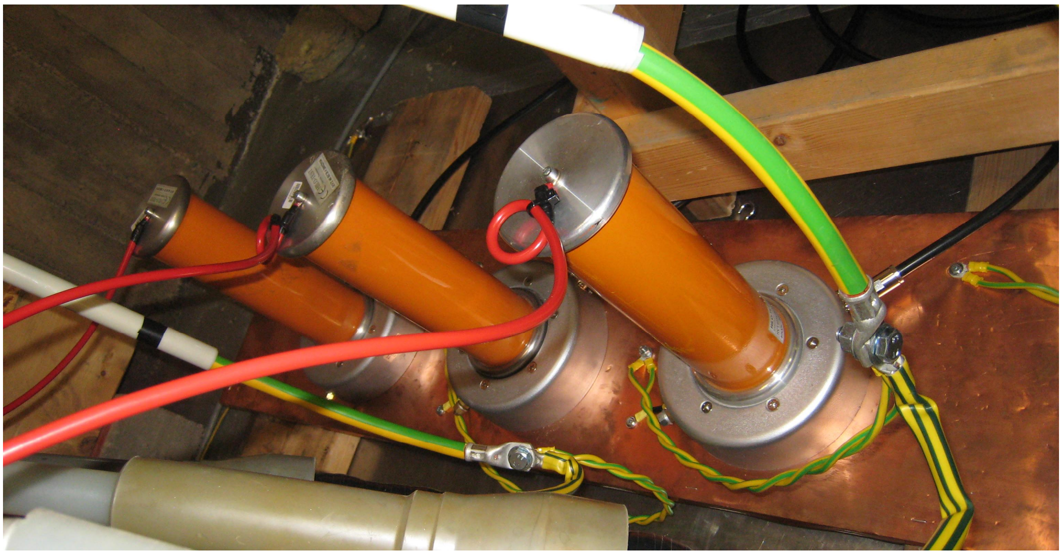

Figure 89 Voltage dividers (HILO) installed at RMU terminal

Figure 90 Current measuremen device used in laboratory experiment

Figure 91 Measurement Data transmitters and battery chargers

Figure 92 Transient data receivers and recorders

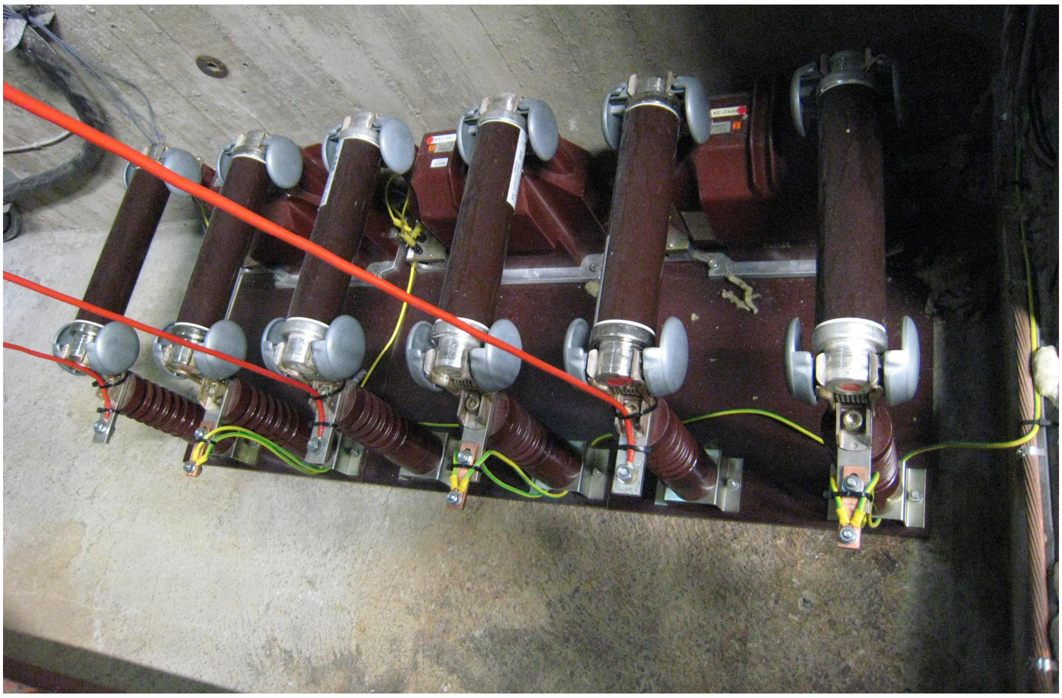

Figure 93 Artificial "grounding transformer" made of three 24 kV rated voltage transformer primary windings connected in wye, connected at the “platform switchgear”

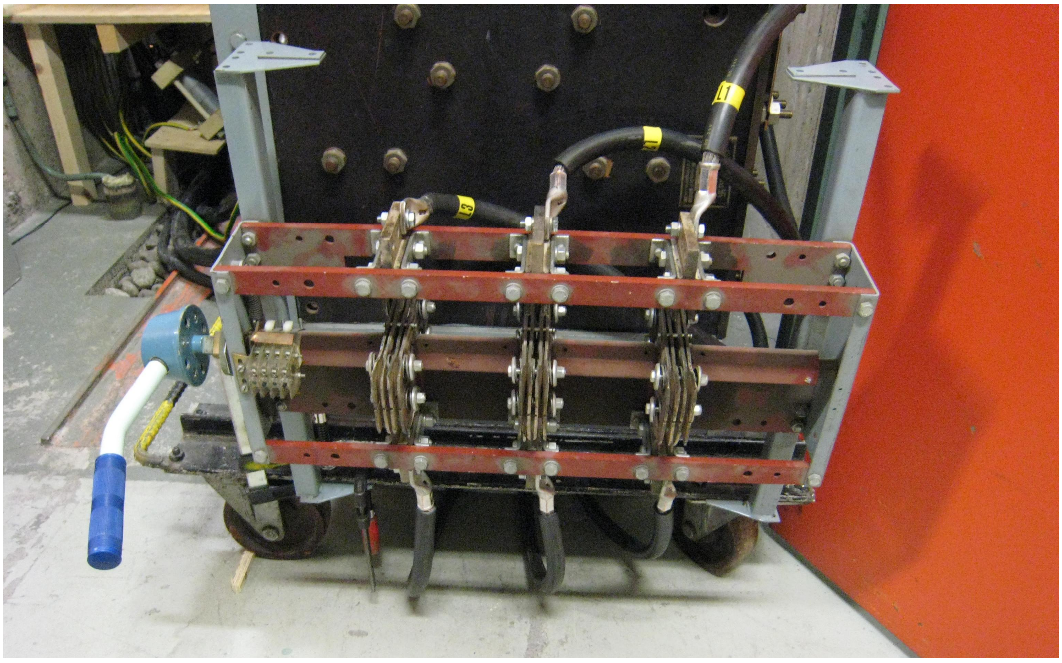

Figure 94 Load switch

Figure 95 Project team (left to right): Muhamad Reza (ABB), Lars Nordin (ABB), Daniel Johannesson (ABB), Antonis Marinopoulos (ABB), Tarik Abdulahovic (Chalmers). Not in picture: Henrik Breder (ABB) and Kailash Srivastava (ABB).

9 Attachment B: project publications

1. M. Reza, K. Srivastava, C. Roy, W. Piasecki, "Proposal to the simulation task force Cigre Working Group A2/C4.39 for studying transients on wind transformers", Cigre Workspot VI, 25-28 April 2010, Foz do Iguacu, Brazil
2. M. Reza, K. Srivastava, T. Abdulahovic, T. Thiringer, "Cable system laboratory for investigation of high frequency transients at wind turbine transformer" , Cigre Workspot VI, 25-28 April 2010, Foz do Iguacu, Brazil
3. F. S. Villar, M. Reza, K. Srivastava, L. C. P. da Silva, "High Frequency Transients Propagation and the Multiple Reflections Effect in Collection Grids for Offshore Wind Parks", IEEE Power and Energy Society General Meeting, 24-28 July 2011, Detroit, Michigan, USA
4. B. Badrzadeh, M. Hogdahl, N. Singh, H. Breder, M. Reza, "Transients in Wind Power Plants – Part II: Case Studies", IEEE Industry Applications Society Annual Meeting, 9-13 October 2011, Orlando, Flordia, USA
5. M. Reza, T. Abdulahovic, B. Badrzadeh, C. Roy, "Brochure Cigre WG A2/C4.39 - Chapter 9.2 Case study: Transients in wind turbine transformer", to be published in 2012
6. T. Abdulahovic, T. Thiringer, M. Reza, H. Breder, "Vacuum Circuit Breaker Parameter Calculation and Modeling for Power System Transient Studies", to be submitted to IEEE Transactions on Industry Applications

ELFORSK

SVENSKA ELFÖRETAGENS FORSKNINGS- OCH UTVECKLINGS - ELFORSK - AB

Elforsk AB, 101 53 Stockholm. Besöksadress: Olof Palmes Gata 31
Telefon: 08-677 25 30, Telefax: 08-677 25 35
www.elforsk.se